Combinatorial Structure of the Moduli Space of Riemann Surfaces and the KP Equations

Motohico Mulase

Michael Penkava

Department of Mathematics, University of California, Davis, CA 95616–8633

E-mail address: mulase@math.ucdavis.edu

Department of Mathematics, University of Wisconsin, Eau Claire, WI 54702–4004

E-mail address: penkavmr@uwec.edu

1991 *Mathematics Subject Classification.* Primary: 32G15, 57R20, 81Q30.
Secondary: 14H15, 30E15, 30E20, 30F30

Contents

Preface

Acknowledgement. The first author thanks Pierre Deligne for comments on the Euler characteristic of algebraic stacks that clarified his understanding of the moduli space of algebraic curves, Maxim Kontsevich for introducing him to the matrix integrals and the moduli theory, and Bill Thurston for discussions on graph complexes and orbifolds. Discussions with Greg Kuperberg were also very useful to him. The second author thanks ... Francesco Bottacin and Regina Parsons read earlier versions and contributed to improve this book, to whom the authors' special thanks are due.

Part 1

Combinatorial Structure of the Moduli Space of Riemann Surfaces

CHAPTER 1

Introduction

1. An Overview

A complex manifold is a patchwork of open domains of the complex Euclidean space. The complex structure of a manifold is the information how these domains are glued together. Since each domain has the standard complex structure, the structure of a complex manifold is a combinatorial information.

The moduli space of a complex manifold is the set of isomorphism classes of the complex structures defined on the underlying topological manifold of a given complex manifold. Therefore, it is natural to expect that the moduli space of a complex manifold may have a combinatorial description.

The moduli problem in algebraic geometry is to determine the algebraic structure of the moduli space of an algebraic object, such as an algebraic variety or an algebraic vector bundle. Often the moduli space does not admit the structure of any algebraic variety. There are two different ways to address this difficulty. The first is to impose a condition on the class of algebraic objects under consideration so that the moduli space can be realized as an open subset of an algebraic variety [**20**]. The second way is to enlarge the notion of the algebraic structure so that the moduli space has an algebraic structure in the extended sense, for example, as an algebraic stack [**3**]. The moduli problem is understood for relatively restricted objects, including the Riemann surfaces or algebraic curves, but even for the case of a Riemann surface, describing the moduli space for a high genus is a hard problem.

The purpose of our study is to give a combinatorial description of the moduli space of Riemann surfaces with marked points and the same number of positive real numbers, and to relate the combinatorial structure with an integrable system of nonlinear partial differential equations through a Hermitian matrix integral.

We will prove that the moduli space of pointed Riemann surfaces with positive real numbers has the structure of a *differentiable orbifold*. An *orbifold* is a patchwork of local pieces, where each local piece is homeomorphic to the quotient space of the real Euclidean space of a fixed dimension by a finite group action [**31**]. If the group action is through orthogonal transformations and the patching is by diffeomorphisms, then the orbifold is said to be *differentiable*. In our study, the finite groups that determine the orbifold structure of the moduli space appear as the automorphism groups of *graphs*, and these graphs are the combinatorial representatives of the holomorphic structures of pointed Riemann surfaces.

The same graph automorphism groups appear in the asymptotic expansion of a Hermitian matrix integral. The integrand of the Hermitian matrix integral we will consider is the exponential function of the trace of an arbitrary polynomial in one matrix variable, and the integral is taken over the space of all Hermitian matrices of a fixed size with respect to the standard Euclidean metric. The technique of

Feynman diagrams can be applied to compute the asymptotic expansion of the Hermitian matrix integral. Due to the fact that the trace of the product of matrix variables is invariant under the cyclic permutation of the variables, the Feynman diagrams appearing in the asymptotic expansion of the Hermitian matrix integral turn out to be graphs drawn on compact oriented surfaces. Through Feynman diagram expansion, the asymptotic series of the Hermitian matrix integral gives us the generating function of the reciprocal of the order of the automorphism group of a graph that is drawn on a Riemann surface.

The Strebel theory [**29**] determines the unique graph for each Riemann surface with marked points and the same number of positive real numbers. Each edge of this graph has a length that is determined by the choice of the complex structure and the positive real numbers. A *metric ribbon graph* is a graph drawn on an oriented surface with a positive real number assigned to each edge. Thus the Strebel theory gives us a description of the moduli space as the set of isomorphism classes of metric ribbon graphs.

The space of metric ribbon graphs forms a stratified space consisting of orbifolds of various dimensions by gluing each piece together by *contraction*. If an edge of a graph is not a loop, then we can remove the edge and join the two endpoints together. This operation is the contraction. The glued union of all the strata has the same dimension everywhere and forms a connected differentiable orbifold, which is shown by *inflating* graphs. The inverse operation of the contraction is the inflation, which inserts a new non-loop edge to a graph such that the contraction of the inserted edge gives us back the original graph. The space of all inflations of a metric ribbon graph is homeomorphic to a real Euclidean space [**28**], and the graph automorphism group acts on this space faithfully, except for the case of genus one with one marked point. The quotient of the space of inflations of a metric ribbon graph by the action of the ribbon graph automorphism group determines the local structure of the moduli space as a differentiable orbifold. Thus we know that, although the moduli space is not a smooth manifold, its singularities are mild. They are modeled by a finite group action on a real Euclidean space through orthogonal transformations.

The space of metric ribbon graphs determines a canonical orbifold cell-decomposition of the moduli space. Using this cell-decomposition, we can give a formula for the orbifold Euler characteristic of the moduli space in terms of the order of the graph automorphism groups. The formula also has an expression in terms of a Hermitian matrix integral known as the Penner model [**21**], which is a special case of the Hermitian matrix integral whose asymptotic expansion is the generating function of the reciprocal of the order of ribbon graph automorphism groups. The asymptotic expansion of the Penner model is explicitly computable by exact asymptotic analysis [**18**], and the coefficients are expressed in terms of special values of the Riemann zeta function. Thus we obtain a formula for the orbifold Euler characteristic of the moduli space in terms of special values of the Riemann zeta function. This recovers a theorem of Harer and Zagier [**10**].

There is no analytic method to calculate the Hermitian matrix integral whose asymptotic expansion gives the generating function of the reciprocal of the order of ribbon graph automorphism groups. But this integral can be characterized by a system of integrable nonlinear partial differential equations known as the Kadomtsev-Petviashvili (KP) equations. Slightly more general Hermitian matrix integrals also

satisfy the KP equations. Since the soliton solutions of the KP equations are written as Hermitian matrix integrals of Dirac delta functions, the Hermitian matrix integrals can be thought of as the continuum limit of the soliton solutions.

The system of the KP equations defines a dynamical system on an infinite-dimensional Grassmannian through the bijective correspondence between the solutions of the KP equations and the points on the Grassmannian [**24**]. Every finite-dimensional orbit of this KP dynamical system is isomorphic to the Jacobian variety of an algebraic curve, and conversely, every Jacobian variety is realized as a finite-dimensional orbit of the KP dynamical system [**1**], [**14**], [**27**]. Let us call a solution to the KP equations *algebraic* if the point of the Grassmannian corresponding to the solution is stabilized by any of the KP flows. All finite-dimensional solutions are algebraic. There are many algebraic solutions which have infinite-dimensional orbits on the Grassmannian, known as *higher-rank* solutions. There is a bijective correspondence between all the algebraic solutions of the KP equations and the set of geometric data consisting of algebraic curves and torsion-free sheaves of arbitrary rank defined on them [**15**].

A generic solution to the KP equations is non-algebraic, or *transcendental*, but it is generally difficult to give an explicit formula for a transcendental solution. The Hermitian matrix integral that gives the generating function of the reciprocal of the order of ribbon graph automorphism groups turns out to be a transcendental solution to the KP equations. This fact follows from a characteristic feature that the point of the Grassmannian corresponding to the Hermitian matrix integral is stabilized by an algebra of differential operators that is isomorphic to $sl(2, \mathbb{C})$. The theory of tau functions of Sato gives us another asymptotic expansion of the Hermitian matrix integral in terms of Young diagrams and Schur polynomials.

These are the topics discussed in the following chapters. Recently the role of quantum field theory and its Feynman path integral expression has won a special attention of the mathematical community. Its power and efficiency has been recognized throughout the mathematical disciplines. The fundamental principle is the following:

Compute a Feynman path integral in two different ways. Since the two expressions come from the same quantum field theory, they should be equal. The equality of the two different expressions will give us a mathematical theorem.

Unfortunately it is very often difficult to prove the equality following the line of arguments suggested by the quantum field theory in background, although here are many successful examples, including the new proof of the Atiyah-Singer index theorem, where the infinite-dimensional integral can be treated rigorously.

The Hermitian matrix integral we are going to study can be thought of as the Feynman path integral expression of a toy quantum field theory. It is finite-dimensional so that it can be analyzed rigorously. In particular, the two formulas of the asymptotic expansion in terms of the Feynman diagram expansion and the classical orthogonal polynomial method gives us a non-trivial equality, which is the formula of Harer and Zagier [**10**].

Yet we add another ramification to the finite-dimensional integral: the KP equations. The Hermitian matrix integral is the partition function of a zero-dimensional quantum field theory, and the partition function as a function with respect to the coupling constants is characterized by the KP nonlinear integrable system. Thus the Hermitian matrix integral connects three different mathematical

world: moduli theory, integrable systems, and the special values of the Riemann zeta function.

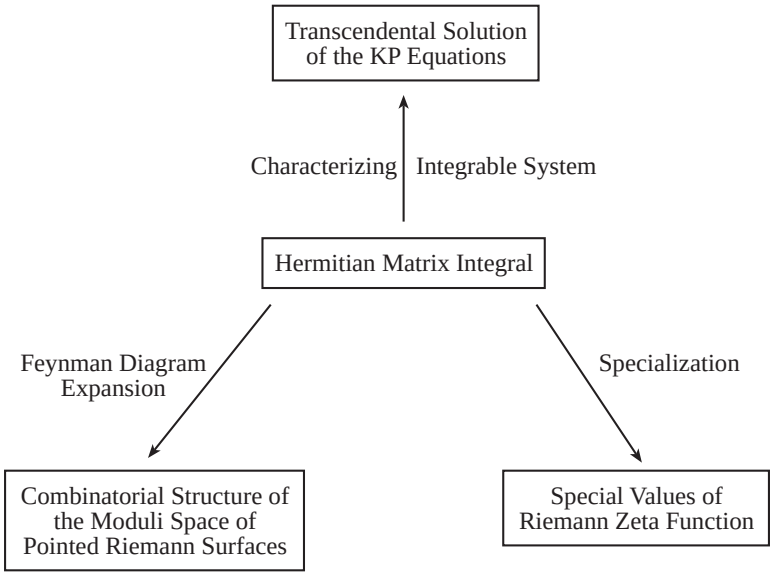

The amzing richness of Witten's world [**33**] is clear. In a sense, our investigation is just the theory of the Gromov-Witten invariants of a 0-dimensional symplectic manifold! In the theory of Gromov-Witten invariants and quantum cohomologies, the homology classes of the compactified moduli spaces of pointed Riemann surfaces play an essential role.

There are other connections between the moduli spaces of algebraic curves and graphs on topological surfaces than the one coming from the Strebel theory. The most interesting among them is Grothendieck's *dessins d'enfant*: the set of isomorphism classes of certain graphs drawn on compact topological surfaces is identified with the moduli space of algebraic curves defined over $\overline{\mathbb{Q}}$. Here the main interests lie in the action of the absolute Galois group $Gal(\overline{\mathbb{Q}}, \mathbb{Q})$ on the algebraic fundamental group (i.e., the profinite completion of π_1) of the moduli spaces [**11**], [**25**]. Of course the KP theory can be built perfectly well on $\overline{\mathbb{Q}}$, but there have been no particular motivation to investigate such a theory until now. With the emergence of the KP theory in the Strebel theory in sight, it is the time to study dessins d'enfant from the point of view of the infinite-dimensional Grassmannian defined over $\overline{\mathbb{Q}}$.

2. A Drawing on a Riemann Surface

A two-dimensional sphere is the foundation and a cylinder is a building block of constructing all compact connected oriented topological surfaces. In this book we consider only connected orientable surfaces. So by a surface we always mean a connected oriented one unless otherwise specified.

A sphere S^2 is itself a compact oriented topological surface. Remove two non-intersecting disks out of it. The surface now has the boundary consisting of two disjoint circles. Since a cylinder has also two circles as its boundary, we can attach

a cylinder to the 2-punctured sphere gluing the boundary circles. The result is a sphere with one handle (Figure 1.1). This surface is homeomorphic to a two-dimensional torus.

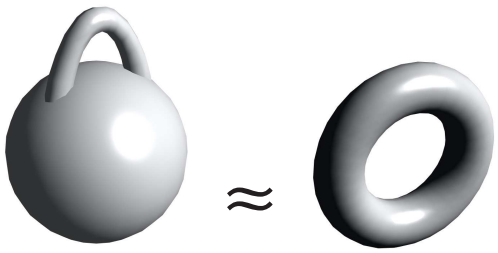

FIGURE 1.1. Sphere with a Handle

The process of attaching a handle can be applied to any compact oriented surface in the same way: first remove two non-intersecting disks from a surface Σ, and then glue a cylinder along the boundary circles. Let us give a recursive definition of the *genus* of a compact oriented surface. The genus of a sphere is defined to be 0. If a surface Σ has genus g, then the surface obtained by attaching a handle to Σ has genus $g+1$.

A surface of genus g is a compact connected oriented surface obtained by attaching g handles to a sphere. The order and the way of attaching the handles do not affect the topological structure, or the structure invariant under homeomorphisms, of the surface. It is known that every compact connected oriented surface is homeomorphic to a surface of genus g.

Let Σ_g be a surface of genus g. Up to homeomorphism, we can realize it in the form of Figure 1.2, where the g handles are aligned around the equator of a sphere. Let P be the north pole of the sphere, and $H_1, \cdots, H_g$ the g handles of Σ_g. Each handle H_j is attached to the sphere along two circles C_j^e and C_j^w, where C_j^e is the east boundary and C_j^w the west boundary of H_j. Let us draw a *drawing*

$$\Gamma = \alpha_1 \cup \beta_1 \cup \cdots \cup \alpha_g \cup \beta_g \tag{1.1}$$

on this surface as in Figure 1.2.

The cycle α_j starts at the north pole P, goes down along a meridian to the west-bound circle C_j^w of the handle H_j, circles around C_j^w, and comes back to P along another meridian. The cycle β_j starts at P, goes down to the east-bound circle C_j^e first, then goes on to the handle H_j, gets out of the handle at the west end, and comes back to P. We choose the paths α_j and β_j so that they intersect only at P. Moreover, we can arrange these cycles for every $j = 1, 2, \cdots, g$ so that none of them intersect except for the common endpoint P. On Figure 1.2, only α_1 and β_1 are drawn, but it is easy to complete the drawing Γ.

None of these cycles are 0-homotopic. Moreover, for every point x of Σ_g that is not on the drawing Γ, there is a path on the surface that connects x and the south pole Q without intersecting Γ. Let us cut the surface along the $2g$ cycles. This is the same as considering the complement of the drawing Γ on the surface. The result is homeomorphic to an open disk bounded by $4g$ edges (Figure 1.3).

In Figure 1.3, an arrow is given to each edge. Since Σ_g is oriented, there are two sides for each cycle. The cutting process is more accurate if we try to cut out

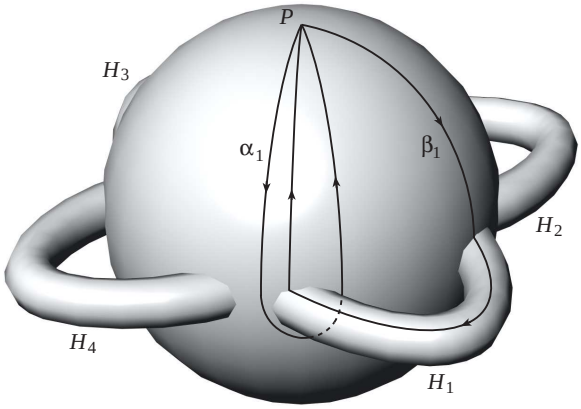

FIGURE 1.2. A Drawing on a Surface of Genus 4

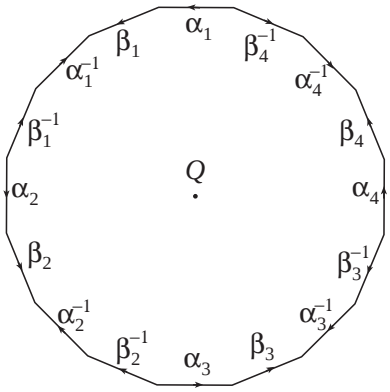

FIGURE 1.3. A $4g$-gon as the Result of Cutting Σ_4 Along the Drawing

a thin neighborhood of the drawing. So when we start from P, we cut along α_1 on its west side. After circling around the west-bound circle C_1^w of the handle H_1, we then cut along the east side of α_1 up to P. Next we cut along the west side of β_1 down to the east-bound circle C_1^e, cut along the inner side of the path on the handle, then go along the east side of β_1 as we go up to the north pole again. We now follow α_1 backward, starting on its west side first, then go up to the north pole along the east side. Finally, we cut along β_1 backward starting with its west side, the outer side on the handle, and the east side as we go up to P. Continuing this cutting process for all cycles, we obtain the $4g$-gon as the complement of the drawing on Σ_g. For each edge of the $4g$-gon, the reversed direction is indicated by the inverse sign of the name the cycle.

We can recover Σ_g by gluing the $4g$ edges of the $4g$-gon pairwise with aligned direction. All the $4g$ corners of the $4g$-gon are identified and recover the north pole P. The center of the $4g$-gon is the south pole Q. Since Σ_g is made of a single $4g$-gon, $2g$-edges after gluing, and a single vertex P, we have the formula for the

Euler characteristic of the surface of genus g:

$$\chi(\Sigma_g) = 1 - 2g + 1 = 2 - 2g. \tag{1.2}$$

The drawing Γ is an example of what we call in later sections a *ribbon graph*. It has one vertex P and $2g$ edges

$$\alpha_1, \beta_1 \cdots, \alpha_g, \beta_g.$$

The vertex P has *degree* $4g$, which is the number of half-rays coming in to, and going out of, P.

A *graph* is a finite collection of points (*vertices*) and line segments (*edges*), such that each vertex bounds an edge and every endpoint of an edge is a vertex. Figure 1.4 is a graph with four vertices of degree 1, 2, 3 and 4.

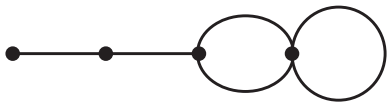

FIGURE 1.4. A Graph

A connected graph Γ is a *ribbon graph* if

(1) it is drawn on a compact connected oriented surface Σ,
(2) it has no vertices of degree 1, and
(3) it induces a cell-decomposition of Σ.

A cell-decomposition of a surface is a decomposition of the surface into the disjoint union of several pieces such that each connected component is homeomorphic to a point, an open line segment, or an open disk, and that an n-dimensional piece is glued to the boundary of an $(n+1)$-dimensional piece, where $n = 0, 1$. The vertices of Γ are the 0-cells and the edges of Γ are the 1-cells of the cell-decomposition. The complement of Γ in Σ is the disjoint union of open disks, which are the 2-cells. The number $v(\Gamma)$ of vertices, the number $e(\Gamma)$ of edges of Γ, the number $b(\Gamma)$ of 2-cells and the genus of Σ satisfy the relation

$$2 - 2g(\Sigma) = v(\Gamma) - e(\Gamma) + b(\Gamma).$$

There are many different cell-decompositions of the same surface by ribbon graphs. Then what properties of a surface does a ribbon graph represent? It is certainly useful to compute the Euler characteristic, but for a surface it is anyway an easy task. Why are we interested in, and what the use of, these ribbon graphs?

The answer comes from a somewhat surprising direction. The different ribbon graphs on the same topological surface represent different *types* of holomorphic structures defined on the surface. In other words, the ribbon graphs represent the combinatorial structure of the *moduli* spaces of Riemann surfaces.

DEFINITION 1.1 (Riemann surfaces and complex structures). Let Σ be a compact connected oriented surface. A *holomorphic structure* on Σ is a finite open covering

$$\Sigma = \bigcup_{j=1}^{n} U_j \tag{1.3}$$

of Σ by open subsets U_j together with homeomorphisms

$$\phi_j : U_j \xrightarrow{\sim} \Omega_j \subset \mathbb{C} \tag{1.4}$$

such that each Ω_j is homeomorphic to an open disk of $\mathbb{C}$, and that the map

$$\phi_j \circ \phi_i^{-1}\big|_{\phi_i(U_i \cap U_j)} : \phi_i(U_i \cap U_j) \xrightarrow{\sim} \phi_j(U_i \cap U_j) \subset \Omega_j$$

is biholomorphic. A compact *Riemann surface* is a compact connected oriented surface with a holomorphic structure defined on it. Two Riemann surfaces $(\Sigma^1, \{U_j^1\})$ and $(\Sigma^2, \{U_k^2\})$ are said to be *isomorphic, conformal, or biholomorphic* if there is a homeomorphism

$$h : \Sigma^1 \longrightarrow \Sigma^2$$

such that

$$\phi_k^2 \circ h \circ (\phi_j^1)^{-1} : \Omega_j^1 \longrightarrow \Omega_k^2$$

and

$$\phi_j^1 \circ h^{-1} \circ (\phi_k^2)^{-1} : \Omega_k^2 \longrightarrow \Omega_j^1$$

are holomorphic maps whenever they are defined.

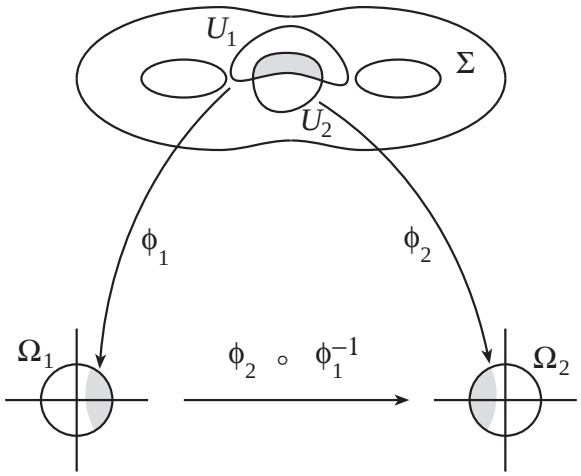

FIGURE 1.5. Coordinate Patch

The *moduli space* $\mathfrak{M}_g$ of Riemann surfaces of genus g is the set of all isomorphism classes of complex structures defined on a compact surface of genus g. What kind of natural geometric structure does the moduli space $\mathfrak{M}_g$ have, and how can we define it? This question goes back to Riemann's paper *Theorie der Abel'schen Functionen* that was published in Crelle's journal in 1847. There have been many results established throughout the 20th century on this moduli problem. The most successful analytic theory on the problem is called *Teichmüller theory*. The techniques developed for the analytic study of $\mathfrak{M}_g$ are used widely in pure and applied mathematics, including fluid dynamics. The literature on this topic is vast. Here we cite only [**6**] and [**12**]. There is also a nice geometric discussion on the subject in [**31**]. The algebro-geometric approach to the moduli problem has evolved into the theory of *algebraic stacks* and *geometric invariant theory*. The standard literature on these subjects are [**3**] and [**20**].

In order to determine the combinatorial representative of a holomorphic structure on a surface, we have to choose some points on it and a the same number of positive real numbers. In later chapters we will show that the collection of these data is equivalent to a ribbon graph with a positive real number assigned to each edge. The key ingredient of our study is the automorphism group of a ribbon graph, which appear in the theory of Riemann surfaces as well as in the asymptotic expansion of certain matrix integrals. The fact that they are the same object gives us a mysterious connection between the totally different objects.

We now begin our more formal treatment of the combinatorial objects we need. It is an unfortunate digression, but without precise definitions we cannot reach to deep theorems. Figures are designed to help forming geometric understanding of the combinatorial objects. The precise algebraic definitions are given so that we will be able to apply the geometric method of counting to the computation of the Hermitian matrix integrals later, where the built-in geometry is not apparent at all. Through an algebraic manipulation of the integrals, we will encounter the combinatorial objects of this chapter, and through the geometric visualization of the combinatorial data, we will see the connection between geometry of Riemann surfaces and analysis of the matrix integrals.

CHAPTER 2

Riemann Surfaces and the Combinatorial Data

Hermann Weyl defined a Riemann surface as a patch-work of complex domains [**32**]. Two open domains are glued together by a biholomorphic function. The complex analytic structure of a Riemann surface is then encoded in the combinatorial data of the coordinate patches.

The combinatorial object we need in our study of the moduli spaces of Riemann surfaces is a type of *graph* drawn on a Riemann surface. Since what we call a graph is not exactly the same as that is found in the common literature of graph theory, we give the precise definition of various kinds of combinatorial objects in this chapter.

We encounter the graph like structures in two different ways. The first one is through Strebel theory, which gives a cell-decomposition of a Riemann surface. The 1-skeleton of the cell complex is a graph drawn on the surface. The other is through Feynman diagram expansion of a Hermitian matrix integral. The fact that these combinatorial data are exactly the same gives us a powerful tool to understand the moduli spaces of Riemann surfaces.

We start with the definition of pairing schemes in Section 1. This is an unusual manner to introduce a graph, but it turns out to be the shortest path to connect Feynman diagram expansion of matrix integrals and the complex analytic structure of a Riemann surface in later chapters. Ribbon graphs (or fatgraphs) are defined in Section 2 as an equivalence class of pairing schemes. The notion of automorphism groups of ribbon graphs is defined. It is this automorphism group that determines the orbifold structure of the moduli space of Riemann surfaces, and at the same time the order of the group appears as the coefficients of the asymptotic expansion of a Hermitian matrix integral. The automorphism group of a ribbon graph naturally acts on the set of edges of the graph. Most of the cases this action is faithful, but there are special graphs which have a non-trivial graph automorphism acting on the set of edges trivially. Section 3 is devoted to classify all the exceptional graphs.

1. Pairing Schemes and Graphs

The object that connects the graphs appearing in the Strebel theory and the Feynman diagrams appearing in the asymptotic expansion of a Hermitian matrix integral is a *pairing scheme*.

DEFINITION 2.1. A *pairing scheme* $P = (\mathcal{V}, p)$ consists of a collection $\mathcal{V} = \{V_1, V_2, \cdots, V_v\}$ of non-empty finite ordered sets $V_j = (V_{j1}, V_{j2}, \cdots, V_{j\ell_j})$, where $j = 1, 2, \cdots, v$, and a bijective *pairing map* $p : \widetilde{\mathcal{V}} \xrightarrow{\sim} \widetilde{\mathcal{V}}$ satisfying that

(1) $p(V) \neq V$ for every $V \in \widetilde{\mathcal{V}}$, and
(2) $p^2 = 1$,

where $\widetilde{\mathcal{V}}$ is the union of all elements of V_j:

$$\widetilde{\mathcal{V}} = \bigcup_{j=1}^{v} V_j = \{V_{11}, \cdots, V_{1\ell_1}, V_{21}, \cdots, V_{2\ell_2}, \cdots, V_{v1}, \cdots, V_{v\ell_v}\}.$$

There is a natural *projection*

$$\widetilde{\mathcal{V}} \ni V_{jk} \longmapsto V_j \in \mathcal{V}. \tag{2.1}$$

The ordered set V_j is called a *vertex* of P of *degree* ℓ_j. The *degree sequence* $(\ell_1, \ell_2, \cdots, \ell_v)$ is always arranged to be non-decreasing:

$$(\ell_1, \ell_2, \cdots, \ell_v) = (\overbrace{1, 1, \cdots, 1}^{n_1\text{-times}}, \overbrace{2, 2, \cdots, 2}^{n_2\text{-times}}, \cdots, \overbrace{m, m, \cdots, m}^{n_m\text{-times}}), \tag{2.2}$$

where $n_i \geq 0$ is the number of vertices of degree i and $n_1 + n_2 + \cdots + n_m = v$. The set of *directed edges* is defined by

$$\overrightarrow{\mathcal{E}} = \{(V, p(V)) \mid V \in \widetilde{\mathcal{V}}\} \subset \widetilde{\mathcal{V}} \times \widetilde{\mathcal{V}}. \tag{2.3}$$

Since $p^2 = 1$, $(V, p(V))$ is contained in $\overrightarrow{\mathcal{E}}$ if and only if $(p(V), V) \in \overrightarrow{\mathcal{E}}$. Thus $\overrightarrow{\mathcal{E}}$ is symmetric under the natural action of $\mathfrak{S}_2$, where $\mathfrak{S}_n$ denotes the symmetric group of n letters. The quotient

$$\mathcal{E} = \overrightarrow{\mathcal{E}}/\mathfrak{S}_2 \subset (\widetilde{\mathcal{V}} \times \widetilde{\mathcal{V}})/\mathfrak{S}_2 \tag{2.4}$$

is the set of *edges*, and each element $(V, p(V)) = (p(V), V) \in \mathcal{E}$ is an *edge* of P.

Two pairing schemes $P = (\mathcal{V}, p)$ and $P' = (\mathcal{V}', p')$ are said to be *isomorphic* if

(1) they have the same degree sequence,
(2) there is a bijection

$$\alpha_j : V_j \xrightarrow{\sim} V'_j \tag{2.5}$$

of a vertex of P of degree ℓ_j to a vertex of P' of the same degree for every $j = 1, 2, \cdots, v$,
(3) the map

$$\alpha : \widetilde{\mathcal{V}} \xrightarrow{\sim} \widetilde{\mathcal{V}}' \tag{2.6}$$

induced by α_j's is a bijection, and
(4) the diagram

$$\begin{array}{ccc} \widetilde{\mathcal{V}} & \xrightarrow[p]{\sim} & \widetilde{\mathcal{V}} \\ {\scriptstyle\alpha}\downarrow\wr & & \wr\downarrow{\scriptstyle\alpha} \\ \widetilde{\mathcal{V}}' & \xrightarrow[p']{\sim} & \widetilde{\mathcal{V}}' \end{array} \tag{2.7}$$

commutes.

We can visualize a pairing scheme by representing each vertex as a set of dots and each edge as a pairing of two dots. The pairing scheme of Figure 2.1 has three vertices of degree 3, 4 and 5, so its degree sequence is $(3, 4, 5)$.

The group

$$G = \prod_{k=1}^{m} \mathfrak{S}_{n_k} \rtimes (\mathfrak{S}_k)^{n_k} \tag{2.8}$$

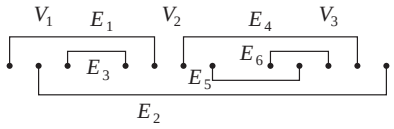

FIGURE 2.1. A Pairing Scheme

acts on the set of all pairing schemes with the same degree sequence. The orbit of this group action at P consists of all pairing schemes that are isomorphic to P.

DEFINITION 2.2. We call an isomorphism class of pairing schemes a *graph* $\Gamma = (\mathcal{V}, \mathcal{E}, i)$ with the *vertex set* $\mathcal{V}$, the *edge set* $\mathcal{E}$, and the *incidence relation*

$$i : \mathcal{E} \longrightarrow (\mathcal{V} \times \mathcal{V})/\mathfrak{S}_2,$$

which is the composition of the inclusion of $\mathcal{E}$ into $(\widetilde{\mathcal{V}} \times \widetilde{\mathcal{V}})/\mathfrak{S}_2$ and the projection $(\widetilde{\mathcal{V}} \times \widetilde{\mathcal{V}})/\mathfrak{S}_2 \longrightarrow (\mathcal{V} \times \mathcal{V})/\mathfrak{S}_2$.

The graph corresponding to the pairing scheme of Figure 2.1 is given in Figure 2.2.

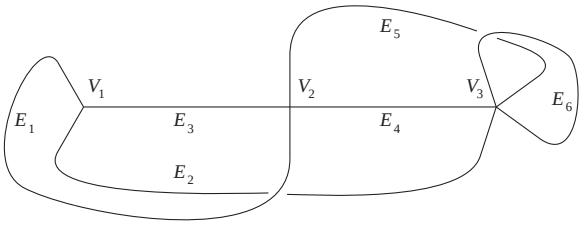

FIGURE 2.2. The Graph Corresponding to the Pairing Scheme of Figure 2.1

Although we use the word *graph* for an isomorphism class of pairing schemes because of its graph-like structure, it is *not* exactly the same object found in the usual literature of graph theory. The biggest difference lies in the notion of *graph automorphism*.

DEFINITION 2.3. Let $P = (\mathcal{V}, p)$ be a pairing scheme with the degree sequence (2.2) and $\Gamma = (\mathcal{V}, \mathcal{E}, i)$ the graph representing the isomorphism class of P. The *graph automorphism group* $\mathrm{Aut}(\Gamma)$ of Γ is the isotropy subgroup of $\prod_{k=1}^{m} \mathfrak{S}_{n_k} \rtimes (\mathfrak{S}_k)^{n_k}$ that preserves P:

$$\mathrm{Aut}(\Gamma) = \left\{ g \in \prod_{k=1}^{m} \mathfrak{S}_{n_k} \rtimes (\mathfrak{S}_k)^{n_k} \;\middle|\; \begin{array}{ccc} \widetilde{\mathcal{V}} & \xrightarrow[p]{\sim} & \widetilde{\mathcal{V}} \\ {\scriptstyle g}\downarrow & & \downarrow{\scriptstyle g} \\ \widetilde{\mathcal{V}} & \xrightarrow[p]{\sim} & \widetilde{\mathcal{V}} \end{array} \text{ commutes} \right\}. \tag{2.9}$$

REMARK. The automorphism group $\mathrm{Aut}(\Gamma)$ does not depend on the choice of the representing pairing scheme P. Let P' be a pairing scheme isomorphic to P. Then there is an $h \in \prod_{k=1}^{m} \mathfrak{S}_{n_k} \rtimes (\mathfrak{S}_k)^{n_k}$ such that $P' = hP$. The isotropy subgroup of P' is conjugate to the isotropy subgroup of P by h in $\prod_{k=1}^{m} \mathfrak{S}_{n_k} \rtimes (\mathfrak{S}_k)^{n_k}$.

For comparison, let us give the usual definition of a graph here.

DEFINITION 2.4. A usual *graph* $\Gamma = (\mathcal{V}, \mathcal{E}, i)$ consists of finite sets $\mathcal{V}$ of *vertices* and $\mathcal{E}$ of *edges*, together with a map

$$i : \mathcal{E} \longrightarrow (\mathcal{V} \times \mathcal{V})/\mathfrak{S}_2$$

called the *incidence relation*. Let $\mathcal{V} = \{V_1, V_2, \cdots, V_v\}$. The number of vertices v is called the *order* of Γ. The *degree*, or *valence*, of a vertex V_j is the number

$$\deg(V_j) = \sum_{k \neq j} a_{jk} + 2a_{jj},$$

where

$$a_{jk} = |i^{-1}(V_j, V_k)|.$$

The *degree sequence* of Γ is the list of degrees of vertices:

$$(\deg(V_1), \deg(V_2), \cdots, \deg(V_v)).$$

The vertices are arranged so that the degree sequence is non-decreasing.

REMARK. In this article we assume $\deg(V_j) > 0$ for every vertex $V_j \in \mathcal{V}$.

DEFINITION 2.5. An *isomorphism* $g = (a, b)$ of a graph $\Gamma = (\mathcal{V}, \mathcal{E}, i)$ to another graph $\Gamma' = (\mathcal{V}', \mathcal{E}', i')$ *in the usual sense* is a pair of bijective maps

$$a : \mathcal{V} \xrightarrow{\sim} \mathcal{V}' \qquad \text{and} \qquad b : \mathcal{E} \xrightarrow{\sim} \mathcal{E}'$$

such that the diagram

$$\begin{array}{ccc} \mathcal{E} & \xrightarrow{\ i\ } & (\mathcal{V} \times \mathcal{V})/\mathfrak{S}_2 \\ {\scriptstyle b}\big\downarrow\wr & & \wr\big\downarrow{\scriptstyle a\times a} \\ \mathcal{E}' & \xrightarrow[\ i'\ ]{} & (\mathcal{V}' \times \mathcal{V}')/\mathfrak{S}_2 \end{array} \tag{2.10}$$

commutes.

Every isomorphism $g = (a, b) : \Gamma \longrightarrow \Gamma'$ in the usual sense preserves the degree sequence. In particular, a maps a vertex of Γ to a vertex of Γ' of the same degree.

Let $\Gamma = (\mathcal{V}, \mathcal{E}, i)$ be an ordinary graph in the above sense. We define the *edge refinement* $\Gamma_{\mathcal{E}} = (\mathcal{V} \cup \mathcal{V}_{\mathcal{E}}, 2\mathcal{E}, i_{\mathcal{E}})$ of Γ to be the graph Γ with the middle point of each edge added as a degree 2 vertex. More precisely, let V_E be the midpoint of an edge $E \in \mathcal{E}$ of Γ. We denote by $\mathcal{V}_{\mathcal{E}}$ the set of all these midpoints of edges. These midpoints are considered to be degree 2 vertices of the new graph $\Gamma_{\mathcal{E}}$. The set of vertices of $\Gamma_{\mathcal{E}}$ is the disjoint union $\mathcal{V} \cup \mathcal{V}_{\mathcal{E}}$, and the set of edges is the disjoint union $\mathcal{E} \coprod \mathcal{E}$, which we denote by $2\mathcal{E}$, because the midpoint V_E divides the edge E into two parts. The incidence relation can now be described by a map

$$i_{\mathcal{E}} : 2\mathcal{E} = \mathcal{E} \coprod \mathcal{E} \longrightarrow \mathcal{V} \times \mathcal{V}_{\mathcal{E}}, \tag{2.11}$$

because each edge of $\Gamma_{\mathcal{E}}$ connects exactly one vertex of $\mathcal{V}$ to a vertex of $\mathcal{V}_{\mathcal{E}}$. An edge of $\Gamma_{\mathcal{E}}$ is called a *half-edge* of Γ. For every vertex $V \in \mathcal{V}$ of Γ, the set $i_{\mathcal{E}}^{-1}(V \times \mathcal{V}_{\mathcal{E}})$ consists of half-edges coming out of V. Note that we have

$$\deg(V) = |i_{\mathcal{E}}^{-1}(V \times \mathcal{V}_{\mathcal{E}})|.$$

In Figure 2.3, the original graph Γ has three vertices V_1, V_2, V_3 and six edges $E_1, E_2, \cdots, E_6$. The edge refinement $\Gamma_{\mathcal{E}}$ has thus six more vertices $V_{E_1}, \cdots, V_{E_6}$. There are five half-edges at V_3, as the degree of the vertex V_3 indicates.

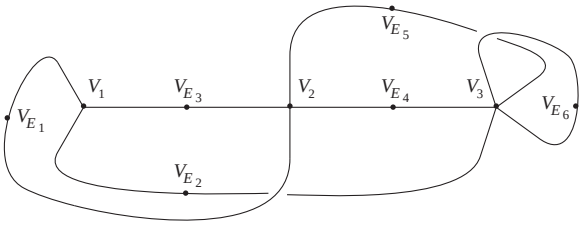

FIGURE 2.3. The Edge Refinement of a Graph

The graph automorphism $\mathrm{Aut}(\Gamma)$ in our sense is the graph automorphism of the edge refinement $\Gamma_{\mathcal{E}}$ in the usual sense that preserves $\mathcal{V}$, $\mathcal{V}_{\mathcal{E}}$ and $\mathcal{E}$. For example, the graph with one degree 4 vertex and two edges has $(\mathbb{Z}/2\mathbb{Z})^3$ as its automorphism, while the usual graph theoretic automorphism is $\mathbb{Z}/2\mathbb{Z}$ (Figure 2.4).

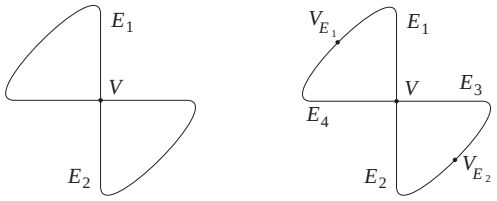

FIGURE 2.4. A Graph and its Edge Refinement

The isomorphism class of a pairing scheme can be recovered from a usual graph through the edge refinement, by defining a vertex of the pairing scheme as the set of half-edges coming out of a vertex of the original graph.

DEFINITION 2.6. Let Γ be a graph. Two edges E_1 and E_2 are *connected* if there is a vertex V of Γ such that both E_1 and E_2 are incident to V. A *sequence of connected edges* is an ordered set

$$(E_1, E_2, \cdots, E_k) \tag{2.12}$$

of edges of Γ such that E_j and E_{j+1} are connected for every $j = 1, 2, \cdots, k-1$. A graph Γ is *connected* if for every pair of vertices V and V' of Γ, there is a sequence of connected edges (2.12) such that E_1 is incident to V and E_k is incident to V'.

REMARK. As a convention, we classify the empty graph as a non-connected graph. Thus we count that the number of graphs with 0 vertices is 1, while the number of *connected* graphs with 0 vertices is 0.

2. Ribbon Graphs

Let us now turn our attention to ribbon graphs.

DEFINITION 2.7. Two isomorphic pairing schemes P and P' with the same degree sequence (2.2) have the same *orientation* if $P' = gP$ for some

$$g \in \prod_{k=1}^{m} \mathfrak{S}_{n_k} \rtimes (\mathbb{Z}/k\mathbb{Z})^{n_k}.$$

The group element g is called an *orientation preserving isomorphism* of P to P'.

DEFINITION 2.8. A *ribbon graph* (or *fatgraph*) Γ *associated with* a pairing scheme $P = (\mathcal{V}, p)$ is the equivalence class of P with respect to the action of the orientation preserving isomorphisms.

PROPOSITION 2.9. *A ribbon graph is a graph* $\Gamma = (\mathcal{V}, \mathcal{E}, i)$ *together with a cyclic ordering on each vertex*

$$V_j = (V_{j1}, V_{j2}, \cdots, V_{j\ell_j}) \in \mathcal{V}$$

of Γ.

PROOF. Since an orientation preserving isomorphism of a pairing scheme to another pairing scheme changes the elements of a vertex only by a cyclic permutation, the notion of a cyclic order at each vertex makes sense. Conversely, if each vertex of a pairing scheme has a cyclic ordering, then it defines an isomorphism class of pairing schemes under orientation preserving isomorphisms. Thus it determines a ribbon graph. □

Each vertex of a ribbon graph of degree d can be placed on a positively oriented plane (i.e., a plane with the counter-clockwise orientation). We can make each of the d half-edges into a road coming in to the vertex. Thus the vertex becomes an intersection of d streets. The cyclic ordering of half-edges defines an orientation to each of the side-walks of a street (Figure 2.5).

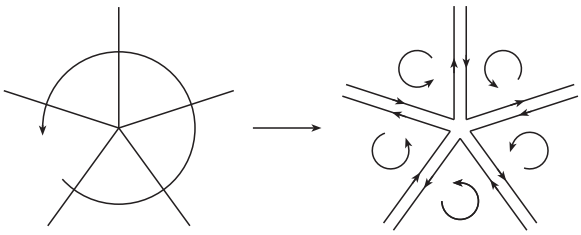

FIGURE 2.5. A Vertex with a Cyclic Ordering and a Cross Road Intersection

The streets are connected following the compatible orientation of the side-walks to form a ribbon like object (Figure 2.6). The graph is no longer placed on an oriented plane. The ribbon graph itself can be considered as an open oriented surface with boundary, which are the connected side-walks.

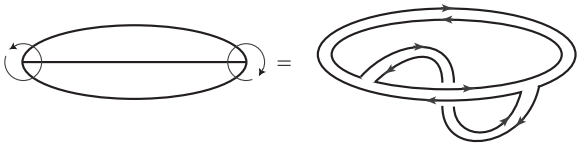

FIGURE 2.6. A Ribbon Graph = A Graph with a Cyclic Order of Half-Edges at each Vertex

The graph of Figure 2.2, when considered as a ribbon graph, is visualized in Figure 2.7.

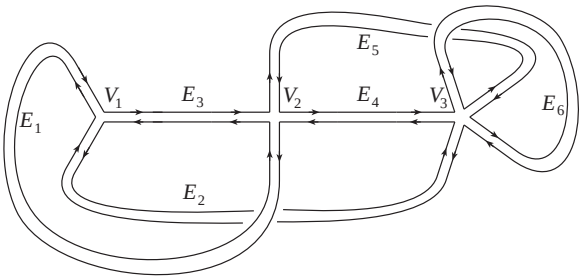

FIGURE 2.7. A Ribbon Graph

DEFINITION 2.10. Let Γ be a ribbon graph associated with a pairing scheme $P = (\mathcal{V}, p)$. Its *automorphism group* $\mathrm{Aut}_{rib}(\Gamma)$ is the isotropy subgroup of

$$\prod_{k=1}^{m} \mathfrak{S}_{n_k} \rtimes (\mathbb{Z}/k\mathbb{Z})^{n_k}$$

that preserves P:

(2.13)

$$\mathrm{Aut}_{rib}(\Gamma) = \left\{ g \in \prod_{k=1}^{m} \mathfrak{S}_{n_k} \rtimes (\mathbb{Z}/k\mathbb{Z})^{n_k} \;\middle|\; \begin{array}{ccc} \widetilde{\mathcal{V}} & \xrightarrow[p]{\sim} & \widetilde{\mathcal{V}} \\ {\scriptstyle g}\downarrow\wr & & \wr\downarrow{\scriptstyle g} \\ \widetilde{\mathcal{V}} & \xrightarrow[p]{\sim} & \widetilde{\mathcal{V}} \end{array} \text{ is commutative} \right\}.$$

As in Definition 2.3, $\mathrm{Aut}_{rib}(\Gamma)$ as an abstract group is independent of the choice of the representing pairing scheme. Since we deal mainly with ribbon graphs from now on, we use the notation $\mathrm{Aut}(\Gamma)$ for the automorphism group of a ribbon graph Γ, unless otherwise stated.

The characteristic difference between a graph and a ribbon graph is that the latter has *boundary*.

DEFINITION 2.11. Let $\Gamma = (\mathcal{V}, \mathcal{E}, i, c)$ be a ribbon graph associated with a pairing scheme $P = (\mathcal{V}, p)$, where c denotes the cyclic ordering of half-edges at each vertex. A *boundary component* of Γ is a sequence of edges

$$(E_1, E_2, \cdots, E_q)$$

with a cyclic order satisfying the following conditions:

(1) Let $E_\nu = (V_{j_\nu k_\nu}, p(V_{j_\nu k_\nu}))$, $\nu = 0, 2, \cdots, q-1$. Then $p(V_{j_\nu k_\nu})$ and $V_{j_{\nu+1} k_{\nu+1}}$ belong to the same vertex $V_{j_{\nu+1}}$, where we consider $q \equiv 0 \mod q$.
(2) $V_{j_{\nu+1} k_{\nu+1}}$ is the predecessor of $p(V_{j_\nu k_\nu})$ with respect to the cyclic order on $V_{j_{\nu+1}}$.

REMARK. Note that the notion of boundary is not defined for ribbon graphs that have vertices of degree 1.

The ribbon graph associated with the pairing scheme of Figure 2.8 has three boundary components (V_{11}, V_{12}), (V_{13}, V_{14}), and $((V_{14}, V_{13}), (V_{12}, V_{11}))$, which correspond to the three topological boundary components of the ribbon graph of Figure 2.9.

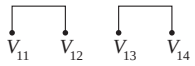

FIGURE 2.8. A Pairing Scheme with a Vertex of Degree 4

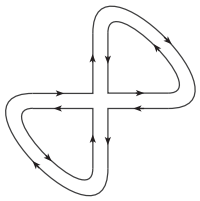

FIGURE 2.9. Visualizing the Boundary Components of a Ribbon Graph of Figure 2.8

The ribbon graphs of Figure 2.6 and Figure 2.7 have only one boundary component. We denote by $b(\Gamma)$ the *number of boundary components* of a ribbon graph Γ.

DEFINITION 2.12. The group of automorphisms of Γ that preserve the boundary components is denoted by $\mathrm{Aut}_\partial(\Gamma)$, which is a subgroup of $\mathrm{Aut}(\Gamma)$.

Since a boundary component of a ribbon graph is defined to be a sequence of edges with a cyclic order, the topological realization of the ribbon graph has a well-defined orientation and each boundary component has the induced orientation that is compatible with the cyclic order. Thus we can attach an oriented disk to each boundary component of a ribbon graph Γ so that the total space, which we denote by $C(\Gamma)$, is a compact oriented topological surface.

The attached disks and the underlying graph $\underline{\Gamma}$ of the ribbon graph Γ defines a cell-decomposition of $C(\Gamma)$. Let $v(\Gamma)$ denote the number of vertices and $e(\Gamma)$ the number of edges of Γ. Then the genus $g(C(\Gamma))$ of the closed surface $C(\Gamma)$ is determined by the following formula for the Euler characteristic:

$$v(\Gamma) - e(\Gamma) + b(\Gamma) = 2 - 2g(C(\Gamma)). \tag{2.14}$$

The ribbon graph of Figure 2.6 has two vertices, three edges and one boundary component. From (2.14), we have $2 - 3 + 1 = 2 - 2 = 0$, hence the surface $C(\Gamma)$ is a torus on which the graph is drawn.

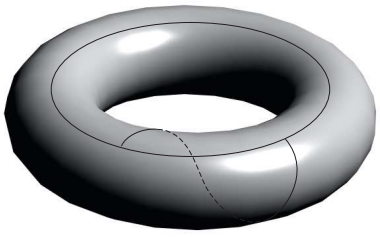

FIGURE 2.10. A Cell-Decomposition of a Torus

The ribbon graph of Figure 2.7 has three vertices, six edges and one boundary component. Thus the genus of the closed surface $C(\Gamma)$ associated with this ribbon graph is 2.

FIGURE 2.11. A Cell-Decomposition of a Surface of Genus 2

The example of Figure 2.9 gives rise to a sphere made up with three disks and a figure 8 shape.

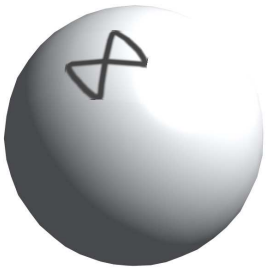

FIGURE 2.12. A Cell-Decomposition of a Sphere with an 8-Shape

Note that (2.14) is invariant under interchanging the number of vertices and boundary components of a ribbon graph. This invariance comes from the *duality* of a cell-decomposition of an oriented surface. Let Z be the cell-decomposition of the surface $C(\Gamma)$ associated with a ribbon graph Γ. Let $\mathcal{V}$ denote the set of vertices, $\mathcal{E}$ the set of edges, and $\mathcal{B}$ the set of boundary components of Γ. The *dual graph* $\Gamma^* = (\mathcal{V}^*, \mathcal{E}^*, i^*)$ of Z consists of the vertex set $\mathcal{V}^* = \mathcal{B}$ and the edge set $\mathcal{E}^*$, which has the same cardinality of $\mathcal{E}$. Two vertices of Γ^* are connected by an edge E^* if the corresponding faces of Z are glued together along an edge E of Γ. The dual graph Γ^* is naturally a ribbon graph, but it may have vertices of degree 1. Thus the boundary components of Γ^* may be ill-defined. If Γ does not have any loop, then Γ^* has well-defined boundaries and it determines the same topological surface

$$C(\Gamma^*) = C(\Gamma).$$

The ribbon graph of Figure 2.7 has only one boundary component. The oriented boundary is a dodecagon as shown in Figure 2.13. The dual graph of the cell-decomposition of Figure 2.11 has thus one vertex of degree 12, six edges, and three boundary components, as shown in Figure 2.14.

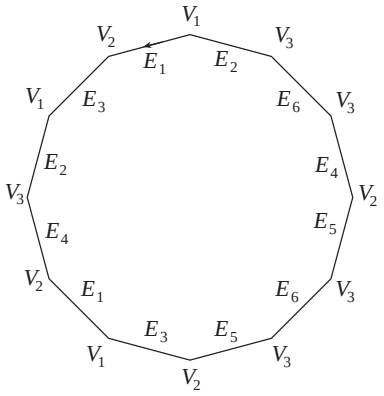

FIGURE 2.13. The Boundary Disk of the Ribbon Graph of Figure 2.7

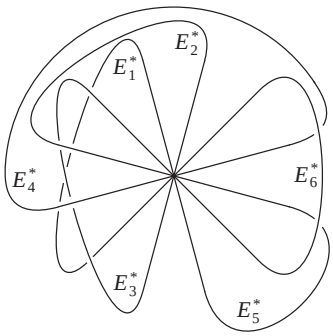

FIGURE 2.14. The Dual of the Cell-Decomposition of Figure 2.11

From now on, we deal only with ribbon graphs whose vertices are of degree 3 or more.

3. Exceptional Graphs

In Chapter 4, we will study *metric ribbon graphs*, which are ribbon graphs with a positive real number assigned to each edge. The set of all metric edges of a ribbon graph forms a topological space, and the automorphism group of the ribbon graph acts on the space. To study the structure of this space, we need to examine the action of the automorphism group of a ribbon graph Γ on the space of metric edges $\mathbb{R}_+^{e(\Gamma)}$. So let us determine all ribbon graphs that have a non-trivial graph automorphism acting trivially on the set of edges.

DEFINITION 2.13. A ribbon graph Γ is *exceptional* if the natural homomorphism

$$\phi_\Gamma : \mathrm{Aut}(\Gamma) \longrightarrow \mathfrak{S}_{e(\Gamma)} \tag{2.15}$$

of the automorphism group of Γ to the permutation group of edges is *not* injective.

The exceptional graphs require a separate treatment when we determine the orbifold structure of the graph complexes in Chapter 3. The geometric structure of the rational cell of the graph complex differs from what we expect from the analytic computation of the invariants through the matrix integral if the graph is exceptional.

Let Γ be an exceptional graph. Since none of the edges are interchanged, the graph can have at most two vertices. If the graph has two vertices, then the graph automorphism interchanges the vertices while all edges are fixed. The only possibility is a graph with two vertices of degree j, ($j \geq 3$), as shown in Figure 2.15.

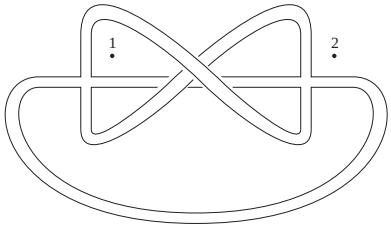

FIGURE 2.15. Exceptional Graph Type 1—A Ribbon

If j is odd, then it has only one boundary component, as in Figure 2.6. The genus of the surface $C(\Gamma)$ is given by

$$g(C(\Gamma)) = \frac{j-1}{2}. \tag{2.16}$$

For an even j, the graph has two boundary components, as in Figure 2.15, and

$$g(C(\Gamma)) = \frac{j-2}{2}. \tag{2.17}$$

In each case, the graph automorphism is the product group

$$\mathrm{Aut}(\Gamma) = \mathbb{Z}/2\mathbb{Z} \times \mathbb{Z}/j\mathbb{Z}, \tag{2.18}$$

and the factor $\mathbb{Z}/2\mathbb{Z}$ acts trivially on the set of edges.

If we label the boundary of the ribbon graph when it has two boundary components, then we can consider the ribbon graph automorphism that preserve the boundary:

$$\mathrm{Aut}_\partial(\Gamma) = \mathbb{Z}/j\mathbb{Z},$$

which is a factor of (2.18). Note that $\mathrm{Aut}_\partial(\Gamma)$ acts faithfully on the set of edges.

To obtain the one-vertex case, we only need to shrink one of the edges of the two-vertex case considered above. The result is a graph with one vertex of degree $2k$, as shown in Figure 2.16.

When k is even, the number of boundary components $b(\Gamma)$ is equal to 1, and the genus of the surface $C(\Gamma)$ is

$$g(C(\Gamma)) = \frac{k}{2}. \tag{2.19}$$

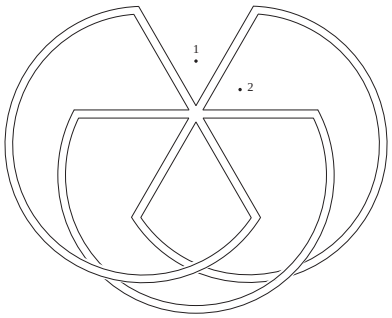

FIGURE 2.16. Exceptional Graph Type 2

If k is odd, then the graph has two boundary components and the genus is

$$g(C(\Gamma)) = \frac{k-1}{2}. \tag{2.20}$$

The graph automorphism is $\mathbb{Z}/(2k)\mathbb{Z}$, but the action on $\mathbb{R}_+^k$ factors through

$$\mathbb{Z}/(2k)\mathbb{Z} \longrightarrow \mathbb{Z}/k\mathbb{Z}.$$

Here again the automorphism group fixing the boundary, $\mathrm{Aut}_\partial(\Gamma) = \mathbb{Z}/k\mathbb{Z}$, acts faithfully on the set of edges.

We have thus classified all exceptional graphs. These exceptional graphs appear for arbitrary genus g. The graph of Figure 2.15 has two distinct labeling of the boundary components, but since they can be interchanged by the action of a ribbon graph automorphism, there is only one equivalence class of ribbon graph with labeled boundary over this underlying ribbon graph. The automorphism group that preserves the boundary is $\mathbb{Z}/4\mathbb{Z}$. Thus the space of metric ribbon graphs with labeled boundary is $\mathbb{R}_+^4/(\mathbb{Z}/4\mathbb{Z})$. The change of labeling, or the action of $\mathfrak{S}_2$, has a non-trivial effect on the graph level, but does not act at all on the space $\mathbb{R}_+^4/(\mathbb{Z}/4\mathbb{Z})$. The space of metric ribbon graphs is also $\mathbb{R}_+^4/(\mathbb{Z}/4\mathbb{Z})$, which is not the $\mathfrak{S}_2$-quotient of the space of metric ribbon graphs with labeled boundary.

The other example of an exceptional graph, Figure 2.16, gives another interesting case. This time the space of metric ribbon graphs with labeled boundary and the space of metric ribbon graphs without referring to the boundary are both $\mathbb{R}_+^3/(\mathbb{Z}/3\mathbb{Z})$. The group $\mathfrak{S}_2$ of changing the labels on the boundary has again no effect on the space.

The analysis of exceptional graphs shows that labeling all edges does not induce labeling of the boundary components of a ribbon graph. However, if we label all half-edges of a ribbon graph, then we have a labeling of the boundary components as well. We will come back to this point when we study the orbifold covering of the space of metric ribbon graphs by the space of metric ribbon graphs with labeled boundary components in Chapter 3.

CHAPTER 3

Theory of Orbifolds

1. The Moduli Space of Riemann Surfaces with Marked Points

Let C be a smooth compact Riemann surface of genus g. A set of n *marked* points of C is an ordered set $(p_1, p_2, \cdots, p_n)$ of n points of C that are labeled. Two sets of data $(C, (p_1, p_2, \cdots, p_n))$ and $(C', (p'_1, p'_2, \cdots, p'_n))$ are said to be *isomorphic* if there is a biholomorphic mapping $f : C \longrightarrow C'$ such that

$$f(p_j) = p'_j \tag{3.1}$$

for $j = 1, 2, \cdots, n$. The *moduli space* $\mathfrak{M}_{g,n}$ is the set of isomorphism classes of smooth compact Riemann surfaces of genus g with n marked points.

We define this space merely as the set of biholomorphic classes for now. The purpose of our study if to give a canonical and explicit combinatorial structure to the space $\mathfrak{M}_{g,n} \times \mathbb{R}^n_+$ and realize it as an *orbifold* [**31**].

The moduli space $\mathfrak{M}_{g,n}$ has been defined as an open complex algebraic variety of complex dimension $3g - 3 + n$ [**20**]. Another algebro-geometric structure as an *algebraic stack* has been introduced to $\mathfrak{M}_{g,n}$ [**3**]. Using the Teichmüller theory, the moduli space is realized as the quotient space of an open domain homeomorphic to $\mathbb{R}^{6g-6+2n}$ by a properly discontinuous action of an infinite discrete group that is known as the *mapping class group* or the *modular group* [**6**]. Since the mapping class group action on the Teichmüller space has fixed points, the quotient space has the structure of an orbifold.

Our approach, which deals with the product space $\mathfrak{M}_{g,n} \times \mathbb{R}^n_+$ rather than the moduli space itself, is more explicit and combinatorial in nature. Our aim is to define an orbifold structure in this product space, and to give a canonical *rational cell-decomposition* of it. This direction of approach to the moduli theory has been studied by [**10**], [**13**], [**21**], [**33**], and many others.

2. Orbifolds and the Euler Characteristic

A space obtained by patching pieces of the form

$$\frac{\text{smooth open ball}}{\text{finite group}}$$

together is called a *V-manifold* by Satake [**23**] and an *orbifold* by Thurston [**31**], from the latter we cite:

Definition 3.1. An *orbifold* $Q = (X(Q), \{U_i\}_{i\in I}, \{G_i\}_{i\in I}, \{\phi_i\}_{i\in I})$ is a set of data consisting of

(1) a Hausdorff topological space $X(Q)$ that is called the *underlying space*,

(2) a locally finite open covering

$$X(Q) = \bigcup_{i \in I} U_i$$

of the underlying space,

(3) a collection of finite groups G_i and a set $\{\phi_i\}$ of homeomorphisms such that for every $i \in I$ there exists an open subset $\widetilde{U}_i$ of $\mathbb{R}^n$ and a faithful G_i-action on $\widetilde{U}_i$ subject to the homeomorphism

$$\phi_i : U_i \xrightarrow{\sim} \widetilde{U}_i/G_i.$$

Whenever $U_i \subset U_j$, there is an injective group homomorphism

$$f_{ij} : G_i \longrightarrow G_j$$

and an embedding

$$\tilde{\phi}_{ij} : \widetilde{U}_i \longrightarrow \widetilde{U}_j$$

such that

$$\tilde{\phi}_{ij}(\gamma x) = f_{ij}(\gamma)\tilde{\phi}_{ij}(x)$$

for every $\gamma \in G_i$ and $x \in \widetilde{U}_i$, and that

$$\begin{array}{ccc}
\widetilde{U}_i & \xrightarrow{\tilde{\phi}_{ij}} & \widetilde{U}_j \\
\downarrow & & \downarrow \\
\widetilde{U}_i/G_i & \xrightarrow{\phi_{ij}=\tilde{\phi}_{ij}/G_i} & \widetilde{U}_j/f_{ij}(G_i) \\
\| & & \downarrow \\
\widetilde{U}_i/G_i & \longrightarrow & \widetilde{U}_j/G_j \\
{\scriptstyle \phi_i}\uparrow{\scriptstyle \wr} & & {\scriptstyle \wr}\uparrow{\scriptstyle \phi_j} \\
U_i & \xrightarrow{\text{inclusion}} & U_j.
\end{array}$$

The space Q is called an orbifold *locally modeled on $\mathbb{R}^n$ modulo finite groups*. An *orbifold with boundary* is a space locally modeled on $\mathbb{R}^n$ modulo finite groups and $\mathbb{R}^n_+$ modulo finite groups. An orbifold is said to be *differentiable* if the group G_i is a finite subgroup of the orthogonal group $O(n)$ acting on $\mathbb{R}^n$, and the local models $\mathbb{R}^n/G_i$ are glued together by a diffeomorphism.

Definition 3.2. A surjective map

$$\pi : Q_0 \longrightarrow Q_1$$

of an orbifold Q_0 onto Q_1 is said to be an *orbifold covering* if the following conditions are satisfied:

(1) The map π induces a surjective continuous map

$$\pi : X(Q_0) \longrightarrow X(Q_1)$$

between the underlying spaces, *which is not generally a covering map of the topological spaces.*

(2) For every $x \in Q_0$, there are an open neighborhood $U \subset Q_0$, an open subset $\widetilde{U} \subset \mathbb{R}^n$, a finite group G_1 and its subgroup $G_0 \subset G_1$ subject to

$$\phi : U \xrightarrow{\sim} \widetilde{U}/G_0$$

and

$$\begin{array}{ccc} U & \xrightarrow{\pi} & \pi(U) \\ \wr\downarrow \phi & & \downarrow \wr \\ \widetilde{U}/G_0 & \longrightarrow & \widetilde{U}/G_1. \end{array}$$

(3) If we start with a point $y \in Q_1$, then there are an open neighborhood $V \subset Q$ of y, an open subset $\widetilde{V} \subset \mathbb{R}^n$, a finite group G_1' and its subgroup $G_0' \subset G_1'$, and a connected component U' of $\pi^{-1}(V) \subset Q_0$ such that

$$\begin{array}{ccc} U' & \xrightarrow{\pi} & V \\ \wr\downarrow & & \downarrow \wr \\ \widetilde{V}/G_0' & \longrightarrow & \widetilde{V}/G_1'. \end{array}$$

If a group G acts on a Riemannian manifold M properly discontinuously by isometries, then

$$\pi : M \longrightarrow M/G$$

is an example of a differentiable covering orbifold.

For every point $x \in Q$, there is a well-defined group G_x associated to it. Let $U = \widetilde{U}/G$ be a local open coordinate neighborhood of $x \in Q$. Then the isotropy subgroup of G that stabilizes any inverse image of x is unique up to conjugation. We define G_x to be this isotropy group. An *orbifold cell-decomposition* of an orbifold is a cell-decomposition of the underlying space $X(Q)$ such that the group G_x is the same along each stratum. We denote by G_C the group associated with a cell C.

Thurston extended the notion of the *Euler characteristic* to orbifolds.

DEFINITION 3.3. If an orbifold Q admits an orbifold cell-decomposition, then we define the *Euler characteristic* by

$$\chi(Q) = \sum_{C:\text{cell}} (-1)^{\dim(C)} \frac{1}{|G_C|}. \tag{3.2}$$

The next theorem gives us a useful method to compute the Euler characteristic.

THEOREM 3.4. *Let*

$$\pi : Q_0 \longrightarrow Q_1$$

be a covering orbifold. We define the sheet number *of the covering π to be the cardinality $k = |\pi^{-1}(y)|$ of the preimage $\pi^{-1}(y)$ of a non-singular point $y \in Q_1$. Then*

$$\chi(Q_1) = \frac{1}{k}\chi(Q_0). \tag{3.3}$$

PROOF. We first observe that for an *arbitrary* point y of Q_1, we have

$$k = \sum_{x:\pi(x)=y} \frac{|G_x|}{|G_y|}.$$

Let

$$Q_1 = \coprod_j C_j$$

be an orbifold cell-decomposition of Q_1, and

$$\pi^{-1}(C_j) = \coprod_i C_{ij}$$

a division of the preimage of C_j into its connected components. Then

$$\begin{aligned} k\chi(Q_1) &= k\sum_j (-1)^{\dim(C_j)} \frac{1}{|G_{C_j}|} \\ &= \sum_j (-1)^{\dim(C_j)} \sum_i \frac{|G_{C_j}|}{|G_{C_{ij}}|} \frac{1}{|G_{C_j}|} \\ &= \sum_{ij} (-1)^{\dim(C_{ij})} \frac{1}{|G_{C_{ij}}|} \\ &= \chi(Q_0). \end{aligned}$$

□

COROLLARY 3.5. *Let G be a finite subgroup of $\mathfrak{S}_n$ that acts on $\mathbb{R}^n_+$ by permutation of the coordinate axes. Then $\mathbb{R}^n_+/G$ is a differentiable orbifold and*

$$\chi\left(\mathbb{R}^n_+/G\right) = \frac{(-1)^n}{|G|}. \tag{3.4}$$

REMARK. We note that in general

$$\chi\left(\mathbb{R}^n_+/G\right) \neq \frac{(-1)^n}{|G|},$$

unless G acts on $\mathbb{R}^n_+$ faithfully.

EXAMPLE 3.1. Let us study the quotient space $\mathbb{R}^n_+/\mathfrak{S}_n$. We denote by

$$\Delta(123\cdots n)$$

the interior of a regular n-hyperhedron of $(n-1)$ dimensions. Thus $\Delta(12)$ is a line segment, $\Delta(123)$ is an equilateral triangle, and $\Delta(1234)$ is a regular tetrahedron. The space $\mathbb{R}^n_+$ is a cone over $\Delta(123\cdots n)$:

$$\mathbb{R}^n_+ = \Delta(123\cdots n) \times \mathbb{R}_+.$$

The closure $\overline{\Delta(123\cdots n)}$ has n vertices $x_1, \cdots, x_n$. Let x_{12} be the midpoint of the line segment $\overline{x_1x_2}$, x_{123} the center of gravity of the triangle $\triangle x_1x_2x_3$, etc., and $x_{123\cdots n}$ the center of gravity of $\Delta(123\cdots n)$.

The $(n-1)$-dimensional region

$$\Delta = \overline{x_1x_{12}x_{123}\cdots x_{123\cdots n}} \tag{3.5}$$

is the fundamental domain of the $\mathfrak{S}_n$-action on $\Delta(123\cdots n)$ by permutation of vertices. Δ can be considered as a cell complex of the orbifold $\mathbb{R}^n_+/\mathfrak{S}_n$. Since the n-hyperhedron does not include the boundary, Δ has only one 0-cell $x_{123\cdots n}$, $\binom{n-1}{1}$ 1-cells

$$\overline{x_1x_{123\cdots n}}$$
$$\overline{x_{12}x_{123\cdots n}}$$

$$\overline{x_{123}x_{123\cdots n}}$$
$$\vdots$$
$$\overline{x_{123\cdots(n-1)}x_{123\cdots n}},$$

$\binom{n-1}{2}$ 2-cells

$$\overline{x_1x_{12}x_{123\cdots n}}$$
$$\overline{x_1x_{123}x_{123\cdots n}}$$
$$\vdots$$
$$\overline{x_{12}x_{123}x_{123\cdots n}}$$
$$\vdots$$
$$\overline{x_{123\cdots(n-2)}x_{123\cdots(n-1)}x_{123\cdots n}},$$

etc. The number of k-cell is $\binom{n-1}{k}$ (Figure 3.1).

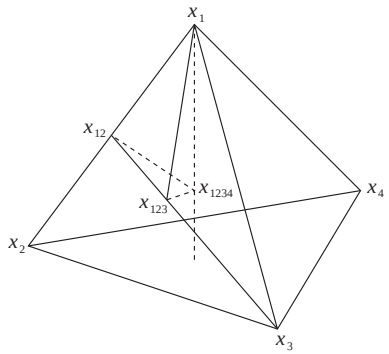

FIGURE 3.1. $\Delta(1234)$

The isotropy group of each cell is easily calculated. For example, the isotropy group of a 2-cell $\overline{x_{12}x_{123}x_{123\cdots n}}$ is

$$\mathfrak{S}(12) \times \mathfrak{S}(456\cdots n),$$

where $\mathfrak{S}(abc\cdots z)$ is the permutation group of the specified letters. The definition of the Euler characteristic (3.2) and the computation using (3.3) gives an interesting combinatorial identity

$$\begin{aligned}\chi\left(\mathbb{R}^n_+/\mathfrak{S}_n\right) &= -\chi\left(\Delta(123\cdots n)/\mathfrak{S}_n\right)\\ &= -\sum_{k=0}^{n-1}(-1)^k \sum_{\substack{m_0+m_1+\cdots+m_k=n\\ m_0\geq 1, m_1\geq 1,\cdots,m_k\geq 1}} \frac{1}{m_0!m_1!\cdots m_k!}\\ &= \frac{(-1)^n}{n!}.\end{aligned} \tag{3.6}$$

The $\mathfrak{S}_n$-action of the cell-decomposition of

$$\Delta(123\cdots n)/\mathfrak{S}_n$$

gives a cell-decomposition of $\Delta(123\cdots n)$ itself, and hence a cell-decomposition of $\mathbb{R}^n_+$. We call this cell-decomposition the *canonical cell-decomposition* of $\mathbb{R}^n_+$, and denote it by $\square(\mathbb{R}^n_+)$. For every subgroup $G \subset \mathfrak{S}_n$, the fixed point set of an element of G is one of the cells of $\square(\mathbb{R}^n_+)$. In particular, $\square(\mathbb{R}^n_+)$ induces a cell-decomposition of the orbifold $\mathbb{R}^n_+/G$, which we call the *canonical orbifold cell-decomposition* of $\mathbb{R}^n_+/G$. We will come back to these canonical orbifold cell-decompositions when we study the space of metric ribbon graphs in the next chapter.

3. The Moduli Space of Pointed Elliptic Curves

An *elliptic curve* E is a quotient group of the complex plane $\mathbb{C}$ by a lattice subgroup $\mathbb{Z}^2$:

$$0 \longrightarrow \mathbb{Z}^2 \xrightarrow{\psi} \mathbb{C} \longrightarrow E \longrightarrow 0.$$

The injective group homomorphism $\psi : \mathbb{Z}^2 \longrightarrow \mathbb{C}$ is determined by its image of the generators $(1,0)$ and $(0,1)$. Let us denote by $\omega = \psi(1,0)$ and $\tau\omega = \psi(0,1)$, where ω is a non-zero complex number, and

$$\tau \in H = \{\tau \in \mathbb{C} \mid Im(\tau) > 0\} \tag{3.7}$$

is an element of the upper half plane. Since the imaginary part of τ is positive, ω and $\tau\omega$ are $\mathbb{R}$-linearly independent in $\mathbb{C}$.

The parameter $\tau \in H$ defines an elliptic curve

$$E_\tau = \frac{\mathbb{C}}{\mathbb{Z}\omega \oplus \mathbb{Z}\tau\omega}. \tag{3.8}$$

The complex structure of E_τ does not depend on the choice of ω, because there is a complex linear automorphism of $\mathbb{C}$ that brings one choice of ω to another. The parameter τ is called the *modular parameter* of an elliptic curve. The elliptic curves E_τ and $E_{\tau'}$ are biholomorphic if and only if there is a fractional linear transformation

$$\tau' = \begin{bmatrix} a & b \\ c & d \end{bmatrix} \cdot \tau = \frac{a\tau + b}{c\tau + d}, \tag{3.9}$$

where

$$\begin{bmatrix} a & b \\ c & d \end{bmatrix} \in PSL(2,\mathbb{Z}).$$

Note that the group $PSL(2,\mathbb{Z})$ acts properly discontinuously on the upper half plane H. Therefore, we can identify the moduli space of elliptic curves as the quotient space $H/PSL(2,\mathbb{Z})$.

Since we have defined an elliptic curve as a quotient abelian group (3.8), it comes with a specific point, namely the identity element $0 \in E_\tau$ of the group. Therefore, the quotient space $H/PSL(2,\mathbb{Z})$ actually represents the moduli space of elliptic curve with one marked point:

$$\mathfrak{M}_{1,1} = H/PSL(2,\mathbb{Z}). \tag{3.10}$$

Indeed, an elliptic curve as an abelian group is an analytic automorphism group of the elliptic curve itself, and this action is transitive. Thus a pointed elliptic curve (E_τ, p_1) is always isomorphic to another pointed elliptic curve (E_τ, p_2) by the translation

$$p_2 - p_1 : E_\tau \ni z \longmapsto z + p_2 - p_1 \in E_\tau.$$

Figure 3.2 shows the fundamental domain of the $PSL_2(\mathbb{Z})$-action on the upper half plane by fractional linear transformations.

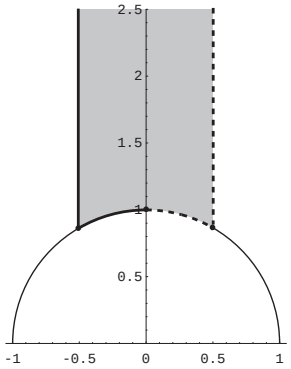

FIGURE 3.2. The Fundamental Domain of $PSL_2(\mathbb{Z})$-Action on H

The complex analytic structure of $\mathfrak{M}_{1,1}$ can be studied by using the *elliptic modular function* $J(\tau)$, which is defined as follows. First, let us define two functions in ω and τ by

$$g_2 = \sum_{\substack{(m,n)\in\mathbb{Z}^2 \\ (m,n)\neq(0,0)}} \frac{60}{(m\omega+n\tau\omega)^4}, \quad \text{and} \quad g_3 = \sum_{\substack{(m,n)\in\mathbb{Z}^2 \\ (m,n)\neq(0,0)}} \frac{140}{(m\omega+n\tau\omega)^6}. \tag{3.11}$$

The ratio

$$J(\tau) = \frac{g_2(\tau)^3}{g_2(\tau)^3 - 27g_3(\tau)^2} \tag{3.12}$$

is a function in one variable τ. The elliptic modular function is a holomorphic mapping

$$J : H \longrightarrow \mathbb{C}$$

which is invariant under the $PSL_2(\mathbb{Z})$-action on H. Thus J induces a canonical bijection

$$\widetilde{J} : H/PSL_2(\mathbb{Z}) \xrightarrow{\sim} \mathbb{C} \tag{3.13}$$

In other words, the elliptic modular function maps the fundamental domain of Figure 3.2 holomorphically onto the entire complex plane $\mathbb{C}$. $J(\tau)$ has a zero of degree 3 at $\tau = e^{\pi i/3}$, and $J(\tau) - 1$ has a zero of degree 2 at $\tau = i$. J maps $i\infty$ to the point at infinity of $\mathbb{P}^1$. Except for these three points i, $e^{\pi i/3}$, and $i\infty$, J has a unique finite value at each point of the fundamental domain and its derivative is non-vanishing. Therefore, the fundamental domain minus two points i and $e^{\pi i/3}$ is mapped *biholomorphically* onto $\mathbb{P}^1$ minus three points:

$$\mathfrak{M}_{1,1} \setminus \{i, e^{\pi i/3}\} \xrightarrow{\sim} \mathbb{P}^1 \setminus \{0, 1, \infty\}.$$

When the complex analytic structure of the moduli space is in question, we *introduce* the holomorphic structure on $\mathfrak{M}_{1,1} = H/PSL_2(\mathbb{Z})$ by the identification $\widetilde{J}$ of (3.13). As an algebraic variety, we *define*

$$\mathfrak{M}_{1,1} = \mathrm{Spec}\mathbb{C}[J]. \tag{3.14}$$

In each case, the underlying topological space is just the real 2-plane $\mathbb{R}^2$.

However, the moduli space $\mathfrak{M}_{1,1}$ has actually a subtler structure, due to the fact that the $PSL_2(\mathbb{Z})$-action on H has fixed points, or equivalently, J^{-1} is not holomorphic at $0 \in \mathbb{C}$ and $1 \in \mathbb{C}$. This subtlety is articulated by the idea of orbifold. Using the elliptic modular function, we can view

$$\mathfrak{M}_{1,1} = \big(\mathbb{P}^1 \setminus \{0, 1, \infty\}\big) \cup U_0/(\mathbb{Z}/2\mathbb{Z}) \cup U_1/(\mathbb{Z}/3\mathbb{Z}), \tag{3.15}$$

where U_p denotes a small open disk of $\mathbb{C}$ centered at a point p. What we have is the complex plane with two *orbifold singularities* at 0 and 1.

To identify the local structure of (3.15) with the quotient $H/PSL_2(\mathbb{Z})$, let us examine the $PSL_2(\mathbb{Z})$-action on the upper half plane H (Figure 3.3).

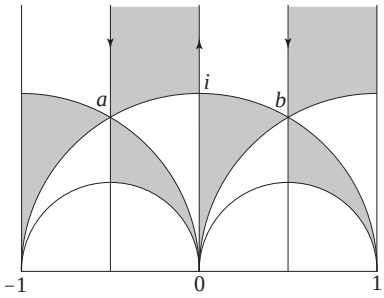

FIGURE 3.3. $PSL_2(\mathbb{Z})$-action on the Upper Half Plane

The boundary of the fundamental domain is glued together in the following way. The vertical line $a + it$ for $t \in [0, \infty)$ is identified with $b + it$, where $a = e^{2\pi i/3}$ and $b = e^{\pi i/3}$. The arc $\overset{\frown}{ai}$ is glued with the arc $\overset{\frown}{bi}$. Thus the resulting orbifold looks as in Figure 3.4.

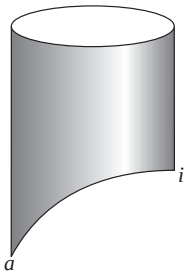

FIGURE 3.4. Orbifold $\mathfrak{M}_{1,1}$

It has two corner-like singularities, corresponding to a and i of Figure 3.3. The isotropy subgroup of $PSL_2(\mathbb{Z})$ that stabilizes i is

$$\left\{ \begin{bmatrix} 1 & \\ & 1 \end{bmatrix}, \begin{bmatrix} & 1 \\ -1 & \end{bmatrix} \right\}.$$

Therefore, the orbifold singularity of $\mathfrak{M}_{1,1}$ at i is modeled on $\mathbb{R}^2/(\mathbb{Z}/2\mathbb{Z})$. Similarly, the singularity a has the isotropy group

$$\left\{ \begin{bmatrix} 1 & \\ & 1 \end{bmatrix}, \begin{bmatrix} 1 & 1 \\ -1 & \end{bmatrix}, \begin{bmatrix} & 1 \\ -1 & -1 \end{bmatrix} \right\},$$

which is modeled on $\mathbb{R}^2/(\mathbb{Z}/3\mathbb{Z})$.

Let us determine the Euler characteristic of $\mathfrak{M}_{1,1}$. The moduli space $\mathfrak{M}_{1,1}$ has an orbifold cell-decomposition consisting of two singularities as 0-cells, two lines $a+it$ and $i+it$ for $t \geq 0$ and the arc $\overset{\frown}{ai}$ as three 1-cells, and two 2-dimensional cells. The isotropy of the cells are already determined, so we conclude

$$\chi\left(\mathfrak{M}_{1,1}\right) = \frac{1}{2} + \frac{1}{3} - 1 - 1 - 1 + 1 + 1 = -\frac{1}{6}. \tag{3.16}$$

Remark. The notion of orbifold is different from *algebraic stack* when there is a group action that is nowhere faithful. The Euler characteristic of $\mathfrak{M}_{1,1}$ as an algebraic stack has been computed by Deligne and Rapoport [**4**]. Their value gives

$$\chi_{\text{stack}}\left(\mathfrak{M}_{1,1}\right) = \zeta(-1) = -\frac{1}{12}. \tag{3.17}$$

The difference between (3.16) and (3.17) is factor 2, which comes from

$$2 = \left| \frac{SL_2(\mathbb{Z})}{PSL_2(\mathbb{Z})} \right|.$$

We will come back to this point later in Chapter 5.

CHAPTER 4

The Space of Metric Ribbon Graphs

The goal of this chapter is to show that the space of all metric ribbon graphs with the fixed Euler characteristic and the number of boundary components forms a differentiable orbifold, and to compute its orbifold Euler characteristic. The metric ribbon graph space can a priori have a complicated singularity, but it will turn out that the space has only the quotient singularities defined by finite group actions on the Euclidean space of a fixed dimension. This characteristic feature is due to the local behavior of deformations of a metric ribbon graph.

The structure of deformations of a metric ribbon graph has a connection to certain questions in computer science. We refer to [**28**] for more discussion on this topic.

1. Contraction and Inflation of Ribbon Graphs

Let $RG_{g,n}$ denote that set of all isomorphism classes of connected ribbon graphs Γ such that

$$\begin{cases} \chi(\Gamma) = v(\Gamma) - e(\Gamma) = 2 - 2g - n \\ b(\Gamma) = n, \end{cases} \tag{4.1}$$

where $v(\Gamma)$ and $e(\Gamma)$ denote the number of vertices and edges of Γ, respectively, and that every vertex has degree at least 3. If an edge E of Γ is incident with two distinct vertices V_1 and V_2, then we can construct another ribbon graph $\Gamma' \in RG_{g,n}$ with

$$e(\Gamma') = e(\Gamma) - 1 \qquad \text{and} \qquad v(\Gamma') = v(\Gamma) - 1 \tag{4.2}$$

by removing E from Γ and putting V_1 and V_2 together. The ribbon graph Γ' is a *contraction* of Γ. The *partial ordering* of $RG_{g,n}$ is defined by

$$\Gamma' \prec \Gamma \tag{4.3}$$

when Γ' is a contraction of Γ, and by extending this relation with the transitivity law

$$\Gamma'' \prec \Gamma' \quad \text{and} \quad \Gamma' \prec \Gamma \Longrightarrow \Gamma'' \prec \Gamma.$$

Since contraction decreases the number of edges and vertices by one, a graph with only one vertex is a minimal graph with respect to this partial ordering, and a degree 3 graph (a graph with only degree 3 vertices), or a *trivalent* graph, is a maximal element of $RG_{g,n}$. Every graph can be obtained by contraction of a degree 3 graph.

The inverse operation of contraction of a ribbon graph is the *inflation*. Every vertex of degree $d \geq 4$ of a ribbon graph Γ can be *inflated* by adding a new edge as shown in Figure 4.1. The arrows represent the contraction.

Let Γ be a ribbon graph and $\Gamma_{\mathcal{E}}$ the edge-refinement of Γ (see Section 1 of Chapter 2). The edges of $\Gamma_{\mathcal{E}}$ are the half-edges of Γ. In the process of inflation, we

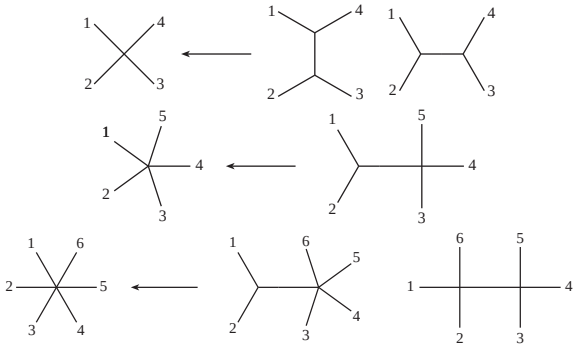

FIGURE 4.1. Inflation of Vertices

identify two ways of inflation if there is a ribbon graph isomorphism from one to the other that preserves all the original half-edges of the graph. Thus when we inflate a vertex of degree $d \geq 4$, there are $d(d-3)/2$ ways of inflating it by adding an edge. The situation is easier to understand by looking at the *dual graph* of Figure 4.2, where the arrows are again the contraction map.

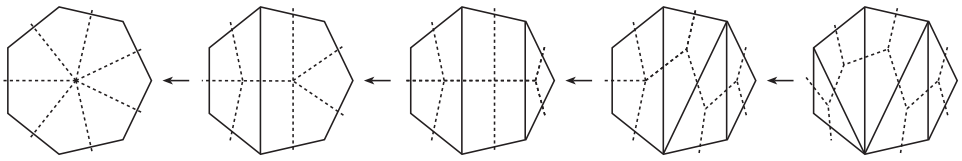

FIGURE 4.2. Inflation of a Vertex of Degree 7 and its Dual Graph

Consider a ribbon graph $*_d$ with a vertex of degree $d \geq 4$ and d half-edges labeled by numbers 1 through d. The dual graph to $*_d$ is a convex polygon with d sides. The process of inflation by adding an edge at the vertex of $*_d$ corresponds to drawing a diagonal line of the d-gon of Figure 4.2. The number $d(d-3)/2$ corresponds to the number of diagonals in a convex d-gon. Inflating the graph further corresponds to adding another diagonal to the polygon in such a way that the added diagonal does not intersect with the original diagonal except at the vertices of the polygon. The inflation process terminates after $d-3$ inflations, because only this much non-intersecting diagonals can be placed in a convex d-gon. Note that the maximal inflation is trivalent at the internal vertices, and its dual defines a triangulation of the polygon. The number of all triangulations of the d-gon is equal to

$$\frac{1}{d-1}\binom{2d-4}{d-2},$$

which is the *Catalan number* (see [**7**], Chapter 20).

2. Space of Metric Ribbon Graphs as an Orbifold

A *metric* ribbon graph is a ribbon graph with a positive real number assigned to each edge. The assigned real number of an edge is called the *length* of the edge.

For a ribbon graph $\Gamma \in RG_{g,n}$, the space of metric ribbon graphs with Γ as the underlying graph is a differentiable orbifold

$$\frac{\mathbb{R}_+^{e(\Gamma)}}{\mathrm{Aut}(\Gamma)}, \tag{4.4}$$

where the action of $\mathrm{Aut}(\Gamma)$ on $\mathbb{R}_+^{e(\Gamma)}$ is through the natural homomorphism

$$\phi : \mathrm{Aut}(\Gamma) \longrightarrow \mathfrak{S}_{e(\Gamma)}. \tag{4.5}$$

We have shown that the above homomorphism ϕ fails to be injective if and only if Γ is an exceptional graph. Therefore, for an exceptional graph Γ_{ex}, we have

$$\frac{\mathbb{R}_+^{e(\Gamma_{\mathrm{ex}})}}{\mathrm{Aut}(\Gamma_{\mathrm{ex}})} = \frac{\mathbb{R}_+^{e(\Gamma_{\mathrm{ex}})}}{\mathrm{Aut}(\Gamma_{\mathrm{ex}})/(\mathbb{Z}/2\mathbb{Z})}, \tag{4.6}$$

because the factor $\mathbb{Z}/2\mathbb{Z}$ acts trivially on $\mathbb{R}_+^{e(\Gamma_{\mathrm{ex}})}$ (see Section 3 of Chapter 2).

For integers g and n subject to

$$\begin{cases} g \geq 0 \\ n \geq 1 \\ 2-2g-n < 0, \end{cases} \tag{4.7}$$

we define the space of all metric ribbon graphs satisfying the topological condition (4.1) by

$$RG_{g,n}^{\mathrm{met}} = \coprod_{\Gamma \in RG_{g,n}} \frac{\mathbb{R}_+^{e(\Gamma)}}{\mathrm{Aut}(\Gamma)}. \tag{4.8}$$

The purpose of this section is to show that $RG_{g,n}^{\mathrm{met}}$ has the natural structure of a differentiable orbifold. Each piece (4.4) of (4.8) is called a *rational cell* of $RG_{g,n}^{\mathrm{met}}$. The rational cells are glued together by the contraction operation of ribbon graphs in an obvious way. A rational cell has a natural quotient topology.

Let us compute the dimension of $RG_{g,n}^{\mathrm{met}}$. We denote by $v_j(\Gamma)$ the number of vertices of a ribbon graph Γ of degree j. Since these numbers satisfy

$$\begin{aligned} -(2-2g-n) &= -v(\Gamma) + e(\Gamma) \\ &= -\sum_{j\geq 3} v_j(\Gamma) + \frac{1}{2}\sum_{j\geq 3} j v_j(\Gamma) \\ &= \sum_{j\geq 3}\left(\frac{j}{2}-1\right) v_j(\Gamma), \end{aligned}$$

the number $e(\Gamma)$ of edges takes its maximum value when all vertices have degree 3. In that case,

$$3v(\Gamma) = 2e(\Gamma)$$

holds, and we have

$$\dim(RG_{g,n}^{\mathrm{met}}) = \max_{\Gamma \in RGg,n}(e(\Gamma)) = 6g-6+3n. \tag{4.9}$$

To prove that $RG_{r,s}^{\mathrm{met}}$ is a differentiable orbifold, we need to show that for every element $\Gamma_{\mathrm{met}} \in RG_{r,s}^{\mathrm{met}}$, there is an open neighborhood $U_\epsilon(\Gamma_{\mathrm{met}})$ of Γ_{met}, an

open disk $\widetilde{U}_\epsilon(\Gamma_{\rm met}) \subset \mathbb{R}^{6g-6+3n}$, and a finite group G_Γ acting on $\widetilde{U}_\epsilon(\Gamma_{\rm met})$ by an orthogonal transformation such that

$$\widetilde{U}_\epsilon(\Gamma_{\rm met})/G_\Gamma \cong U_\epsilon(\Gamma_{\rm met}).$$

DEFINITION 4.1. Let $\Gamma_{\rm met} \in RG^{\rm met}_{g,n}$ be a metric ribbon graph, and $\epsilon > 0$ a positive number smaller than the half of the length of the shortest edge of $\Gamma_{\rm met}$. The *ϵ-neighborhood* $U_\epsilon(\Gamma_{\rm met})$ of $\Gamma_{\rm met}$ in $RG^{\rm met}_{g,n}$ is the set of all metric ribbon graphs $\Gamma'_{\rm met}$ that satisfy the following conditions:

(1) $\Gamma \preceq \Gamma'$.
(2) The edges of $\Gamma'_{\rm met}$ that are contracted in $\Gamma_{\rm met}$ have length less than ϵ.
(3) Let E' be a non-contracting edge of $\Gamma'_{\rm met}$ that corresponds to an edge E of $\Gamma^{\rm met}$. Then the length L' of E' is in the range of
$$L - \epsilon < L' < L + \epsilon,$$
where L is the length of E.

REMARK. Since $\epsilon < L/2$, the edge E' has length $L' > \epsilon$.

The topology of the space $RG^{\rm met}_{g,n}$ is defined by these ϵ-neighborhoods.

DEFINITION 4.2. Let $\Gamma \in RG_{g,n}$ be a ribbon graph and $\Gamma_{\mathcal{E}}$ its edge-refinement. We choose a labeling of all edges of $\Gamma_{\mathcal{E}}$, i.e., the half-edges of Γ. The set $X_{\succeq\Gamma}$ consists of Γ itself and all its inflations. Two inflations are identified if there is a ribbon graph isomorphism of one inflation to the other that preserves all the original half-edges coming from $\Gamma_{\mathcal{E}}$. The *space of metric inflations* of Γ, which is denoted by $X^{\rm met}_{\succeq\Gamma}$, is the set of all graphs in $X_{\succeq\Gamma}$ with metric on each edge.

DEFINITION 4.3. The *codimension* of $\Gamma \in RG_{g,n}$ is the integer

$$\mathrm{codim}(\Gamma) = 6g - 6 + 3n - e(\Gamma).$$

To understand the structure of $X^{\rm met}_{\succeq\Gamma}$, let us consider the inflation process of a vertex of degree $d \geq 4$. Since inflation is essentially a local operation, we can obtain the whole picture out of it. Let $*_d$ denote the tree graph consisting of a single vertex of degree d with d half-edges attached to it. Although $*_d$ is not the type of ribbon graphs we are considering, we can define the space $X^{\rm met}_{\succeq *_d}$ of metric inflations of $*_d$ in the same way as in Definition 4.2. Since the edges of $*_d$ correspond to half-edges of our ribbon graphs, we do not assign any metric to them. Thus $\dim(X^{\rm met}_{\succeq *_d}) = d-3$. As we have noted in Figure 4.2, the inflation process of $*_d$ can be more effectively visualized by the dual polygon. A maximal inflation corresponds to a triangulation of the starting d-gon by non-intersecting diagonals. Since there are $d-3$ additional edges in the maximal inflation tree graph, each maximal graph determines the space $\mathbb{R}_+^{d-3}$ of metric trees. There is a set of $d-4$ non-intersecting diagonals in the d-gon that is obtained by removing one diagonal from a triangulation T_1 of the d-gon, or removing another diagonal from another triangulation T_2. The transformation of the tree graph corresponding to T_1 to the tree corresponding to T_2 is the so-called *fusion move*. If we consider the trivalent trees as *binary trees*, then the fusion move is known as *rotation* [**28**].

Two $(d-3)$-dimensional cells are glued together along a $(d-4)$-dimensional cell. The number of $(d-3)$-dimensional cells in $X_{\succeq *_d}$ is equal to the Catalan number

$$\frac{1}{d-1}\binom{2d-4}{d-2}.$$

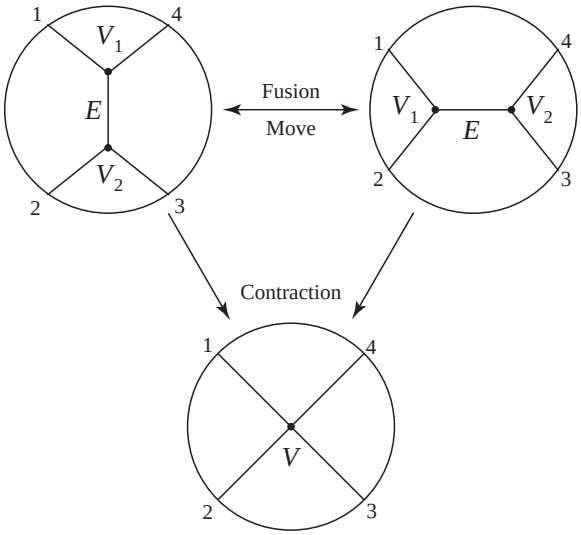

FIGURE 4.3. Fusion Move

THEOREM 4.4. *The space $X^{\mathrm{met}}_{\succeq *_d}$ is homeomorphic to $\mathbb{R}^{d-3}$, and its combinatorial structure defines a cell-decomposition of $\mathbb{R}^{d-3}$, where each cell is a convex cone with vertex at the origin. The origin is the only 0-cell of the cell complex and is corresponding to the graph $*_d$.*

The group $\mathbb{Z}/d\mathbb{Z}$ acts on $X^{\mathrm{met}}_{\succeq *_d}$ through orthogonal transformation with respect to the natural Euclidean structure of $\mathbb{R}^{d-3}$.

REMARK. In the reference [**28**], the rotation distance between the top dimensional cells of $X^{\mathrm{met}}_{\succeq *_d}$ is studied in terms of hyperbolic geometry. The research in this direction has a close relation to the structure of binary search trees.

PROOF. Draw a convex d-gon on the xy plane of the coordinate $\mathbb{R}^3$ with vertical axis z. Let $\mathcal{V}$ be the set of vertices of the d-gon, and consider the set of all functions

$$f : \mathcal{V} \longrightarrow \mathbb{R}.$$

An element $f \in \mathbb{R}^{\mathcal{V}} = \mathbb{R}^d$ is visualized by its function graph

$$Graph(f) = \{(V, f(V)) \mid V \in \mathcal{V}\} \subset \mathbb{R}^3. \tag{4.10}$$

$Graph(f)$ is the set of d points in $\mathbb{R}^3$ such that its projection image onto the xy plane is the vertex set $\mathcal{V}$. Let us denote by $CH(Graph(f))$ the convex hull of $Graph(f)$ in $\mathbb{R}^3$. If we view the convex hull from the top, it is a d-gon with a set of non-intersecting diagonals.

Viewing the convex hull from the positive direction of the z-axis, we obtain a map

$$\xi : \mathbb{R}^{\mathcal{V}} \longrightarrow X_{\succeq *_d}, \tag{4.11}$$

where we identify $X_{\succeq *_d}$ with the set of arrangements of non-intersecting diagonals of the convex d-gon. A generic point of $\mathbb{R}^{\mathcal{V}}$ corresponds to a triangulation of the d-gon as in Figure 4.4, but special points give fewer number of diagonals on the d-gon. For example, if f is a constant function, then the function graph $Graph(f)$

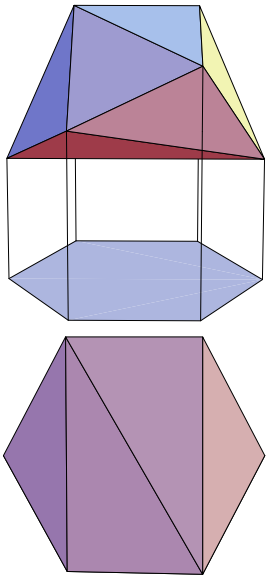

FIGURE 4.4. The Convex Hull of the Function Graph of $f \in \mathbb{R}^{\mathcal{V}}$ and its View from the Top

is flat and the top view of its convex hull is just the d-gon without any diagonals in sight.

This consideration leads us to note that the map ξ factors through

$$\begin{array}{ccc} \mathbb{R}^{\mathcal{V}} & \xrightarrow{pr} & \frac{\mathbb{R}^{\mathcal{V}}}{\text{Affine}(\mathbb{R}^2,\mathbb{R})} \\ \| & & \downarrow \eta \\ \mathbb{R}^{\mathcal{V}} & \xrightarrow{\xi} & X_{\succeq *_d}, \end{array} \tag{4.12}$$

where

$$\text{Affine}(\mathbb{R}^2, \mathbb{R}) \cong \mathbb{R}^3$$

is the space of affine maps of $\mathbb{R}^2$ to $\mathbb{R}$. Such an affine map induces a map of $\mathcal{V}$ to $\mathbb{R}$, but the image is flat and no diagonals are produced in the d-gon.

The map η of (4.12) is surjective, because we can explicitly construct a function f that corresponds to an arbitrary element of $X_{\succeq *_d}$. We also note that the inverse image of m-diagonal arrangement $(0 \leq m \leq d-3)$ is a cone of dimension m with vertex at the origin. It is indeed a convex cone, because if two points of

$$\frac{\mathbb{R}^{\mathcal{V}}}{\text{Affine}(\mathbb{R}^2, \mathbb{R})} = \mathbb{R}^{d-3} \tag{4.13}$$

correspond to the same diagonal arrangement of $X_{\succeq *_d}$, then every point on the line segment connecting these two points corresponds to the same arrangement. To see this, let $\mathcal{V} = \{V_1, V_2, \cdots, V_d\}$, and let a function $f \in \mathbb{R}^{\mathcal{V}}$ satisfy

$$f(V_{d-2}) = f(V_{d-1}) = f(V_d) = 0.$$

Then f can be thought of an element of the quotient space (4.13). Take two such functions f and g that correspond to the same m-diagonal arrangement of the d-gon. The line segment connecting these two functions is

$$h_t = f + t(g - f), \tag{4.14}$$

where $0 \leq t \leq 1$. This means that the point $h_t(V_j) \in \mathbb{R}^3$ is on the vertical line segment connecting $f(V_j)$ and $g(V_j)$ for all $j = 1, 2, 3, \cdots, d-3$. Thus the top roof of the convex hull $CH(Graph(h_t))$ determines the same arrangement of the diagonals on the d-gon as $CH(Graph(f))$ and $CH(Graph(g))$ do.

Since the inverse image of an m-diagonal arrangement is an m-dimensional convex cone, it is homeomorphic to $\mathbb{R}^m_+$. Hence $X_{\succeq *_d}$ defines a cell-decomposition of $\mathbb{R}^{d-3}$, which is homeomorphic to $X^{\mathrm{met}}_{\succeq *_d}$, as claimed.

The convex d-gon on the plane can be taken as a regular d-gon centered at the origin. The cyclic group $\mathbb{Z}/d\mathbb{Z}$ naturally acts on $\mathcal{V}$ by a rotation. This action induces an action on $\mathbb{R}^{\mathcal{V}}$ through permutation of axes, which is an orthogonal transformation with respect to the standard Euclidean structure of $\mathbb{R}^d$. A rotation of $\mathcal{V}$ induces a rotation of the horizontal plane $\mathbb{R}^2$, thus the space of affine maps of $\mathbb{R}^2$ to $\mathbb{R}$ is invariant under the $\mathbb{Z}/d\mathbb{Z}$-action. Therefore, the cyclic group acts on the quotient space $\mathbb{R}^{d-3}$.

Let $\mathrm{Affine}(\mathbb{R}^2, \mathbb{R})^\perp$ denote the orthogonal complement of $\mathrm{Affine}(\mathbb{R}^2, \mathbb{R})$ in $\mathbb{R}^{\mathcal{V}}$. Since $\mathrm{Affine}(\mathbb{R}^2, \mathbb{R})$ is invariant under the finite group $\mathbb{Z}/d\mathbb{Z}$ of orthogonal transformations, the action descends to the orthogonal complement $\mathrm{Affine}(\mathbb{R}^2, \mathbb{R})^\perp$. Thus $\mathbb{Z}/d\mathbb{Z}$ acts on

$$X^{\mathrm{met}}_{\succeq *_d} \cong \mathrm{Affine}(\mathbb{R}^2, \mathbb{R})^\perp \cong \mathbb{R}^{d-3}$$

by an orthogonal transformation with respect to its natural Euclidean structure.

This completes the proof. □

Example 4.1. The space of metric inflations of a vertex of degree 5 is a cell-decomposed plane. There are five 1-cells and also five 2-cells arranged like a cherry blossom (Figure 4.5). The arrows indicate the contraction. Each of the 2-cells has two boundary components, and two 1-cells are attached to the boundary. Two 2-cells have one boundary in common, and the boundary is attached to a 1-cell. The five 1-cells are glued together at the origin. The space of metric inflations covers the whole plane.

The rotation of the central pentagon through the angle $2\pi/5$ induces the rotation of the angle $4\pi/5$ of the plane.

Example 4.2. The space of metric inflations of a vertex of degree 6 is a cell-decomposed $\mathbb{R}^3$. There are nine 1-cells, twenty-one 2-cells, and fourteen 3-cells. In Figure 4.6, the line going down to the left is the x-axis, the line going down to the right is the y-axis, and the vertical line is the z-axis. The $\mathbb{Z}/6\mathbb{Z}$-action on $\mathbb{R}^3$ is generated by the orthogonal transformation

$$\begin{pmatrix} -\frac{1}{2} & 0 & \frac{\sqrt{3}}{2} \\ 0 & -1 & 0 \\ -\frac{\sqrt{3}}{2} & 0 & -\frac{1}{2} \end{pmatrix}.$$

Theorem 4.5. *Let $\Gamma \in RG_{g,n}$. Then*

$$X^{\mathrm{met}}_{\succeq \Gamma} \cong \mathbb{R}^{e(\Gamma)}_+ \times \mathbb{R}^{\mathrm{codim}(\Gamma)}. \tag{4.15}$$

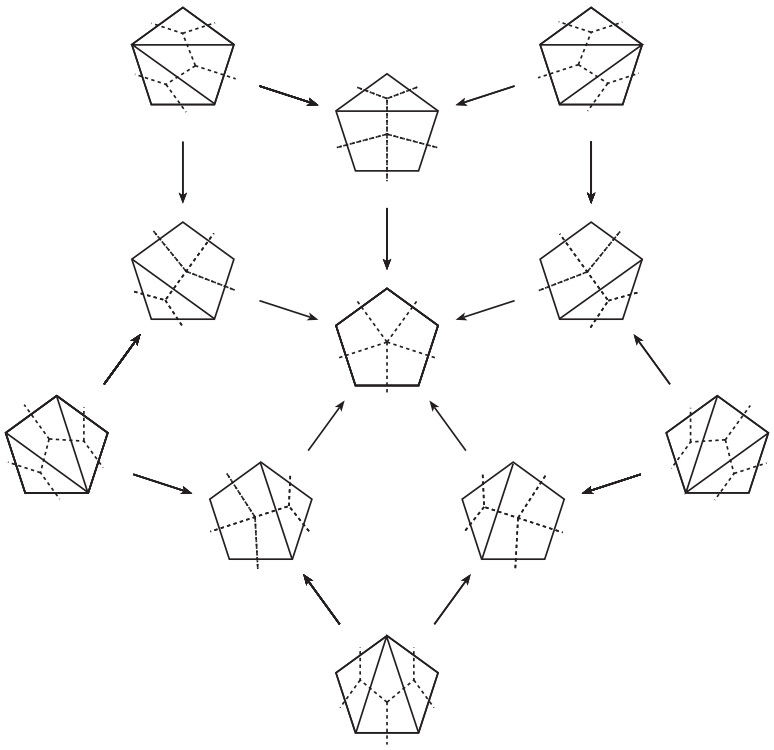

FIGURE 4.5. The Space of Metric Inflations of a Vertex of Degree 5

The combinatorial structure of $X^{\mathrm{met}}_{\succeq\Gamma}$ *determines a cell-decomposition of* $\mathbb{R}_+^{e(\Gamma)} \times \mathbb{R}^{\mathrm{codim}(\Gamma)}$. *The group* $\mathrm{Aut}(\Gamma)$ *acts on* $X_{\succeq\Gamma}$ *by automorphism of a cell complex, which is an orthogonal transformation with respect to the natural Euclidean structure of* $X^{\mathrm{met}}_{\succeq\Gamma}$ *via the homeomorphism (4.15). The action of* $\mathrm{Aut}(\Gamma)$ *on the metric edge space* $\mathbb{R}_+^{e(\Gamma)}$ *may be non-faithful (when* Γ *is exceptional), but its action on* $\mathbb{R}^{\mathrm{codim}(\Gamma)}$ *is always faithful except for the case* $(g,n) = (1,1)$.

PROOF. The inflation process of Γ takes place at each vertex of degree 4 or more. Since we identify inflations only when there is an isomorphism fixing all original half-edges coming from Γ, the inflation can be done independently at each vertex. Let $*(1), \cdots, *(v)$ be the list of vertices of Γ and d_j the degree of $*(j)$. We arrange the degree sequence of Γ as

$$(\overbrace{3,3,\cdots,3}^{n_3\text{-times}},\overbrace{4,4,\cdots,4}^{n_4\text{-times}},\cdots,\overbrace{m,m,\cdots,m}^{n_m\text{-times}}).$$

Note that

$$n_3 + n_4 + \cdots + n_m = v$$

is the number of vertices of Γ. Then

$$X^{\mathrm{met}}_{\succeq\Gamma} = \mathbb{R}_+^{e(\Gamma)} \times \prod_{j=1}^{v} X^{\mathrm{met}}_{\succeq *(j)},$$

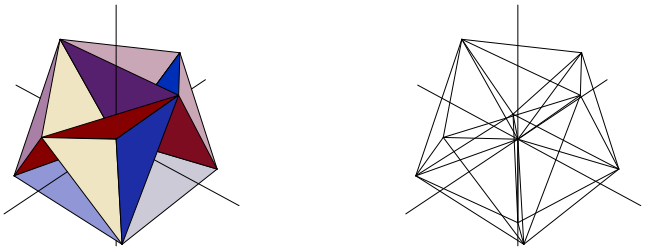

FIGURE 4.6. The Space of Metric Inflations of a Vertex of Degree 6

and the second factor is homeomorphic to

$$\prod_{j=1}^{v} X^{\mathrm{met}}_{\succeq *(j)} \cong \prod_{\mu=3}^{m} \left(\mathbb{R}^{\mu-3}\right)^{n_\mu} = \mathbb{R}^{\mathrm{codim}(\Gamma)},$$

because $X^{\mathrm{met}}_{\succeq *(j)}$ is a single point if the jth vertex has degree 3.

The group

$$G(\Gamma) = \prod_{\mu=3}^{m} \mathfrak{S}_{n_\mu} \rtimes \mathbb{Z}/\mu\mathbb{Z}$$

acts on $\prod_{j=1}^{v} X^{\mathrm{met}}_{\succeq *(j)}$ through an orthogonal transformation in the natural way because each factor $\mathbb{Z}/\mu\mathbb{Z}$ acts on $X^{\mathrm{met}}_{\succeq *(j)}$ through an orthogonal transformation if $d_j = \mu$, and the symmetric group $\mathfrak{S}_{n_\mu}$ acts on $\left(\mathbb{R}^{\mu-3}\right)^{n_\mu}$ by permutation of factors, which is also an orthogonal transformation.

Since $\mathrm{Aut}(\Gamma)$ is a subgroup of $G(\Gamma)$, it acts on $\prod_{j=1}^{v} X^{\mathrm{met}}_{\succeq *(j)}$ through an orthogonal transformation. It's action on $\mathbb{R}_+^{e(\Gamma)}$ is by permutation of axes, thus it is also orthogonal if we embed $\mathbb{R}_+^{e(\Gamma)}$ into $\mathbb{R}^{e(\Gamma)}$ in the natural way. Therefore, $\mathrm{Aut}(\Gamma)$ acts on $X^{\mathrm{met}}_{\succeq \Gamma}$ through an orthogonal transformation with respect to the natural Euclidean structure of $X^{\mathrm{met}}_{\succeq \Gamma}$.

The action of $\mathrm{Aut}(\Gamma)$ on $\mathbb{R}^{\mathrm{codim}(\Gamma)}$ is faithful because all half-edges of Γ are labeled in $X^{\mathrm{met}}_{\succeq \Gamma}$, except for the case $(g,n) = (1,1)$. There are only two graphs in $RG_{1,1}$, and both are exceptional. Thus $\mathrm{Aut}(\Gamma)$-action on $X^{\mathrm{met}}_{\succeq \Gamma}$ has a redundant factor $\mathbb{Z}/2\mathbb{Z}$ for $RG_{1,1}$. This completes the proof. □

A cell complex like $RG^{\mathrm{met}}_{g,n}$ does not have to be an orbifold in general, because it can have more complicated singularities than an orbifold. For example, we can

glue one 0-cell, six $\mathbb{R}_+$'s, and twelve $\mathbb{R}^2_+$'s to form the singular real algebraic variety of Figure 4.7.

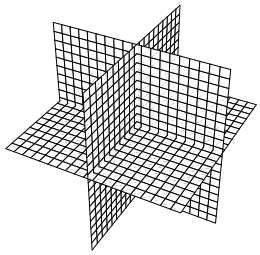

FIGURE 4.7. Cell-Decomposition of A Singular Variety

The space of metric ribbon graphs $RG^{\mathrm{met}}_{g,n}$ does not have this type of singularities. In fact, the worst singularity it has is modeled by the quotient space of $\mathbb{R}^{6g-6+3n}$ by a finite group action. For every codimension 1 rational cell, there are only up to two top dimensional pieces glued together. Thus the situation of Figure 4.7, where four top dimensional cells are glued to one codimension 1 cell, does not happen in our graph complex. This is because a codimension 1 piece corresponds to a ribbon graph with all vertices of degree 3 except for one vertex of degree 4. There are only two inflations for this graph, which means only (up to) two top dimensional rational cells are glued to this piece.

THEOREM 4.6. *The space*

$$RG^{\mathrm{met}}_{g,n} = \coprod_{\Gamma \in RG_{g,n}} \frac{\mathbb{R}_+^{e(\Gamma)}}{\mathrm{Aut}(\Gamma)}$$

of metric ribbon graphs is a differentiable orbifold locally modeled by

$$\frac{X^{\mathrm{met}}_{\succeq \Gamma}}{\mathrm{Aut}(\Gamma)}. \tag{4.16}$$

PROOF. For every ribbon graph $\Gamma \in RG_{g,n}$, there is a natural map

$$\widetilde{\mu}_\Gamma : X^{\mathrm{met}}_{\succeq \Gamma} \longrightarrow RG^{\mathrm{met}}_{g,n}, \tag{4.17}$$

assigning to each metric inflation of Γ its isomorphism class as a metric ribbon graph. Since the $\mathrm{Aut}(\Gamma)$-action on $X^{\mathrm{met}}_{\succeq \Gamma}$ induces ribbon graph isomorphism, the map (4.17) factors through the map μ_Γ of the quotient space:

$$X^{\mathrm{met}}_{\succeq \Gamma} \longrightarrow \frac{X^{\mathrm{met}}_{\succeq \Gamma}}{\mathrm{Aut}(\Gamma)} \xrightarrow{\mu_\Gamma} RG^{\mathrm{met}}_{g,n}. \tag{4.18}$$

The inverse image $\widetilde{\mu}_\Gamma^{-1}(U_\epsilon(\Gamma_{\mathrm{met}}))$ of the ϵ-neighborhood $U_\epsilon(\Gamma_{\mathrm{met}})$ is an open subset of $X^{\mathrm{met}}_{\succeq \Gamma}$ that is homeomorphic to a disk. We claim that

$$\mu_\Gamma : \frac{\widetilde{\mu}_\Gamma^{-1}(U_\epsilon(\Gamma_{\mathrm{met}}))}{\mathrm{Aut}(\Gamma)} \xrightarrow{\sim} U_\epsilon(\Gamma_{\mathrm{met}}) \tag{4.19}$$

is a homeomorphism for every metric ribbon graph Γ_{met} if $\epsilon > 0$ is chosen sufficiently small compared to the shortest edge length of Γ_{met}.

Take a point $\Gamma^0_{\mathrm{met}} \in U_\epsilon(\Gamma_{\mathrm{met}})$, and let

$$\Gamma^j_{\mathrm{met}} \in \widetilde{\mu}_\Gamma^{-1}(\Gamma^0_{\mathrm{met}}), \qquad j = 1, 2,$$

be its inverse images. The ribbon graph isomorphism $\widetilde{\alpha}$ that brings Γ^1_{met} to Γ^2_{met} preserves the set K of contracting edges. Since Γ^j_{met} modulo the contracting edges K is the graph Γ_{met}, $\widetilde{\alpha}$ induces an automorphism $\alpha \in \mathrm{Aut}(\Gamma)$. Thus $\widetilde{\alpha}$ factors into the product of an automorphism α of Γ and a permutation of K. As an element of $X^{\mathrm{met}}_{\succeq\Gamma}$, a permutation of elements of contracting edges in K does not create any difference. Thus Γ^2_{met} is an α-image of Γ^1_{met} in $X^{\mathrm{met}}_{\succeq\Gamma}$. This shows that (4.19) is a natural bijection.

Since the topology of the space of metric ribbon graphs is determined by these ϵ-neighborhoods, the map μ_Γ is continuous. Thus for a small enough ϵ, we have a homeomorphism (4.19).

The metric ribbon graph space is covered by local coordinate patches

$$\bigcup_{\Gamma \in RG^{\mathrm{met}}_{g,n}} \mu_\Gamma \left(\frac{\widetilde{\mu}_\Gamma^{-1}(U_\epsilon(\Gamma_{\mathrm{met}}))}{\mathrm{Aut}(\Gamma)} \right) = RG^{\mathrm{met}}_{g,n}, \tag{4.20}$$

where

$$\frac{\widetilde{\mu}_\Gamma^{-1}(U_\epsilon(\Gamma_{\mathrm{met}}))}{\mathrm{Aut}(\Gamma)} \subset \frac{X^{\mathrm{met}}_{\succeq\Gamma}}{\mathrm{Aut}(\Gamma)}$$

is a differentiable orbifold. Let

$$\Gamma''_{\mathrm{met}} \in \mu_\Gamma \left(\frac{\widetilde{\mu}_\Gamma^{-1}(U_\epsilon(\Gamma_{\mathrm{met}}))}{\mathrm{Aut}(\Gamma)} \right) \cap \mu_{\Gamma'} \left(\frac{\widetilde{\mu}_{\Gamma'}^{-1}(U_\epsilon(\Gamma'_{\mathrm{met}}))}{\mathrm{Aut}(\Gamma')} \right)$$

be a metric ribbon graph in the intersection of two coordinate patches. Then $\Gamma'' \succeq \Gamma$ and $\Gamma'' \succeq \Gamma'$. There is a small δ such that

$$\mu_{\Gamma''} \left(\frac{\widetilde{\mu}_{\Gamma''}^{-1}(U_\delta(\Gamma''_{\mathrm{met}}))}{\mathrm{Aut}(\Gamma'')} \right) \subset \mu_\Gamma \left(\frac{\widetilde{\mu}_\Gamma^{-1}(U_\epsilon(\Gamma_{\mathrm{met}}))}{\mathrm{Aut}(\Gamma)} \right) \cap \mu_{\Gamma'} \left(\frac{\widetilde{\mu}_{\Gamma'}^{-1}(U_\epsilon(\Gamma'_{\mathrm{met}}))}{\mathrm{Aut}(\Gamma')} \right).$$

If we label the edges of Γ'' that are not contracting in Γ, then we have an embedding

$$X^{\mathrm{met}}_{\succeq\Gamma''} \subset X^{\mathrm{met}}_{\succeq\Gamma}$$

that induces

$$\frac{\widetilde{\mu}_{\Gamma''}^{-1}(U_\delta(\Gamma''_{\mathrm{met}}))}{\mathrm{Aut}(\Gamma'')} \subset \frac{\widetilde{\mu}_\Gamma^{-1}(U_\epsilon(\Gamma_{\mathrm{met}}))}{\mathrm{Aut}(\Gamma)}.$$

These inclusion maps are injective diffeomorphisms with respect to the natural differentiable structure of $X^{\mathrm{met}}_{\succeq\Gamma}$. The same is true for Γ'' and Γ'. This implies that the local coordinate neighborhoods of (4.20) are patched together by diffeomorphisms. This completes the proof. □

Remark. The local map μ_Γ of (4.19) is not a homeomorphism if ϵ takes a large value. In particular,

$$\frac{X^{\mathrm{met}}_{\succeq\Gamma}}{\mathrm{Aut}(\Gamma)}$$

does not map injectively to $RG^{\mathrm{met}}_{g,n}$ via the natural map μ_Γ.

THEOREM 4.7. *The Euler characteristic of $RG^{\mathrm{met}}_{g,n}$ as an orbifold is given by*

$$\chi(RG^{\mathrm{met}}_{g,n}) = \sum_{\Gamma\in RG_{g,n}} \frac{(-1)^{e(\Gamma)}}{|\mathrm{Aut}(\Gamma)|}, \qquad (g,n)\neq(1,1). \tag{4.21}$$

For $(g,n)=(1,1)$, we have

$$\chi(RG^{\mathrm{met}}_{1,1}) = \sum_{\Gamma\in RG_{1,1}} \frac{(-1)^{e(\Gamma)}}{|\mathrm{Aut}(\Gamma)|/2} = -\frac{1}{3}+\frac{1}{2}=\frac{1}{6}. \tag{4.22}$$

PROOF. Since the $\mathrm{Aut}(\Gamma)$-action on $\mathbb{R}^{e(\Gamma)}_+$ is through the representation

$$\mathrm{Aut}(\Gamma)\longrightarrow \mathfrak{S}_{e(\Gamma)},$$

we have the canonical orbifold cell-decomposition of $\mathbb{R}^{e(\Gamma)}_+/\mathrm{Aut}(\Gamma)$ defined in Example 3.1. Gluing all these canonical cell-decompositions of the rational cells of the orbifold $RG^{\mathrm{met}}_{g,n}$, we obtain an orbifold cell-decomposition of the entire space $RG^{\mathrm{met}}_{g,n}$. To determine the isotropy subgroups of each orbifold cell, we need the local model (4.19). We note that $\mathrm{Aut}(\Gamma)$-action on $\widetilde{\mu}_\Gamma^{-1}(U_\epsilon(\Gamma_{\mathrm{met}}))$ is faithful if $(g,n)\neq(1,1)$.

If $\mathrm{Aut}(\Gamma)$ acts on $\mathbb{R}^{e(\Gamma)}_+$ faithfully, then the contribution of the rational cell $\mathbb{R}^{e(\Gamma)}_+/\mathrm{Aut}(\Gamma)$ to the Euler characteristic of $RG^{\mathrm{met}}_{g,n}$ is

$$\frac{(-1)^{e(\Gamma)}}{|\mathrm{Aut}(\Gamma)|}.$$

But if Γ is exceptional, then the rational cell

$$\frac{\mathbb{R}^{e(\Gamma)}_+}{\mathrm{Aut}(\Gamma)} = \frac{\mathbb{R}^{e(\Gamma)}_+}{\mathrm{Aut}(\Gamma)/(\mathbb{Z}/2\mathbb{Z})}$$

itself is a singular set of $X^{\mathrm{met}}_{\succeq\Gamma}/\mathrm{Aut}(\Gamma)$. The contribution of the Euler characteristic of $RG^{\mathrm{met}}_{g,n}$ from this rational cell is thus

$$\frac{(-1)^{e(\Gamma)}}{2\cdot|\mathrm{Aut}(\Gamma)/(\mathbb{Z}/2\mathbb{Z})|} = \frac{(-1)^{e(\Gamma)}}{|\mathrm{Aut}(\Gamma)|}.$$

Summing all these, we obtain the formula for the Euler characteristic.

The case of $(g,n)=(1,1)$ is still different because all graphs in $RG_{1,1}$ are exceptional. The general formula (4.21) gives $-1/6+1/4=1/12$, but since the factor $\mathbb{Z}/2\mathbb{Z}$ of $\mathrm{Aut}(\Gamma)$ acts trivially on $X^{\mathrm{met}}_{\succeq\Gamma}$, the factor 2 has to be modified. We will study more on $RG_{1,1}$ in Section 2 of Chapter 5. □

3. Ribbon Graphs with Labeled Boundary and the Orbifold Covering

Let $RGB_{g,n}$ denote the set of all isomorphism classes of connected ribbon graphs with labeled boundary components subject to the topological condition (4.1), and

$$RGB^{\mathrm{met}}_{g,n} = \coprod_{\Gamma^b\in RGB_{g,n}} \frac{\mathbb{R}^{e(\Gamma^b)}_+}{\mathrm{Aut}_\partial(\Gamma^b)} \tag{4.23}$$

the space of metric ribbon graphs with labeled boundary components, where

$$\mathrm{Aut}_\partial(\Gamma^b)$$

is the automorphism group of a ribbon graph Γ^b preserving the boundary labeling. The same argument of the previous section applies without any alteration to show that $RGB^{\mathrm{met}}_{g,n}$ is a differentiable orbifold locally modeled by

$$\frac{X^{\mathrm{met}}_{\succeq\Gamma}}{\mathrm{Aut}_\partial(\Gamma)}.$$

The definition of the space of metric inflations $X^{\mathrm{met}}_{\succeq\Gamma}$ does not refer to the labeling of the boundary components of a ribbon graph Γ, but it requires labeling of all half-edges of Γ. As we have noted at the end of Chapter 1, labeling all half-edges induce labeling of the boundary components. Thus every inflation of Γ appearing in $X^{\mathrm{met}}_{\succeq\Gamma}$ has a boundary labeling that is consistent with the boundary labeling of Γ.

THEOREM 4.8. *For every genus $g \geq 0$ and $n \geq 1$ subject to (4.7), the natural* forgetful *projection*

$$pr : RGB^{met}_{g,n} \longrightarrow RG^{met}_{g,n} \tag{4.24}$$

is an orbifold covering of degree $n!$.

PROOF. Let Γ be a ribbon graph. We label the boundary components of Γ, and denote by B the set of all permutations of the boundary components. The cardinality $|B|$ of B is $n!$. The automorphism group $\mathrm{Aut}(\Gamma)$ acts on the set B, and by definition the isotropy subgroup of $\mathrm{Aut}(\Gamma)$ of each element of B is isomorphic to the group $\mathrm{Aut}_\partial(\Gamma)$ consisting of the graph automorphisms of Γ that preserve the boundary components. The orbit space $B/\mathrm{Aut}(\Gamma)$ is the set of ribbon graphs with labeled boundary. Thus the inverse image of the local model $X^{\mathrm{met}}_{\succeq\Gamma}/\mathrm{Aut}(\Gamma)$ by pr^{-1} is the disjoint union of $|B/\mathrm{Aut}(\Gamma)|$ copies of $X^{\mathrm{met}}_{\succeq\Gamma}/\mathrm{Aut}_\partial(\Gamma)$:

$$pr^{-1}\left(\frac{X^{\mathrm{met}}_{\succeq\Gamma}}{\mathrm{Aut}(\Gamma)}\right) = \overbrace{\frac{X^{\mathrm{met}}_{\succeq\Gamma}}{\mathrm{Aut}_\partial(\Gamma)} \coprod \cdots \coprod \frac{X^{\mathrm{met}}_{\succeq\Gamma}}{\mathrm{Aut}_\partial(\Gamma)}}^{|B/\mathrm{Aut}(\Gamma)|\text{-copies}}. \tag{4.25}$$

Since the projection restricted on each local model

$$pr : \frac{X^{\mathrm{met}}_{\succeq\Gamma}}{\mathrm{Aut}_\partial(\Gamma)} \longrightarrow \frac{X^{\mathrm{met}}_{\succeq\Gamma}}{\mathrm{Aut}(\Gamma)}$$

is an orbifold covering of degree $|\mathrm{Aut}(\Gamma)/\mathrm{Aut}_\partial(\Gamma)|$, the map

$$pr_\Gamma : pr^{-1}\left(\frac{X^{\mathrm{met}}_{\succeq\Gamma}}{\mathrm{Aut}(\Gamma)}\right) \longrightarrow \frac{X^{\mathrm{met}}_{\succeq\Gamma}}{\mathrm{Aut}(\Gamma)} \tag{4.26}$$

is an orbifold covering of degree

$$|B/\mathrm{Aut}(\Gamma)| \cdot |\mathrm{Aut}(\Gamma)/\mathrm{Aut}_\partial(\Gamma)| = |B| = n!.$$

Since the projection of (4.24) is just a collection of pr_Γ of (4.26),

$$pr : RGB^{\mathrm{met}}_{g,n} \longrightarrow RG^{\mathrm{met}}_{g,n}$$

is an orbifold covering of degree $n!$ as desired. This completes the proof. □

As an immediate consequence, we have

COROLLARY 4.9. *The Euler characteristic of* $RGB_{g,n}^{\mathrm{met}}$ *is given by*

$$\chi(RGB_{g,n}^{\mathrm{met}}) = n! \cdot \chi(RG_{g,n}^{\mathrm{met}}). \tag{4.27}$$

CHAPTER 5

Strebel Differentials on a Riemann Surface

A Riemann surface is a patchwork of a collection of complex domains. Let us ask a question in the opposite direction: If we are *given* a compact Riemann surface, then how can we find a patchwork of coordinate patches that represents the complex structure?

In this chapter we give a canonical coordinate system of a Riemann surface once a finite number of points on the surface and the same number of positive real numbers are chosen. The key technique is the theory of Strebel differentials [**29**]. Using Strebel differentials, we can encode the holomorphic structure of a Riemann surface in the combinatorial data of ribbon graphs.

1. Strebel Differentials and Measured Foliations on a Riemann Surface

Let C be a compact Riemann surface. We choose a set of finitely many labeled points $\{p_1, p_2, \cdots, p_n\}$ on C, and call them *marked points* on the Riemann surface. The bridge that connects the complex structure of a Riemann surface and combinatorial data is the idea of *tiling*. Let $\square$ be a cell-decomposition of a Riemann surface C. Then C is made of patching *tiles* along the edges of $\square$. If each edge has a definite length, then each tile can be realized as a polygon on a complex plane with the specified edge length. In particular, each tile has a unique complex structure. By patching them in a compatible way, we give a combinatorial description of the complex structure on a compact surface. Thus a complex structure of a Riemann surface is essentially a collection of combinatorial data that is expressed in terms of tiling.

In order to obtain a tiling, or a cell-decomposition, of a Riemann surface, we use the *Strebel differential* on the Riemann surface. A Strebel differential defines a specific foliation on a Riemann surface, and a cell arises as the union of certain types of leaves.

Let $\mathcal{T}_C$ be the holomorphic tangent sheaf of C, and ${\mathcal{T}_C}^* = K_C$ the holomorphic cotangent sheaf, or the canonical line bundle, of C. A holomorphic *quadratic differential* defined on C is an element of $H^0(C, K_C^{\otimes 2})$, where $K_C^{\otimes 2}$ denotes the symmetric tensor product of the canonical sheaf. In a local coordinate z of C, a quadratic differential q is represented by $q = f(z)\big(dz\big)^2$ with a locally defined holomorphic function $f(z)$. With respect to a coordinate change $w = w(z)$, the local expressions

$$q = f(z)\big(dz\big)^2 = g(w)\big(dw\big)^2$$

transform into one another by

$$f(z) = g(w(z))\left(\frac{dw(z)}{dz}\right)^2. \tag{5.1}$$

A *meromorphic* quadratic differential on C is a holomorphic quadratic differential q defined on C except for a finite set $\{p_1, \cdots, p_n\}$ of points of C such that at each *singularity* p_j of q, there is a local expression $q = f_j(z)\big(dz\big)^2$ with a meromorphic function f_j that has a pole at $z = p_j$. If $f_j(z)$ has a pole of order r at p_j, then we say q has a pole of order r at $z = p_j$.

Let $q = f(z)\big(dz\big)^2$ be a meromorphic quadratic differential defined on C. A real parametric curve

$$\gamma : (a, b) \ni t \longmapsto \gamma(t) = z \in C \tag{5.2}$$

parametrized on an open interval (a, b) of a real axis is a *horizontal leaf* (or in the classical terminology, a horizontal *trajectory*) of q if

$$f(\gamma(t)) \left(\frac{d\gamma(t)}{dt}\right)^2 > 0 \tag{5.3}$$

for every $t \in (a, b)$. If

$$f(\gamma(t)) \left(\frac{d\gamma(t)}{dt}\right)^2 < 0 \tag{5.4}$$

holds instead, then the parametric curve γ of (5.2) is called a *vertical leaf* of q. The collection of all horizontal or vertical leaves form a *real codimension 1 foliation* on the Riemann surface C minus the singular points and zeroes of q. There are three important examples of the foliations for our study.

EXAMPLE 5.1. Let $q = \big(dz\big)^2$. Then the horizontal lines

$$\alpha(t) = t + ci, \qquad t \in \mathbb{R}$$

are the horizontal leaves of q, and

$$\beta(t) = it + c, \qquad t \in \mathbb{R}$$

are the vertical leaves for every $c \in \mathbb{R}$. Each of these defines a simple foliation on the complex plane $\mathbb{C}$. In Figure 5.1, horizontal leaves are described by straight lines, and vertical leaves are indicated by broken lines.

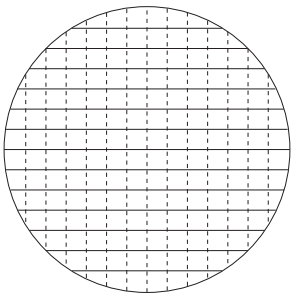

FIGURE 5.1. Foliations Defined by $(dz)^2$

If a quadratic differential $q = f(z)(dz)^2$ is holomorphic and non-zero at $z = z_0$, then on a neighborhood of z_0 we can introduce a *canonical coordinate*

$$w(z) = \int_{z_0}^{z} \sqrt{f(z)}dz. \tag{5.5}$$

It follows from (5.1) that in w-coordinate the quadratic differential is given by $q = (dw)^2$. Therefore, the leaves of q near z_0 look exactly as in Figure 5.1 in the canonical coordinate. This explains the classical terminology of horizontal and vertical trajectories. We remark here that although the coordinate $w(z)$ is called *canonical*, still there is an ambiguity of coordinate change

$$w(z) \longmapsto -w(z) + a \tag{5.6}$$

with an arbitrary complex constant a.

Using the canonical coordinate, it is obvious to see the following:

PROPOSITION 5.1. *Let S be an open Riemann surface and q a holomorphic quadratic differential on S. Then for every point $p \in S$, there is a unique horizontal leaf and a vertical leaf passing through p. Moreover, these leaves intersect at the right angle with respect to the conformal structure of S near p.*

When a holomorphic quadratic differential has a zero, then the foliation behaves differently.

EXAMPLE 5.2. Let $q = z^m(dz)^2$. Then $(m+2)$ half rays

$$\alpha_k : (0, \infty) \ni t \longmapsto t \cdot \exp\left(\frac{2\pi i k}{m+2}\right) \in \mathbb{C}, \qquad k = 0, 1, \cdots, m+1$$

give the horizontal leaves that have $z = 0$ on the boundary (the straight lines of Figure 5.2), and another set of $(m+2)$ half rays

$$\beta_k : (0, \infty) \ni t \longmapsto t \cdot \exp\left(\frac{\pi i + 2\pi i k}{m+2}\right) \in \mathbb{C}, \qquad k = 0, 1, \cdots, m+1$$

gives the vertical leaves (the broken lines of Figure 5.2).

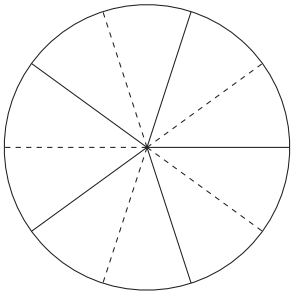

FIGURE 5.2. Horizontal and Vertical Leaves of $z^3(dz)^2$

The foliation become quite wild at singularities of q. However, the situation is milder around a quadratic pole with a negative real coefficient .

EXAMPLE 5.3. Let $q = -\left(\frac{dz}{z}\right)^2$. Then every concentric circle centered at 0,

$$\alpha(t) = re^{it}, \qquad t \in \mathbb{R}, r > 0,$$

is a horizontal leaf, and all the half-rays

$$\beta(t) = te^{i\theta}, \qquad t > 0, 0 \leq \theta < 2\pi,$$

give the vertical leaves. We note that all horizontal leaves are compact curves (Figure 5.3).

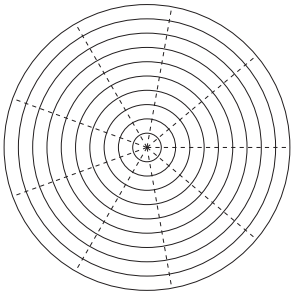

FIGURE 5.3. Horizontal Compact Leaves and Vertical Leaves of $-\frac{1}{z^2}(dz)^2$

The fundamental theorem we need is:

THEOREM 5.2 (Strebel [**29**], Theorem 23.5). *Let g and n be integers satisfying that*

$$\begin{cases} g \geq 0 \\ n \geq 1 \\ 2-2g-n < 0. \end{cases} \tag{5.7}$$

Let $(C, (p_1, \cdots, p_n))$ be a smooth Riemann surface of genus g with n marked points $p_1, \cdots, p_n$. Choose an ordered n-tuple $(a_1, \cdots, a_n) \in \mathbb{R}_+^n$ of positive real numbers. Then there is a unique meromorphic quadratic differential q on C satisfying the following conditions:

1. *q is holomorphic on $C \setminus \{p_1, \cdots, p_n\}$.*
2. *q has a double pole at each p_j, $j = 1, \cdots, n$.*
3. *The union of all non-compact horizontal leaves forms a closed subset of C of measure zero.*
4. *Every compact horizontal leaf α is a simple loop circling around one of the poles, say p_j, and it satisfies*

$$a_j = \oint_\alpha \sqrt{q}, \tag{5.8}$$

where the branch of the square root is chosen so that the integral has a positive value with respect to the positive orientation of α that is determined by the complex structure of C.

This unique quadratic differential is called the *Strebel differential*. Note that the integral (5.8) is automatically a real number because of (5.3). Every non-compact horizontal leaf of a Strebel differential defined on C is bounded by zero points of q, and every zero of degree m of q bounds $m+2$ horizontal leaves, as we have seen in Example 5.2.

Let $\gamma(t)$ be a non-compact horizontal leaf bounded by two zeros $z_0 = \gamma(t_0)$ and $z_1 = \gamma(t_1)$ of $q = f(z)(dz)^2$. Then we can assign a positive real number

$$L(\gamma) = \int_{z_0}^{z_1} \sqrt{q} = \int_{t_0}^{t_1} \sqrt{f(\gamma(t))} \frac{d\gamma(t)}{dt} dt \tag{5.9}$$

by choosing a branch of $\sqrt{f(z)}$ near z_0 and z_1 so that the integral becomes positive. (As before, the integral is a real number because γ is a horizontal leaf.) We call

$L(\gamma)$ the *length* of the *edge* γ with respect to q. Note that the length (5.9) is independent of the choice of the parameter t. The length is also defined to any compact horizontal leaf by (5.8). Thus every horizontal leaf has a uniquely defined length, and hence the Strebel differential q defines a *measured* foliation on the open subset of the Riemann surface that is the complement of the set of zeroes and poles of q.

Around every marked point p_j there is a foliated disk of compact horizontal leaves with length equal to the prescribed value a_j. As the loop becomes larger in size (but not in length, because it is a constant), it hits zeroes of q and the shape becomes a polygon (Figure 5.4).

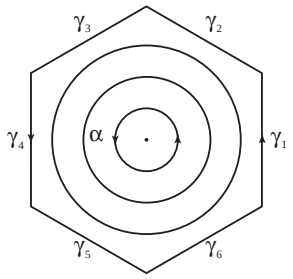

FIGURE 5.4. Foliated Disk

Let the polygon be an m-gon, $\gamma_1, \cdots, \gamma_m$ the non-compact horizontal leaves surrounding p_j, and α a compact horizontal leaf around the point. Then we have

$$a_j = L(\alpha) = L(\gamma_1) + \cdots L(\gamma_m). \tag{5.10}$$

We note that some of the γ_j's may be the same non-compact horizontal leaf on the Riemann surface C. The collection of all compact horizontal leaves surrounding p_j forms a punctured disk with its center at p_j. Glue all these punctured disks to non-compact horizontal leaves and the zeroes of the Strebel differentials, and fill the punctures with points $\{p_1, \cdots, p_n\}$. Then we obtain a compact surface, which is the underlying topological surface of the Riemann surface C.

COROLLARY 5.3. *Let g and n be integers satisfying (5.7), and*

$$(C, (p_1, p_2, \cdots, p_n), (a_1, a_2, \cdots, a_n)) \tag{5.11}$$

a non-singular Riemann surface of genus g with n marked points and an ordered n-tuple of positive real numbers. Then there is a unique cell-decomposition $\square_q$ of C consisting of v 0-cells, e 1-cells, and n 2-cells, where v is the number of zeroes of the Strebel differential q associated with (5.11), and

$$e = v - 2 + 2g + n.$$

PROOF. The 0-cells, or the *vertices*, of $\square_q$ are the zeroes of the Strebel differential q of (5.11). The 1-cells, or the *edges*, are the non-compact horizontal leaves that connect the 0-cells. Since each 1-cell has a finite positive length and the union of all 1-cells is closed and has measure zero on C, the number of 1-cells is finite. The union of all compact horizontal leaves that are homotopic to p_j (together with the center p_j) forms a 2-cell, or a *face*, that is homeomorphic to a 2-disk. There are n

such 2-cells. The boundary of an edge is one or two vertices, and the boundary of a face is a union of some edges and vertices. The formula for the Euler characteristic

$$v - e + n = 2 - 2g$$

determines the number of edges. □

The 1-skeleton, or the union of the 0-cells and 1-cells, of the cell-decomposition $\square_q$ that is defined by the Strebel differential is a ribbon graph. The cyclic ordering of the half-edges at each vertex is determined by the orientation of the Riemann surface. The next chapter is devoted to study these graphs appearing from the cell-decompositions of a Riemann surface. A vertex of the graph that comes from a zero of degree m of the Strebel differential is a vertex of degree $m+2$. Thus the graph we are considering here does not have any vertices of degree less than 3. Since each edge of the graph has the unique length by (5.9), the graph is a metric ribbon graph.

2. Examples of Strebel Differentials

Let us give some explicit examples of the Strebel differentials.

EXAMPLE 5.4. We begin with recalling the *Weierstrass elliptic function*

$$\begin{aligned}\wp(z) &= \frac{1}{z^2} + \sum_{\substack{(m,n)\in\mathbb{Z}^2\\(m,n)\neq(0,0)}} \left(\frac{1}{(z-m\omega-n\tau\omega)^2} - \frac{1}{(m\omega+n\tau\omega)^2}\right) \\ &= \frac{1}{z^2} + \frac{g_2 z^2}{20} + \frac{g_3 z^4}{28} + \frac{g_2^2 z^6}{1200} + \frac{3g_2 g_3 z^8}{6160} + \cdots\end{aligned} \tag{5.12}$$

defined on an elliptic curve

$$E_\tau = \frac{\mathbb{C}}{\mathbb{Z}\omega \oplus \mathbb{Z}\tau\omega}$$

of (3.8), where g_2 and g_3 are defined in (3.11). With respect to a coordinate z on $\mathbb{C}$ of (3.8), the Strebel differential of $((E_\tau, 0), a) \in \mathfrak{M}_{1,1} \times \mathbb{R}_+$ is given by

$$q = (-a\wp(z) + c)\,(dz)^2, \tag{5.13}$$

where c is a suitable complex constant so that q satisfies the conditions of Theorem 5.2. It is customary to write

$$\omega_1 = \omega/2, \quad \omega_2 = (\omega + \tau\omega)/2, \quad \text{and} \quad \omega_3 = \tau\omega/2.$$

We also use the traditional notation

$$e_j = \wp(\omega_j), \qquad j = 1, 2, 3.$$

It is known that g_2, g_3 and e_j's satisfy the following relation:

$$4x^3 - g_2 x - g_3 = 4(x - e_1)(x - e_2)(x - e_3).$$

Let us consider now the case when τ is pure imaginary. We choose a positive real ω. Then it is easy to see from (3.11) that g_2 and g_3 are real, and it can be shown that e_1, e_2, e_3 are also real in this case. The Weierstrass $\wp$-function maps the interior of the rectangle spanned by $0, \omega_1, \omega_2, \omega_3$ biholomorphically onto the upper half plane (see for example, [**22**]). The boundary rectangle is mapped to the real axis, and we have

$$e_3 < e_2 < e_1.$$

The Strebel differential is then given by

$$q = a\left(-\wp(z) + e_2\right)(dz)^2.$$

The series expansion of (5.12) tells us that the horizontal leaves near 0 are closed loops that are centered at the origin. The differential q has a double zero at ω_2, which we see from the Weierstrass differential equation

$$\wp'(z)^2 = 4\wp(z)^3 - g_2\wp(z) - g_3 = 4\left(\wp(z) - e_1\right)\left(\wp(z) - e_2\right)\left(\wp(z) - e_3\right).$$

The real curve $\omega_1 + it$ is a horizontal leaf, because on the edge $\overline{\omega_1\omega_2}$ the Weierstrass function $\wp(z)$ takes values in $[e_2, e_1]$. The curve $\omega_3 + t$ is also a horizontal leaf, because on the edge $\overline{\omega_3\omega_2}$ the function $\wp(z)$ takes values in $[e_3, e_2]$. In the above consideration we used the fact that $\wp(z)$ is an even function:

$$\wp(z) = \wp(-z).$$

The case $\tau = i$ is of special interest. E_i belongs to the boundary of the fundamental domain Figure 3.2, which is fixed by the $\mathbb{Z}/2\mathbb{Z}$ symmetry $\tau \to -1/\tau$. In this case, we have $g_2 = 4$, $g_3 = 0$, $e_1 = -e_3 = 1$ and $e_2 = 0$. Therefore, the Strebel differential (5.13) is simply given by

$$q = -a\wp(z)(dz)^2.$$

The extra $\mathbb{Z}/2\mathbb{Z}$ symmetry comes from the transformation property

$$\wp(iz) = -\wp(z).$$

The metric graph corresponding to this case certainly has the $\mathbb{Z}/2\mathbb{Z}$-invariance corresponding to interchanging the edges (Figure 5.5).

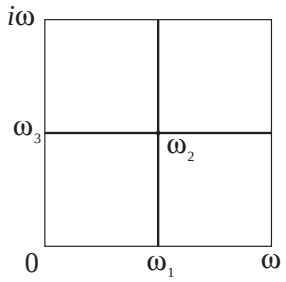

FIGURE 5.5. Elliptic Curve with $\tau = i$

The other special point of $\mathfrak{M}_{1,1}$ is $\tau = e^{\pi i/3}$, which corresponds to $g_2 = 0$, $g_3 = 4$, and

$$e_1 = 1, \quad e_2 = e^{2\pi i/3}, \quad e_3 = e^{4\pi i/3}.$$

The zeroes of $\wp(z)$ are

$$p = \frac{\omega_1 + \omega_2 + \omega_3}{3} \quad \text{and} \quad 2p = \frac{2(\omega_1 + \omega_2 + \omega_3)}{3}.$$

The Weierstrass function $\wp(z)$ maps the line segment $\overline{p\omega_1}$ onto $[0, 1]$, $\overline{p\omega_2}$ to $\overline{0e_2}$, and $\overline{p\omega_3}$ to $\overline{0e_3}$, respectively (Figure 5.6).

The Strebel differential is again

$$q = -a\wp(z)(dz)^2,$$

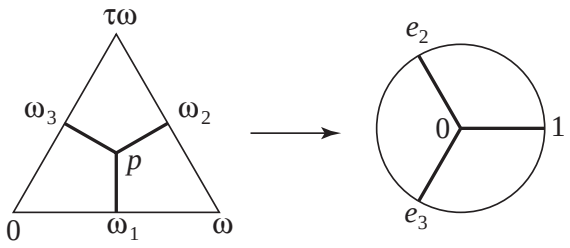

FIGURE 5.6. Weierstrass $\wp$-Function for $g_2 = 0, g_3 = 4$

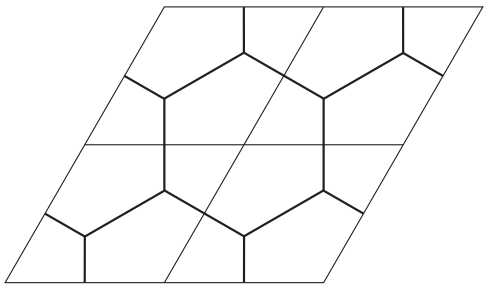

FIGURE 5.7. Honeycomb

and the non-compact leaves form a regular hexagonal network, which possesses a $\mathbb{Z}/3\mathbb{Z}$-symmetry (Figure 5.7).

It is interesting to investigate what happens if we add a holomorphic quadratic differential $c(dz)^2$ to the Strebel differential. The addition does not affect the local behavior of compact horizontal leaves around the pole, but the global picture of the foliation is altered so that the conditions of Theorem 5.2 do not hold. For example, the non-compact horizontal leaves of a quadratic differential

$$q_1 = -\left(\wp(z) + \frac{1}{2}\right)(dz)^2$$

for the case $\tau = i$ looks as in Figure 5.8. Since the central vertical line $\omega_1 + it$ remains as a horizontal leaf of q_1, it has a compact horizontal leaf that is not homotopic to the pole of q_1.

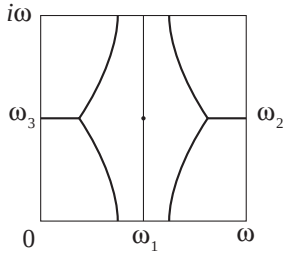

FIGURE 5.8. Non-Strebel Case

3. The Canonical Coordinate System on a Riemann Surface

In Section 1, we have seen that the horizontal leaves of the Strebel differential determine a canonical cell-decomposition of a Riemann surface once a set of n marked points and an n-tuple of positive real numbers are specified. In this section we will see that the vertical leaves give us a canonical coordinate system of the Riemann surface and a patchwork of open domains that determines the complex structure.

Let $(C, (p_1, p_2, \cdots, p_n), (a_1, a_2, \cdots, a_n))$ be the set of data of (5.11), and q the Strebel differential associated with the data. We recall that for every point of a vertical leaf there is a horizontal leaf intersecting perpendicularly at the point (Proposition 5.1). Since the set of all the compact horizontal leaves of q forms an open dense subset of C, which is indeed the disjoint union of punctured open 2-disks, every vertical leaf of q extends to one of the points p_j. In particular, a vertical leaf starting at a zero of q should end at one of the poles. In other words, there is no vertical leaf that has both endpoints at the zeroes of q.

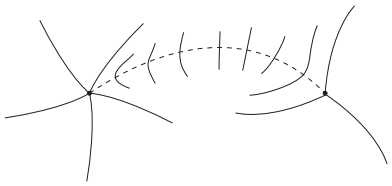

FIGURE 5.9. No Vertical Leaf Connects Zeroes of q

In Figure 5.9, the broken line represents a vertical leaf connecting two zeroes of q. The horizontal leaves intersecting the vertical leaf are mostly closed loops that are homotopic to a single point. But this is impossible, unless there is a pole of q on the vertical leaf.

Thus there are finitely many vertical leaves that connect zeroes and poles of q.

THEOREM 5.4. *The set of all vertical leaves that connect zeroes and poles of q, together with the cell-decomposition $\square_q$ of C by the non-compact horizontal leaves, defines a triangulation Δ_q of C.*

PROOF. The cell-decomposition $\square_q$ of C defined by the non-compact horizontal leaves of q defines a polygonalization of C. Each polygon Figure 5.4 has a unique center, which is a pole of q. The vertical leaves that connect zeroes and poles supply the edges necessary for a triangulation of each polygon (Figure 5.10). □

Let Γ_q denote the graph consisting of zeroes of q as vertices and non-compact horizontal leaves of q as edges. Since there is a unique and well-defined cyclic order of half-edges at each vertex of Γ_q, it is a ribbon graph. By the property of the Strebel differential, we have

$$\begin{cases} \chi(\Gamma_q) = v(\Gamma_q) - e(\Gamma_q) = 2 - 2g \\ b(\Gamma_q) = n. \end{cases} \tag{5.14}$$

In particular, the closed surface associated with the ribbon graph Γ_q is the underlying topological surface of the Riemann surface C. For every edge E of Γ_q, there are

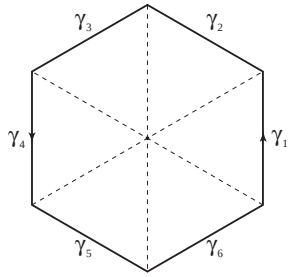

FIGURE 5.10. Triangulation of a Polygon

two triangles of Δ_q that share E. Gluing these two triangles along E, we obtain a diamond shape as in Figure 5.11. This is the set of all vertical leaves that intersect with E. Let V and V' be the endpoints of E, and give a direction to E from V to V'. We allow the case that E has only one endpoint. In that case, we assign a direction either way. For a point P in the triangles, the canonical coordinate

$$z = z(P) = \int_V^P \sqrt{q} \tag{5.15}$$

maps the diamond shape to a strip

$$U_E = \{z \in \mathbb{C} \mid 0 < Re(z) < L\} \tag{5.16}$$

of infinite height and width L in the complex plane, where L is the length of E. We identify the open set U_E as the union of two triangles on the Riemann surface C by the canonical coordinate z (Figure 5.11). The local expression of q on U_E is of course

$$q = (dz)^2. \tag{5.17}$$

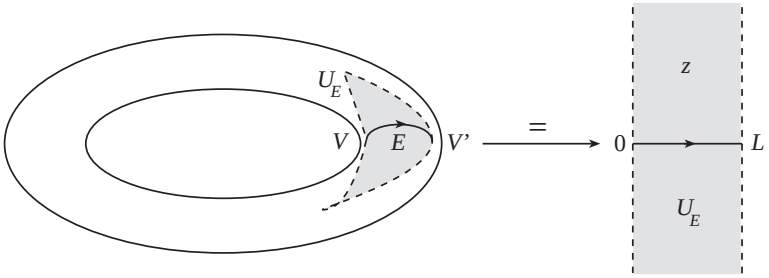

FIGURE 5.11. Triangulation and Canonical Coordinate System

Let the degree of V be m. We note that every quadratic differential has an expression

$$q = \frac{m^2}{4} w^{m-2} (dw)^2 \tag{5.18}$$

around a zero of degree $m-2$. So we use (5.18) as the expression of the Strebel differential q on an open neighborhood U_V around V with a coordinate w such that

V is given by $w = 0$. On the intersection

$$U_E \cap U_V,$$

we have

$$q = (dz)^2 = \frac{m^2}{4} w^{m-2} (dw)^2 \tag{5.19}$$

from (5.17) and (5.18). Solving this differential equation with the initial condition that $z = 0$ and $w = 0$ define the same point V, we obtain the coordinate transform

$$w = w(z) = cz^{2/m}, \tag{5.20}$$

where c satisfies that $c^m = 1$. Thus U_E and U_V are glued on the Riemann surface C in the way described in Figure 5.12.

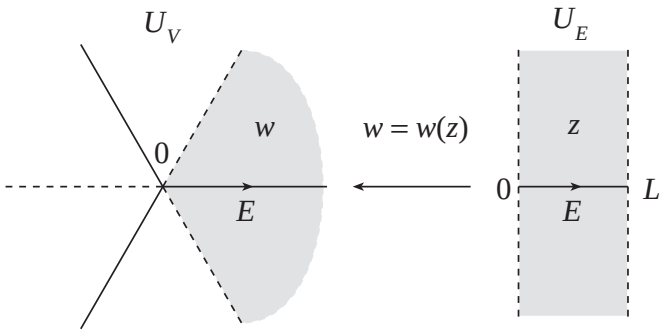

FIGURE 5.12. Gluing a Strip to a Neighborhood of a Vertex by $w = w(z) = z^{2/3}$

Since we have

$$\oint \sqrt{q} = a_j$$

around a quadratic pole p_j, we can choose a local coordinate u on an open disk U_j centered at p_j such that

$$q = -\frac{a_j^2}{4\pi^2} \frac{(du)^2}{u^2}. \tag{5.21}$$

Because of the definition of the Strebel differential, the coordinate disk U_j, which is the union of the horizontal leaves that are zero-homotopic to p_j, can be defined so that its boundary contains a zero of q. Actually, the boundary of U_j consists of a collection of edges $E_1, \cdots, E_\mu$ for some μ. Let z_k be the canonical coordinate on U_{E_k}. Equations (5.17) and (5.21) give us a differential equation

$$(dz_k)^2 = -\frac{a_j^2}{4\pi^2} \frac{(du)^2}{u^2}. \tag{5.22}$$

Its solution is given by

$$u = u(z_k) = \gamma e^{2\pi i z_k / a_j}, \tag{5.23}$$

where γ is a constant of integration. Since the edges $E_1, \cdots, E_\mu$ surround the point p_j, the constant of integration for each z_k is arranged so that the solution u of (5.23)

covers the entire disk. The precise form of gluing function of open sets U_{E_k}'s and U_j is given by

$$u = u(z_k) = \exp\left(2\pi i \frac{L_1 + L_2 + \cdots + L_{k-1} + z_k}{L_1 + L_2 + \cdots + L_\mu}\right), \qquad k = 1, 2, \cdots, \mu, \tag{5.24}$$

where the length L_k satisfies the condition

$$a_j = L_1 + L_2 + \cdots + L_\mu.$$

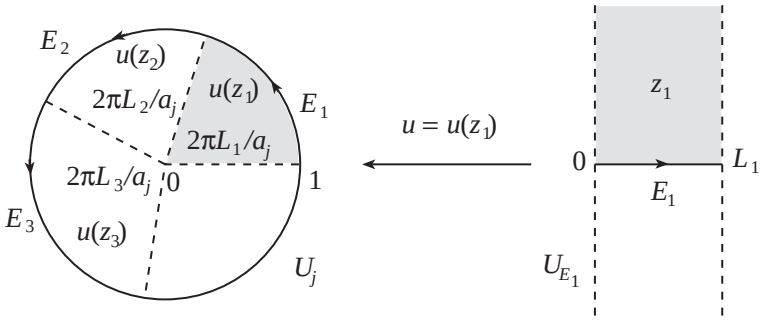

FIGURE 5.13. Gluing a Strip to a Neighborhood of a Pole by $u = u(z_1) = \exp(2\pi i z_1/a_j)$

The open coordinate charts U_E's, U_V's and U_j's cover the whole Riemann surface C. We call them the *canonical coordinate charts*.

DEFINITION 5.5. The *canonical coordinate system* of the data

$$(C, (p_1, p_2, \cdots, p_n), (a_1, a_2, \cdots, a_n))$$

is the covering

$$C = \bigcup_E U_E \cup \bigcup_V U_V \cup \bigcup_{j=1}^{n} U_j \tag{5.25}$$

of the Riemann surface C by the canonical coordinate charts, where the union is defined by the gluing functions (5.20) and (5.24).

We note that the canonical coordinate z we have chosen for the strip U_E around an edge E depends on the direction of the edge. If we use the opposite direction, then the coordinate changes to

$$z \longmapsto L - z, \tag{5.26}$$

where L is the length of E, as before. This change of coordinate does not affect the differential equations (5.19) and (5.22), because

$$(dz)^2 = (d(L - z))^2.$$

CHAPTER 6

Combinatorial Description of the Moduli Spaces

We have defined the space of metric ribbon graphs with labeled boundary components by

$$RGB_{g,n}^{\mathrm{met}} = \coprod_{\Gamma \in RGB_{g,n}} \frac{\mathbb{R}_+^{e(\Gamma)}}{\mathrm{Aut}_\partial(\Gamma)}.$$

The Strebel theory defines a map

$$\sigma : \mathfrak{M}_{g,n} \times \mathbb{R}_+^n \longrightarrow RGB_{g,n}^{\mathrm{met}}. \tag{6.1}$$

In Section 1 below, we will prove that the map σ is a bijection. Since $RGB_{g,n}^{\mathrm{met}}$ is a differentiable orbifold, we can introduce the structure of a differentiable orbifold to $\mathfrak{M}_{g,n} \times \mathbb{R}_+^n$. The case of $(g,n) = (1,1)$ is in many ways exceptional. Section 2 is devoted to study $\mathfrak{M}_{1,1} \times \mathbb{R}_+$. For $(g,n) = (0,3)$, all Strebel differentials are explicitly computable. Thus we can construct the identification map

$$\mathfrak{M}_{0,3} \times \mathbb{R}_+^3 = RGB_{0,3}^{\mathrm{met}}$$

directly. This topic is studied in Section 3. We will also examine the orbifold covering $RGB_{0,3}^{\mathrm{met}} \to RG_{0,3}^{\mathrm{met}}$ there.

The product group $\mathbb{R}_+^n$ acts naturally on $\mathfrak{M}_{g,n} \times \mathbb{R}_+^n$. Therefore it acts on the space $RGB_{g,n}^{\mathrm{met}}$ through the bijection σ. However, the $\mathbb{R}_+^n$-action on $RGB_{g,n}^{\mathrm{met}}$ is complicated. The example of Section 3 shows that the action does not preserve the rational cells.

1. The Bijection between the Moduli Space and the Space of Metric Ribbon Graphs with Labeled Boundary

In this section we establish the following theorem:

THEOREM 6.1. *There is a natural bijection*

$$\mathfrak{M}_{g,n} \times \mathbb{R}_+^n = RGB_{g,n}^{met}.$$

PROOF. The proof breaks down into three steps. In Step 1, we construct a map

$$\coprod_{\Gamma \in RGB_{g,n}} \mathbb{R}_+^{e(\Gamma)} \longrightarrow \mathfrak{M}_{g,n} \times \mathbb{R}_+^n. \tag{6.2}$$

We then prove that the map descends to

$$\beta : RGB_{g,n}^{\mathrm{met}} \longrightarrow \mathfrak{M}_{g,n} \times \mathbb{R}_+^n \tag{6.3}$$

by considering the action of the graph automorphism groups preserving the boundary order in Step 2. From the construction of Step 1 we will see that β is a right-inverse of the map σ of (6.1), i.e., $\sigma \circ \beta$ is the identity of $RGB_{g,n}^{\mathrm{met}}$. In Step 3

we prove that β is also a left-inverse of the map σ. This will complete the proof of our theorem.

STEP 1. Our starting point is a metric ribbon graph Γ_{met} with labeled boundary components. We label all edges, and give an arbitrary direction to each edge. To each directed edge $\overrightarrow{E}$ of Γ_{met}, we assign a strip

$$U_{\overrightarrow{E}} = \{z \in \mathbb{C} \mid 0 < Re(z) < L\}$$

of infinite length and width L, where L is the length of E (see Figure 6.1). The open real line segment $(0, L) \subset U_{\overrightarrow{E}}$ is identified with the edge $\overrightarrow{E}$. The strip $U_{\overrightarrow{E}}$ has a complex structure defined by the coordinate z, and a holomorphic quadratic differential $(dz)^2$ on it. Every horizontal leaf of the foliation defined by this quadratic differential is a horizontal line of length L. If we use the opposite direction of $\overrightarrow{E}$, then $U_{\overrightarrow{E}}$ should be rotated 180° about the real point $L/2$, and the coordinate is changed to $L - z$.

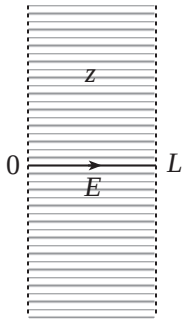

FIGURE 6.1. A Strip of Infinite Length with Horizontal Leaves

Let V be a degree m vertex of Γ. There are m half-edges attached to V, although some of them may belong to the same edge. Let $1, 2, \cdots, m$ be the cyclic order of the half-edges chosen at V. We give a direction to each edge by defining the positive direction to be the one coming out from V, and name the edges $\overrightarrow{E}_1, \overrightarrow{E}_2, \cdots, \overrightarrow{E}_m$. If an edge goes out as a half-edge number j and comes back as another half-edge number k, then we use the convention that $\overrightarrow{E}_j = \overleftarrow{E}_k$, where $\overleftarrow{E}_k$ denotes the edge E_k with the opposite direction. We denote by L_j the length of E_j.

Let us place the vertex V at the origin of the w-plane. We glue a neighborhood of the boundary point 0 of each of the strips $U_{\overrightarrow{E}_1}, \cdots, U_{\overrightarrow{E}_m}$ together on the w-plane by

$$w = e^{2\pi i(j-1)/m} z_j^{2/m}, \qquad j = 1, 2, \cdots, m \tag{6.4}$$

as shown in Figure 6.2.

An open neighborhood U_V of $w = 0$ is covered by this gluing, if we include the boundary of each $U_{\overrightarrow{E}_j}$. It follows from (6.4) that the expression of the quadratic differential $(dz_j)^2$ changes into

$$(dz_j)^2 = \frac{m^2}{4} w^{m-2} (dw)^2 \tag{6.5}$$

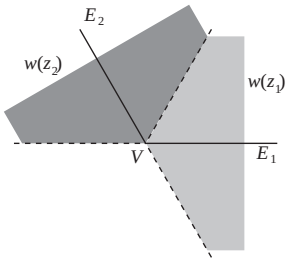

FIGURE 6.2. Gluing Strips at a Vertex

in the w-coordinate for every j. So we define a holomorphic quadratic differential q on U_V by (6.5). Note that q has a zero of degree $m-2$ at $w=0$. At least locally on U_V, the horizontal leaves of the foliation defined by q that have V as a boundary point coincide with the image of the edges $E_1, \cdots, E_m$ via (6.4).

Next, let us consider the case when edges $\overrightarrow{E}_1, \overrightarrow{E}_2, \cdots, \overrightarrow{E}_h$ form an oriented boundary component B of Γ, where the direction of $\overrightarrow{E}_k$ is chosen to be compatible with the orientation of B. Here again we allow that some of the edges are actually the same, with the opposite direction. As before, let L_k be the length of E_k, and put

$$a_B = L_1 + L_2 + \cdots L_h. \tag{6.6}$$

This time we glue the upper half of the strips $U_{\overrightarrow{E}_1}, \cdots, U_{\overrightarrow{E}_h}$ (or the lower half, if the edge has the opposite direction) into the unit disk of the u-plane by

$$u = \exp\left(\frac{2\pi i}{a_B}(L_1 + L_2 + \cdots + L_{k-1} + z_k)\right), \qquad k = 1, 2, \cdots, h. \tag{6.7}$$

We note that the entire unit disk on the u-plane, which we denote by U_B, is covered by this gluing, if the boundary lines of the strips are included (Figure 6.3).

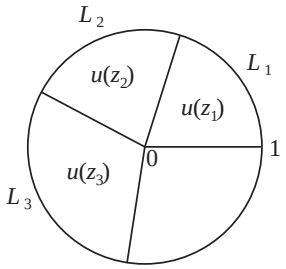

FIGURE 6.3. Gluing Strips along a Loop

It follows from this coordinate transform that

$$(dz_k)^2 = -\frac{a_B^2}{4\pi^2}\frac{(du)^2}{u^2}. \tag{6.8}$$

Thus the holomorphic quadratic differential q naturally extends to a meromorphic quadratic differential on the union

$$U_B \cup \bigcup_{k=1}^{h} U_{\overrightarrow{E}_k}$$

which has a pole of order 2 at $u = 0$ with a negative real coefficient. The horizontal leaves of the foliation defined by q are concentric circles that are centered at $u = 0$, which correspond to the horizontal lines on $U_{\overrightarrow{E}_k}$ through (6.7). Note that the length of a compact horizontal leaf around $u = 0$ is always a_B.

Now define a compact Riemann surface $C(\Gamma_{\mathrm{met}})$ by gluing all the U_V's, U_B's and the strips $U_{\overrightarrow{E}}$'s by (6.4) and (6.7):

$$C(\Gamma_{\mathrm{met}}) = \bigcup_{V\text{: vertex of } \Gamma} U_V \cup \bigcup_{E\text{: edge of } \Gamma} U_{\overrightarrow{E}} \cup \bigcup_{\substack{B\text{: boundary} \\ \text{component of } \Gamma}} U_B. \tag{6.9}$$

Since there are two directions for every edge E, both the upper-half part and the lower-half part of a strip $U_{\overrightarrow{E}}$ are included in the union of all U_B's. Thus the union (6.9) is compact. The Riemann surface $C(\Gamma_{\mathrm{met}})$ has $n = b(\Gamma)$ marked points each of which is the center of the unit disk U_B. The ordering of the boundary components of the ribbon graph determines an ordering of the marked points on the Riemann surface. Attached to each marked point we have a positive real number a_B. The Riemann surface also comes with a meromorphic quadratic differential whose local expressions are given by $(dz_j)^2$, (6.5), and (6.8). It is the Strebel differential on $C(\Gamma_{\mathrm{met}})$. The metric ribbon graph corresponding to this Strebel differential is, by construction, exactly the original graph Γ_{met}, which has a natural ordering of the boundary components.

Out of a metric ribbon graph Γ_{met} with labeled boundary, we have made $e(\Gamma)$ strips with infinite length and various width that is specified by the length of the edges. The combinatorial structure of the ribbon graph gives us the unique way of sewing these strips. The result is a compact Riemann surface with marked points and a positive real number attached to each marked point. Thus we have constructed a map (6.2).

Step 2. Let us now consider the effect of a graph automorphism $f \in \mathrm{Aut}_\partial(\Gamma)$ on (6.9). Let $p_1, \cdots, p_n$ be the marked points of $C(\Gamma_{\mathrm{met}})$, and $a_1, \cdots, a_n$ the corresponding positive numbers. We denote by $E_1, \cdots, E_e$ the edges of Γ, and by $U_{\overrightarrow{E}_1}, \cdots, U_{\overrightarrow{E}_e}$ the corresponding strips with a choice of direction. Then the union of the closures of these strips cover the Riemann surface minus the marked points:

$$C(\Gamma_{\mathrm{met}}) \setminus \{p_1, \cdots, p_n\} = \bigcup_{j=1}^{e} \overline{U}_{\overrightarrow{E}_j}.$$

A graph automorphism $f : \Gamma_{\mathrm{met}} \to \Gamma_{\mathrm{met}}$ induces a permutation of edges and flip of directions, and hence a permutation of strips $U_{\overrightarrow{E}_1}, \cdots, U_{\overrightarrow{E}_e}$ and a change of coordinate z_j to $L_j - z_j$. If f fixes a vertex V of degree m, then it acts on U_V by rotation of angle an integer multiple of $2\pi/m$, which is a holomorphic automorphism of U_V. The permutation of vertices induced by f is a holomorphic transformation of the union of U_V's. Since f preserves the boundary components of Γ, it does not permute U_B's, but it may rotate each U_B following the effect of the permutation of edges. In this case, the origin of U_B, which is one of the marked points, is fixed,

and the orientation of the boundary is also fixed. Thus the graph automorphism induces a holomorphic automorphism of $C(\Gamma_{\text{met}}) \setminus \{p_1, \cdots, p_n\}$. The holomorphic automorphism preserves the ordering of the marked points. Thus we conclude that (6.2) descends to a map β which satisfies that $\sigma \circ \beta = id$.

STEP 3. We still need to show that $\beta \circ \sigma$ is the identity map of $\mathfrak{M}_{g,n} \times \mathbb{R}_+^n$. So we start with a Riemann surface C with n marked points $p_1, \cdots, p_n$ and an ordered n-tuple $(a_1, \cdots, a_n)$ of positive real numbers. Let q be the unique Strebel differential on C, and Γ_{met} the corresponding metric ribbon graph with ordered boundary. In Chapter 4, we have introduced the canonical coordinate system on C. The gluing of these coordinate charts is the same as in the construction of Step 1.

This completes the proof of Theorem 6.1. □

From the computation of the Euler characteristic of $RGB_{g,n}^{\text{met}}$ of (4.27), we obtain

$$\chi\left(\mathfrak{M}_{g,n} \times \mathbb{R}_+^n\right) = \sum_{\Gamma \in RGB_{g,n}} \frac{(-1)^{e(\Gamma)}}{|\text{Aut}_\partial(\Gamma)|} = n! \sum_{\Gamma \in RG_{g,n}} \frac{(-1)^{e(\Gamma)}}{|\text{Aut}(\Gamma)|} \tag{6.10}$$

as a corollary of Theorem 6.1.

To illustrate the gluing procedure, let us apply it to the graph Figure 2.9 with one vertex of degree 4 and two edges.

EXAMPLE 6.1. We glue two strips to the graph and construct $\mathbb{P}^1$ with three marked points. First we label the boundary of the strips as in Figure 6.4.

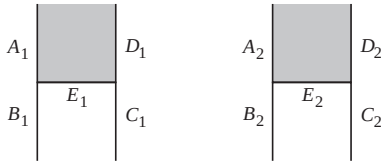

FIGURE 6.4. Two Strips

Since the edges E_1 and E_2 bound only one vertex V, the gluing process around the two loops of the figure 8 shape makes the strips into a twin-cone (Figure 6.5).

The two cones are glued at the vertex V. The two entrances of the wigwam are sewn together along the lines $B_1 = C_2$ and $C_1 = B_2$. Looking from the above, the connected twin-cone becomes a figure 8 shape (Figure 6.6).

The process completes with gluing the outside of the figure 8 shape. The result is Figure 6.7, which is $\mathbb{P}^1$ with three marked points. We have already encountered this shape in Figure 2.12.

EXAMPLE 6.2. We consider the Riemann surface corresponding to an exceptional graph of Figure 6.8. The starting point is the same strips of Figure 6.4.

To make a better picture, we cut the strips into pieces and reassemble them as a square. Gluing the corresponding sides of the square of Figure 6.9, we obtain an elliptic curve with one marked point.

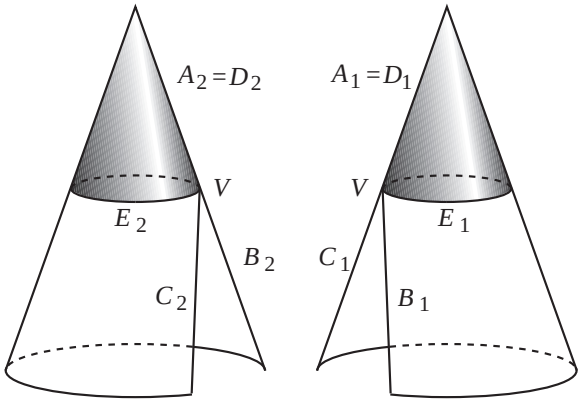

FIGURE 6.5. Twin-Cone

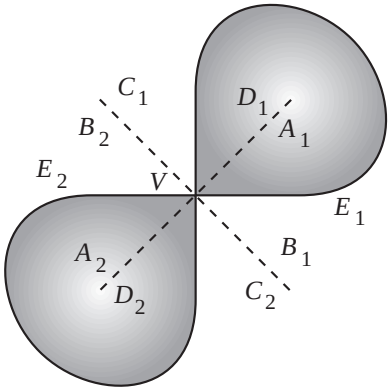

FIGURE 6.6. Glued Cones

2. The Moduli Space $\mathfrak{M}_{1,1}$ and $RG^{\mathrm{met}}_{1,1}$

Recall that $\mathfrak{M}_{1,1}$ has two 0-cells, three 1-cells and two 2-cells (see Section 3 of Chapter 2). We now know that $RG^{\mathrm{met}}_{1,1}$ has two 1-cells, three 2-cells and one 3-cell. The action of $\mathbb{Z}/3\mathbb{Z}$ on $\mathbb{R}^3_+$ is by cyclic permutation of three coordinates. Thus the fundamental domain for this action is the 1/3 of $\mathbb{R}^3_+$ surrounded by the three shaded planes in Figure 6.10: the vertical plane on the left, the vertical plane standing diagonally, and the plane going up from left to right. As an orbifold with boundary, $\mathbb{R}^3_+/(\mathbb{Z}/3\mathbb{Z})$ has one 1-cell defined by $x = y = z$, one 2-cell defined by $x = y$, and one 3-cell. The vertical wall defined by $y = 0$ is the boundary of the orbifold, which is not a cell.

In Figure 6.10, the origin is located at the left lower corner of the backside of the cube, and x, y and z denote the length of the three edges of a trivalent graph on an elliptic curve. Shrinking one of the edges, we obtain a degree 4 graph with two edges. The space of such graphs with metric is $\mathbb{R}^2_+/\mathfrak{S}_2$, and that can be identified with the half of the wall $y = 0$ on Figure 6.10. It has one 1-cell, $x = z, y = 0$, and one 2-cell. Since one half of the wall $y = 0$ is glued with the other half by the reflection along the line $x = z, y = 0$, it is natural to insert one more wall

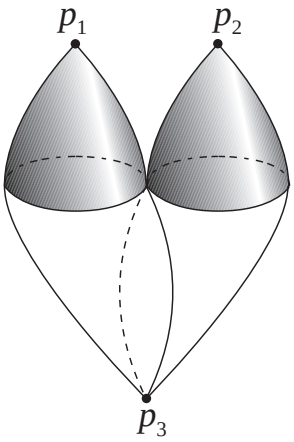

FIGURE 6.7. $\mathbb{P}^1$ with 3 Marked Points

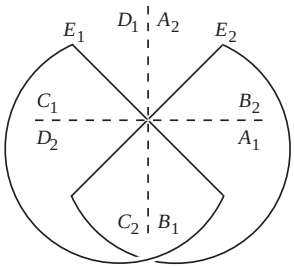

FIGURE 6.8. Gluing for $g = s = 1$

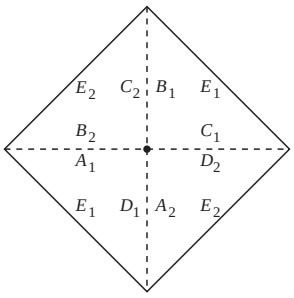

FIGURE 6.9. An Elliptic Curve with One Marked Point

into the picture: the one connecting the lines $x = y = z$ and $x = z, y = 0$ (see Figure 6.10). Altogether, we now have two 1-cells, three 2-cells and two 3-cells, as we have expected. The Euler characteristic can be calculated as follows. The 3-cells contribute with $-1-1$. The two 2-cells of $\mathbb{R}^3_+/(\mathbb{Z}/3\mathbb{Z})$ contribute with $1+1$. The 1-cell in $\mathbb{R}^3_+/(\mathbb{Z}/3\mathbb{Z})$ has the entire group $\mathbb{Z}/3\mathbb{Z}$ as its isotropy group, thus it contributes with $-1/3$. The boundary piece $\mathbb{R}^2_+/\mathfrak{S}_2$ has Euler characteristic $1-1/2$ coming from the two cells in it. As we glue the wall to the boundary of $\mathbb{R}^3_+/(\mathbb{Z}/3\mathbb{Z})$,

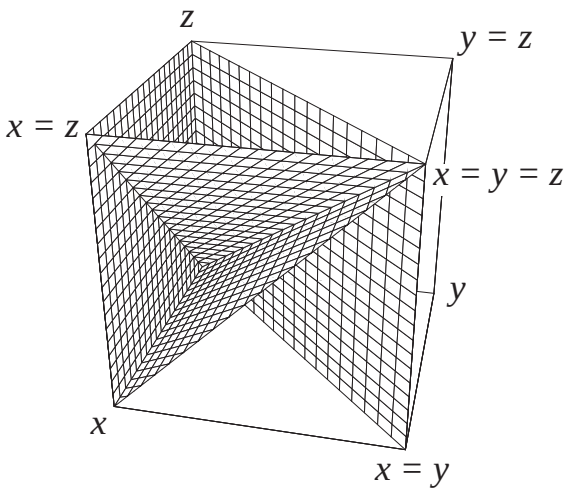

FIGURE 6.10. Orbifold $RG^{\mathrm{met}}_{1,1}$

it becomes just as one of the same kind of walls separating the chamber. Therefore, the total Euler characteristic is computed as

$$\chi\left(RG^{\mathrm{met}}_{1,1}\right) = -\frac{1}{2} - \frac{1}{3} + 1 + 1 + 1 - 1 - 1 = \frac{1}{6},$$

which is in agreement with (3.16).

Geometrically, $\mathfrak{M}_{1,1} \times \mathbb{R}_+$ can be viewed as a cone over the fundamental domain of Figure 3.3 minus the vertex. The vertex of the cone corresponds to the origin of Figure 6.10. The ray $a \times \mathbb{R}_+$, which has the $\mathbb{Z}/3\mathbb{Z}$-symmetry, corresponds to the 1-cell $x = y = z$ of Figure 6.10. The ray $i \times \mathbb{R}_+$ corresponds to the line $x = z, y = 0$, both of which enjoy the $\mathbb{Z}/2\mathbb{Z}$-symmetry. The cones over the three 1-cells of the envelop Figure 3.4 are seen in Figure 6.10 as the three walls separating the chamber. As we have seen in Example 5.4, the vertical line of Figure 3.3 defined by $i + it$ with $t \geq 0$ corresponds to degree 4 graphs. The cone over this line, which is the vertical wall $y = 0$ of the chamber of Figure 6.10, is exactly the space of degree 4 graphs with two edges. Therefore, as a differentiable orbifold with boundary, we have an isomorphism

$$\mathfrak{M}_{1,1} \times \mathbb{R}_+ \cong RG^{\mathrm{met}}_{1,1}. \tag{6.11}$$

Recall that the Euler characteristic of $RG^{\mathrm{met}}_{1,1}$ does not agree with the general formula (4.21). The general formula gives $1/12$, while our computation shows that it is $1/6$. The difference comes from the factor $\mathbb{Z}/2\mathbb{Z}$ of the graph automorphism groups that act trivially on the metric edge spaces. It also corresponds to the factor 2 difference between (3.16) and (3.17).

3. The Moduli Space of Three-Pointed Riemann Sphere

EXAMPLE 6.3. Let us consider another example, the complex projective line $\mathbb{P}^1$ with three ordered marked points, to illustrate the equality

$$\mathfrak{M}_{0,3} \times \mathbb{R}^3_+ = RGB^{\mathrm{met}}_{0,3}$$

and the covering map

$$RGB_{0,3}^{\mathrm{met}} \longrightarrow RG_{0,3}^{\mathrm{met}}.$$

The holomorphic automorphism group of $\mathbb{P}^1$ is $PSL(2,\mathbb{C})$, which acts on $\mathbb{P}^1$ triply transitively. Therefore, we have a biholomorphic equivalence

$$(\mathbb{P}^1,(p_1,p_2,p_3)) \cong (\mathbb{P}^1,(0,1,\infty)).$$

In other words, $\mathfrak{M}_{0,3}$ is just a point. Choose a triple (a_0,a_1,a_∞) of positive real numbers. The unique Strebel differential is given by

$$q = -\left(a\left(\frac{dz}{z}\right)^2 + b\left(\frac{dz}{1-z}\right)^2 + c\left(\frac{dz}{z(1-z)}\right)^2\right),$$

where

$$\begin{cases} a = \frac{1}{2}\left(a_0^2 + a_\infty^2 - a_1^2\right) \\ b = \frac{1}{2}\left(a_1^2 + a_\infty^2 - a_0^2\right) \\ c = \frac{1}{2}\left(a_0^2 + a_1^2 - a_\infty^2\right). \end{cases}$$

The behavior of the foliation of the Strebel differential q depends on the *discriminant*

$$ab+bc+ca = \frac{1}{4}\left(a_0+a_1+a_\infty\right)\left(a_0+a_\infty-a_1\right)\left(a_1+a_\infty-a_0\right)\left(a_0+a_1-a_\infty\right).$$

Case 1. $ab+bc+ca>0$. The graph is of degree 3 with two vertices and three edges, as given in Figure 6.11. The two vertices are located at

$$\frac{a \pm i\sqrt{ab+bc+ca}}{a+b}, \tag{6.12}$$

and the length of edges L_1, L_2 and L_3 are given by

$$\begin{cases} L_1 = \frac{1}{2}\left(a_0+a_\infty-a_1\right) = \frac{1}{2}\left(\sqrt{a+c}+\sqrt{a+b}-\sqrt{b+c}\right) \\ L_2 = \frac{1}{2}\left(a_1+a_\infty-a_0\right) = \frac{1}{2}\left(\sqrt{b+c}+\sqrt{a+b}-\sqrt{a+c}\right) \\ L_3 = \frac{1}{2}\left(a_0+a_1-a_\infty\right) = \frac{1}{2}\left(\sqrt{a+c}+\sqrt{b+c}-\sqrt{a+b}\right). \end{cases} \tag{6.13}$$

Note that positivity of L_1, L_2 and L_3 follows from $ab+bc+ca>0$. The space of metric ribbon graphs with ordered boundary in this case is just $\mathbb{R}_+^3$ because there is only one ribbon graph with boundary order of this type and a graph automorphism that preserves the boundary order is just the identity transformation.

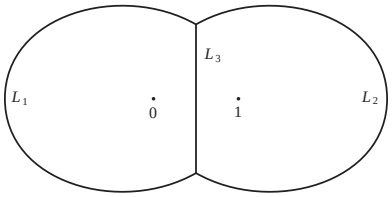

Figure 6.11. Case 1

The natural $\mathfrak{S}_3$-action on the space of (a_0,a_1,a_∞) induces faithful permutations of L_1, L_2 and L_3 through (6.13). The geometric picture can be easily seen from Figure 6.12. The normal subgroup $\mathbb{Z}/3\mathbb{Z}$ of $\mathfrak{S}_3$ acts on $\mathbb{P}^1$ as rotation about the axis connecting the north pole and the south pole, where the poles of Figure 6.12

represent the zeroes (6.12) of the Strebel differential. Note that the three non-compact leaves intersect at a zero of q with 120° angles. The action of the whole group $\mathfrak{S}_3$ is the same as the dihedral group D_3 action on the triangle $\triangle 01\infty$. As a result, $\mathfrak{S}_3$ acts on (L_1, L_2, L_3) as its full permutation group.

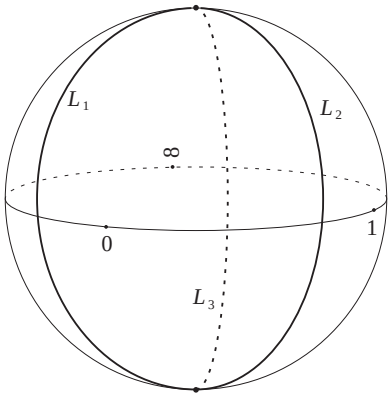

FIGURE 6.12. Degree 3 Graph on a Sphere

CASE 2. $ab+bc+ca = 0$. There are three ribbon graphs with labeled boundary components in this case, whose underlying graph is a degree 4 graph with 1 vertex and two edges (Figure 6.13). The vertex is located at $a/(a+b)$. Each of the three graphs corresponds to one of the three factors, $(a_0 + a_\infty - a_1)$, $(a_1 + a_\infty - a_0)$, and $(a_0 + a_1 - a_\infty)$, of the discriminant that is equal to 0. For example, when $(a_0 + a_1 - a_\infty) = 0$, the length of edges are given by

$$\begin{cases} L_1 = a_0 = \sqrt{a+c} \\ L_2 = a_1 = \sqrt{b+c} \\ L_3 = 0. \end{cases}$$

The $\mathfrak{S}_3$-action on (a_0, a_1, a_∞) interchanges the three types of ribbon graphs with boundary order in Case 2. The automorphism group of the ribbon graph of Case 2 is $\mathbb{Z}/2\mathbb{Z}$, and only the identity element preserves the boundary order.

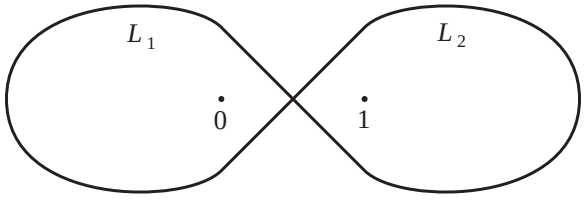

FIGURE 6.13. Case 2

CASE 3. $ab+bc+ca < 0$. The underlying graph is of degree 3 with two vertices and three edges, but the topological type is different from Case 1 (Figure 6.14). The

two vertices are on the real axis located at

$$\frac{a \pm \sqrt{-(ab+bc+ca)}}{a+b}.$$

There are again three different ribbon graphs with boundary order, each of which corresponds to one of the three factors of the discriminant that is negative. For example, if $(a_0 + a_1 - a_\infty) < 0$, then the length of edges are given by

$$\begin{cases} L_1 = a_0 = \sqrt{a+c} \\ L_2 = a_1 = \sqrt{b+c} \\ L_3 = \frac{1}{2}\left(-a_0 - a_1 + a_\infty\right) = \frac{1}{2}\left(-\sqrt{a+c} - \sqrt{b+c} + \sqrt{a+b}\right). \end{cases}$$

L_3 is positive because $ab + bc + ca < 0$.

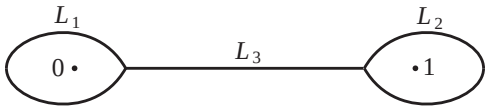

FIGURE 6.14. Case 3

In Case 2 and Case 3, the automorphism group of the ribbon graph without boundary order is $\mathbb{Z}/2\mathbb{Z}$. In every case, we can make the length of edges arbitrary by a suitable choice of (a_0, a_1, a_∞). The discriminant $ab+bc+ca$ breaks the space $\mathbb{R}^3_+$ of the triples (a_0, a_1, a_∞) into 7 pieces: 3 copies of $\mathbb{R}^3_+$ along each of the a_0-, a_1- and a_∞-axis where the discriminant is negative, the center piece of $\mathbb{R}^3_+$ characterized by positivity of the discriminant, and 3 copies of $\mathbb{R}^2_+$ separating the 4 chambers that correspond to the zero points of the discriminant (Figure 6.15):

$$\mathbb{R}^3_+ = \mathbb{R}^3_+ \coprod \mathbb{R}^2_+ \coprod \mathbb{R}^2_+ \coprod \mathbb{R}^2_+ \coprod \mathbb{R}^3_+ \coprod \mathbb{R}^3_+ \coprod \mathbb{R}^3_+. \tag{6.14}$$

The product group $\mathbb{R}^3_+$ acts on the space of (a_0, a_1, a_∞) by multiplication, but the action does not preserve the canonical rational cell-decomposition of $RGB^{\mathrm{met}}_{0,3}$. Indeed, this action changes the sign of the discriminant.

The three $\mathbb{R}^3_+$'s along the axes are equivalent under the $\mathfrak{S}_3$-action on the space of (a_0, a_1, a_∞), and each has a $\mathfrak{S}_2$-symmetry. The three walls separating the chambers are also equivalent under the $\mathfrak{S}_3$-action, and again have the same symmetry. Only the central chamber is acted by the full $\mathfrak{S}_3$. Thus we have

$$\begin{array}{ccc} \mathbb{R}^3_+ & = & \mathbb{R}^3_+ \coprod \mathbb{R}^2_+ \coprod \mathbb{R}^2_+ \coprod \mathbb{R}^2_+ \coprod \mathbb{R}^3_+ \coprod \mathbb{R}^3_+ \coprod \mathbb{R}^3_+ \\ \downarrow & & \downarrow \\ \mathbb{R}^3_+/\mathfrak{S}_3 & = & \mathbb{R}^3_+/\mathfrak{S}_3 \coprod \mathbb{R}^2_+/\mathfrak{S}_2 \coprod \mathbb{R}^3_+/\mathfrak{S}_2. \end{array} \tag{6.15}$$

4. The Moduli Space $\mathfrak{M}_{g,1}$

The multiplicative group $\mathbb{R}_+$ naturally acts on the ribbon graph complexes $RG^{\mathrm{met}}_{g,n}$ and $RGB^{\mathrm{met}}_{g,n}$ through the multiplication of a constant to the edge length. Since the graph automorphism groups $\mathrm{Aut}(\Gamma)$ and $\mathrm{Aut}_\partial(\Gamma)$ act on the edge space $\mathbb{R}^{e(\Gamma)}_+$ through a permutation of coordinate axes, the multiplicative $\mathbb{R}_+$-action and

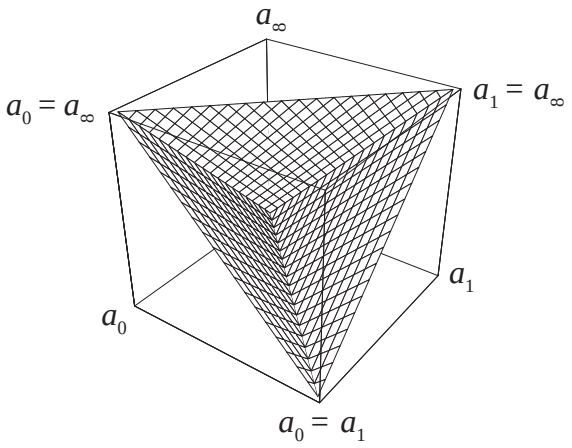

FIGURE 6.15. Partition of $\mathbb{R}^3_+$

the action of the graph automorphism groups are compatible one another. Therefore, we have quotient complexes $RG^{\mathrm{met}}_{g,n}/\mathbb{R}_+$ and $RGB^{\mathrm{met}}_{g,n}/\mathbb{R}_+$. Since $\mathbb{R}^{e(\Gamma)}_+$ is a cone over the $(e(\Gamma)-1)$-dimensional regular $e(\Gamma)$-hyperhedron $\Delta(123\cdots e(\Gamma))$ and since the graph automorphism groups act on the hyperhedron, the quotient of each rational cell is a rational simplex

$$\frac{\Delta(123\cdots e(\Gamma))}{\mathrm{Aut}(\Gamma)}.$$

Thus the quotient complexes $RG^{\mathrm{met}}_{g,n}/\mathbb{R}_+$ and $RGB^{\mathrm{met}}_{g,n}/\mathbb{R}_+$ are rational simplicial complexes.

These quotient complexes are orbifolds modeled on

$$\frac{X^{\mathrm{met}}_{\succeq\Gamma}/\mathbb{R}_+}{G},$$

where G denotes either $\mathrm{Aut}(\Gamma)$ or $\mathrm{Aut}_\partial(\Gamma)$. From (4.15), we have

$$\frac{X^{\mathrm{met}}_{\succeq\Gamma}/\mathbb{R}_+}{\mathrm{Aut}(\Gamma)} = \frac{\Delta(123\cdots e(\Gamma))\times\mathbb{R}^{\mathrm{codim}(\Gamma)}}{\mathrm{Aut}(\Gamma)}. \tag{6.16}$$

Since $\Delta(123\cdots e(\Gamma))$ is homeomorphic to $\mathbb{R}^{e(\Gamma)-1}_+$, the quotient complexes are topological orbifolds.

On the moduli space $\mathfrak{M}_{g,n}\times\mathbb{R}^n_+$, the multiplicative group $\mathbb{R}_+$ acts on the space of n-tuples $\mathbb{R}^n_+$ through the multiplication of a constant. The action has no effect on $\mathfrak{M}_{g,n}$. Thus we have the quotient space

$$\frac{\mathfrak{M}_{g,n}\times\mathbb{R}^n_+}{\mathbb{R}_+} = \mathfrak{M}_{g,n}\times\Delta(123\cdots n).$$

The bijection of Theorem 6.1 is equivariant under the $\mathbb{R}_+$-action, and we have

$$\mathfrak{M}_{g,n}\times\Delta(123\cdots n) = \coprod_{\Gamma\in RGB_{g,n}} \frac{\Delta(123\cdots e(\Gamma))}{\mathrm{Aut}_\partial(\Gamma)}. \tag{6.17}$$

This gives us an orbifold realization of the space $\mathfrak{M}_{g,n} \times \Delta(123\cdots n)$ as a rational simplicial complex. When $n = 1$, the space $\Delta(1)$ consists of just a point. Therefore, we have a rational simplicial complex realization

$$\mathfrak{M}_{g,1} = \coprod_{\Gamma \in RG_{g,1}} \frac{\Delta(123\cdots e(\Gamma))}{\mathrm{Aut}(\Gamma)}. \tag{6.18}$$

Part 2

Asymptotic Expansion of Hermitian Matrix Integrals

CHAPTER 7

Feynman Diagram Expansion of Hermitian Matrix Integrals

We have introduced the orbifold structure in $\mathfrak{M}_{g,n} \times \mathbb{R}_+^n$ through the natural bijection

$$\mathfrak{M}_{g,n} \times \mathbb{R}_+^n = \coprod_{\Gamma \in RGB_{g,n}} \frac{\mathbb{R}_+^{e(\Gamma)}}{\mathrm{Aut}_\partial(\Gamma)}$$

and proved that the orbifold Euler characteristic of this space is given by

$$n! \sum_{\Gamma \in RG_{g,n}} \frac{(-1)^{e(\Gamma)}}{|\mathrm{Aut}(\Gamma)|}. \tag{7.1}$$

In this section we explain how a Hermitian matrix integral gives the generating function of the quantities $1/|\mathrm{Aut}(\Gamma)|$. The computation of (7.1) using a special Hermitian matrix integral will be performed in the next chapter.

The relation between integrals and graph theory was discovered by Feynman. We refer to the volume edited by Schwinger [**26**] for original papers on this subject, and to [**8**] for the history of the birth of Feynman diagrams.

Feynman's method gives us the asymptotic expansion of the Hermitian matrix integral in question in terms of ribbon graphs. The notion of the graph automorphism group that arises naturally from the asymptotic analysis is exactly the same notion defined in Chapter 1. We recall that the graph automorphism we use is different from the one commonly found in graph theory.

In Section 1 we define asymptotic expansion. Section 2 describes Feynman diagram expansion of a scalar integral. We will see how the pairing scheme of Chapter 1 fits into computing the asymptotic expansion. It was G. 'tHooft [**30**] who first applied Feynman's method to a Hermitian matrix integral. Section 3 describes his method to compute the asymptotic expansion of a Hermitian matrix integral. In order to study all ribbon graphs, we need to consider the integral in infinitely many parameters and to deal with asymptotic series in an infinite number of variables. A mathematical method of dealing with these objects is presented in Section 4.

1. Asymptotic Expansion

A holomorphic function defined on a domain is completely determined by its convergent Taylor expansion at a point in the domain. At a boundary point of the domain where the function is not holomorphic, there is no longer a Taylor expansion, but we still have a useful power series expansion called an *asymptotic expansion*.

DEFINITION 7.1. Let Ω be an open domain of the complex plane $\mathbb{C}$ having the origin 0 on its boundary, and let $h(z)$ be a holomorphic function defined on Ω. A formal power series

$$\sum_{v=0}^{\infty} a_v z^v$$

is said to be an *asymptotic* expansion of $h(z)$ on Ω at $z = 0$ if

$$\lim_{\substack{z\to 0\\ z\in\Omega}} \frac{h(z) - \sum_{v=0}^{m} a_v z^v}{z^{m+1}} = a_{m+1} \tag{7.2}$$

holds for all $m \geq 0$.

Formula (7.2) shows that if $h(z)$ admits an asymptotic expansion, then it is unique. If a function $h(z)$ is holomorphic in the neighborhood of $z = 0$, then the Taylor series expansion of $h(z)$ at the origin is by definition the asymptotic expansion. In general, the asymptotic expansion does not determine the original holomorphic function. As an example, let us compute the asymptotic expansion of $e^{1/z}$ defined on a domain

$$\Omega_\epsilon = \{z \in \mathbb{C} \mid \pi/2 + \epsilon < \arg(z) < 3\pi/2 - \epsilon\} \tag{7.3}$$

for a small $\epsilon > 0$ (Figure 7.1).

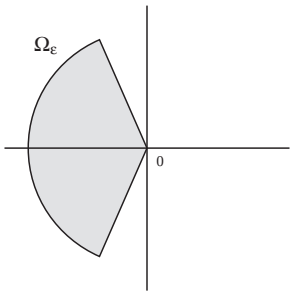

FIGURE 7.1. Domain Ω_ϵ

Since

$$\lim_{\substack{z\to 0\\ z\in\Omega_\epsilon}} \frac{e^{1/z} - 0}{z^{m+1}} = 0$$

for any $m \geq 0$, the asymptotic expansion of $e^{1/z}$ at the origin is the 0-series. Thus the asymptotic expansion does not recognize the difference between $e^{1/z}$ and the 0-function. We will use this fact many times later when we compute the Penner model. This example also shows us that even when $h(z)$ is not holomorphic at $z = 0$, its asymptotic expansion can be a convergent power series.

To indicate that the asymptotic expansion of a holomorphic function is *not equal* to the original function, we use the notation

$$\mathcal{A}\big(h(z)\big) = \sum_{v=0}^{\infty} a_v z^v. \tag{7.4}$$

If two holomorphic functions $h(z)$ and $f(z)$ defined on a domain Ω have the same asymptotic expansion at $z = 0$, then we write

$$h(z) \stackrel{A}{\equiv} f(z). \tag{7.5}$$

Thus $0 \stackrel{A}{\equiv} e^{1/z}$ at $z = 0$ as holomorphic functions defined on the domain Ω_ϵ. For two holomorphic functions $f(z)$ and $g(z)$ defined on Ω admitting the asymptotic expansions at 0, we have

$$\begin{aligned}\mathcal{A}\big(f(z) + g(z)\big) &= \mathcal{A}\big(f(z)\big) + \mathcal{A}\big(g(z)\big)\\ \mathcal{A}\big(f(z) \cdot g(z)\big) &= \mathcal{A}\big(f(z)\big) \cdot \mathcal{A}\big(g(z)\big).\end{aligned}$$

We note that the asymptotic expansion of a holomorphic function depends on the choice of the domain Ω. For example, $e^{1/z}$ does not admit any asymptotic expansion at $z = 0$ as a holomorphic function on the right half plane. However, if

$$\Omega_1 \subset \Omega_2, \qquad 0 \in \partial\Omega_1 \cap \partial\Omega_2,$$

as in Figure 7.2, and $h(z)$ has an asymptotic expansion on Ω_2 at $z = 0$, then it also admits an asymptotic expansion on Ω_1 at $z = 0$, which is actually the same series.

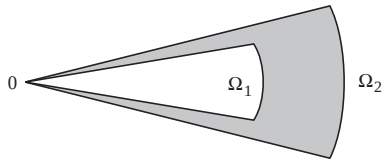

FIGURE 7.2. Domains $\Omega_1 \subset \Omega_2$

We can also define the asymptotic expansion of a real analytic function: if K is an open interval of the real axis with 0 as one of its boundary points and $h(z)$ a real analytic function on K, then the same formula (7.2), replacing Ω by K, defines the asymptotic expansion of $h(z)$ at $z = 0$.

2. The Feynman Diagram Expansion of a Scalar Integral

Now let us compute the asymptotic expansion of

$$Z(t, m) = \int_{-\infty}^{\infty} e^{-x^2/2} \exp\left(\sum_{j=1}^{2m} \frac{t_j}{j!} x^j\right) \frac{dx}{\sqrt{2\pi}}, \tag{7.6}$$

where $m > 0$ is a positive integer and

$$t = (t_1, t_2, t_3, \cdots, t_{2m}) \in \mathbb{C}^{2m}$$

is a complex vector. We choose t_{2m} such that $t_{2m} \in \Omega_\epsilon$. Then the integral $Z(t, m)$ converges and defines a holomorphic function in

$$t = (t_1, t_2, \cdots, t_{2m-1}, t_{2m}) \in \mathbb{C}^{2m-1} \times \Omega_\epsilon. \tag{7.7}$$

We can expand $Z(t, m)$ as a Taylor series in $(t_1, t_2, \cdots, t_{2m-1}) \in \mathbb{C}^{2m-1}$ and as an asymptotic series in $t_{2m} \in \Omega_\epsilon$ at the origin. Fix a value of $t_{2m} \in \Omega_\epsilon$. Then

$$\exp\left(\frac{t_{2m}}{(2m)!} x^{2m}\right)$$

acts as a uniformizing factor so that the power series expansion of the integrand in terms of x converges uniformly on $(-\infty, \infty)$ for all values of $t_1, t_2, \cdots, t_{2m-1} \in \mathbb{C}$. Therefore, we can interchange the infinite integral and the infinite sums:

$$\begin{aligned}
&Z(t,m)\\
&= \int_{-\infty}^{\infty} e^{-x^2/2} \exp\left(\sum_{j=1}^{2m} \frac{t_j}{j!} x^j\right) \frac{dx}{\sqrt{2\pi}}\\
&= \int_{-\infty}^{\infty} e^{-x^2/2} \exp\left(\frac{t_1}{1!}x\right) \cdots \exp\left(\frac{t_{2m-1}}{(2m-1)!}x^{2m-1}\right) \cdot \exp\left(\frac{t_{2m}}{(2m)!}x^{2m}\right) \frac{dx}{\sqrt{2\pi}}\\
&= \int_{-\infty}^{\infty} e^{-x^2/2} \left(\sum_{v_1=0}^{\infty} \frac{{t_1}^{v_1}}{v_1! \cdot (1!)^{v_1}}\right) \cdots \left(\sum_{v_{2m-1}=0}^{\infty} \frac{{t_{2m-1}}^{v_{2m-1}}}{v_{2m-1}! \cdot ((2m-1)!)^{v_{2m-1}}}\right)\\
&\quad \times \left(\sum_{v_{2m}=0}^{\infty} \frac{{t_{2m}}^{v_{2m}}}{v_{2m}! \cdot ((2m)!)^{v_{2m}}}\right) x^{v_1+2v_2+\cdots+(2m)v_{2m}} \frac{dx}{\sqrt{2\pi}}\\
&= \left(\sum_{v_1=0}^{\infty} \frac{{t_1}^{v_1}}{v_1! \cdot (1!)^{v_1}}\right) \cdots \left(\sum_{v_{2m-1}=0}^{\infty} \frac{{t_{2m-1}}^{v_{2m-1}}}{v_{2m-1}! \cdot ((2m-1)!)^{v_{2m-1}}}\right)\\
&\quad \times \int_{-\infty}^{\infty} e^{-x^2/2} \left(\sum_{v_{2m}=0}^{\infty} \frac{{t_{2m}}^{v_{2m}}}{v_{2m}! \cdot ((2m)!)^{v_{2m}}}\right) x^{v_1+2v_2+\cdots+(2m)v_{2m}} \frac{dx}{\sqrt{2\pi}}.
\end{aligned}$$

LEMMA 7.2. *As a holomorphic function in $z \in \Omega_\epsilon$,*

$$h(z) = \int_{-\infty}^{\infty} e^{-x^2/2} \exp\left(\frac{z}{(2m)!}x^{2m}\right) \frac{dx}{2\pi}$$

admits the asymptotic expansion

$$\mathcal{A}\left(\int_{-\infty}^{\infty} e^{-x^2/2} \exp\left(\frac{z}{(2m)!}x^{2m}\right) \frac{dx}{2\pi}\right) = \sum_{v=0}^{\infty} \frac{z^v}{v! \cdot ((2m)!)^v} \int_{-\infty}^{\infty} e^{-x^2/2} x^{(2m)v} \frac{dx}{2\pi}$$

at $z = 0$.

PROOF. For a fixed positive integer k, we have

$$\begin{aligned}
&\int_{-\infty}^{\infty} e^{-x^2/2} \exp\left(\frac{z}{(2m)!}x^{2m}\right) \frac{dx}{2\pi}\\
&= \int_{-\infty}^{\infty} e^{-x^2/2} \sum_{v=0}^{\infty} \frac{z^v}{v! \cdot ((2m)!)^v} x^{(2m)v} \frac{dx}{2\pi}\\
&= \sum_{v=0}^{k} \frac{z^v}{v! \cdot ((2m)!)^v} \int_{-\infty}^{\infty} e^{-x^2/2} x^{(2m)v} \frac{dx}{2\pi}\\
&\qquad + \int_{-\infty}^{\infty} e^{-x^2/2} \sum_{v=k+1}^{\infty} \frac{z^v}{v! \cdot ((2m)!)^v} x^{(2m)v} \frac{dx}{2\pi}.
\end{aligned}$$

Therefore,

$$\lim_{\substack{z\to 0\\ z\in\Omega_\epsilon}} \frac{\int_{-\infty}^{\infty} e^{-x^2/2}\exp\left(\frac{z}{(2m)!}x^{2m}\right)\frac{dx}{2\pi} - \sum_{v=0}^{k}\frac{z^v}{v!\cdot((2m)!)^v}\int_{-\infty}^{\infty} e^{-x^2/2}x^{(2m)v}\frac{dx}{2\pi}}{z^{k+1}}$$

$$= \lim_{\substack{z\to 0\\ z\in\Omega_\epsilon}} \int_{-\infty}^{\infty} e^{-x^2/2}\sum_{v=k+1}^{\infty}\frac{z^{v-k-1}}{v!\cdot((2m)!)^v}x^{(2m)v}\frac{dx}{2\pi}$$

$$= \frac{1}{(k+1)!\cdot((2m)!)^{k+1}}\int_{-\infty}^{\infty} e^{-x^2/2}x^{(2m)(k+1)}\frac{dx}{2\pi}.$$

This completes the proof. □

Thus we have

$$\mathcal{A}\left(\int_{-\infty}^{\infty} e^{-x^2/2}\left(\sum_{v_{2m}=0}^{\infty}\frac{{t_{2m}}^{v_{2m}}}{v_{2m}!\cdot((2m)!)^{v_{2m}}}\right)x^{v_1+2v_2+\cdots+(2m)v_{2m}}\frac{dx}{\sqrt{2\pi}}\right)$$

$$= \sum_{v_{2m}=0}^{\infty}\frac{{t_{2m}}^{v_{2m}}}{v_{2m}!\cdot((2m)!)^{v_{2m}}}\int_{-\infty}^{\infty} e^{-x^2/2}x^{v_1+2v_2+\cdots+(2m)v_{2m}}\frac{dx}{\sqrt{2\pi}},$$

and hence

$$\mathcal{A}\left(\int_{-\infty}^{\infty} e^{-x^2/2}\exp\left(\sum_{j=1}^{2m}\frac{t_j}{j!}x^j\right)\frac{dx}{\sqrt{2\pi}}\right) \tag{7.8}$$

$$= \sum_{v_1=0}^{\infty}\frac{{t_1}^{v_1}}{v_1!\cdot(1!)^{v_1}}\cdots\sum_{v_{2m}=0}^{\infty}\frac{{t_{2m}}^{v_{2m}}}{v_{2m}!\cdot((2m)!)^{v_{2m}}}\int_{-\infty}^{\infty} e^{-x^2/2}x^{v_1+2v_2+\cdots+(2m)v_{2m}}\frac{dx}{\sqrt{2\pi}}.$$

Note that (7.8) is exactly the process of interchanging the infinite sum and infinite integral. We know that these two operations are not interchangeable, but if we do interchange them, then we obtain the asymptotic expansion of the original holomorphic function, which is no longer equal to the original function.

To complete the computation, we have to evaluate the integral

$$\int_{-\infty}^{\infty} e^{-x^2/2}x^{v_1+2v_2+\cdots+(2m)v_{2m}}\frac{dx}{\sqrt{2\pi}}. \tag{7.9}$$

The standard technique is the following:

$$\int_{-\infty}^{\infty} e^{-x^2/2}x^{v_1+2v_2+\cdots+(2m)v_{2m}}\frac{dx}{\sqrt{2\pi}}$$

$$= \int_{-\infty}^{\infty} e^{-x^2/2}\left(\frac{d}{dy}\right)^{v_1+2v_2+\cdots+(2m)v_{2m}} e^{xy}\Big|_{y=0}\frac{dx}{\sqrt{2\pi}}$$

$$= \left(\frac{d}{dy}\right)^{v_1+2v_2+\cdots+(2m)v_{2m}}\int_{-\infty}^{\infty} e^{-x^2/2}e^{xy}\frac{dx}{\sqrt{2\pi}}\Big|_{y=0}$$

$$= \left(\frac{d}{dy}\right)^{v_1+2v_2+\cdots+(2m)v_{2m}}\int_{-\infty}^{\infty} e^{-(x-y)^2/2}e^{y^2/2}\frac{dx}{\sqrt{2\pi}}\Big|_{y=0}$$

$$= \left(\frac{d}{dy}\right)^{v_1+2v_2+\cdots+(2m)v_{2m}} e^{y^2/2}\Big|_{y=0},$$

where we have used the translational invariance of the integral

$$\int_{-\infty}^{\infty} e^{-(x-y)^2/2} \frac{dx}{\sqrt{2\pi}} = 1$$

for every $y \in \mathbb{R}$. The integration is reduced to a differentiation, which can be computed by a combinatorial counting. Let us denote the differential operator d/dy by a dot $\bullet$. We have altogether $v_1 + 2v_2 + \cdots + (2m)v_{2m}$ dots in the scene. We partition them into v_1 groups of single dots, v_2 groups of double dots, v_3 groups of triple dots, etc., and v_{2m} groups of $2m$ dots. Since y is set to be 0 after the differentiation, the single differentiation gives zero value:

$$\frac{d}{dy}\, e^{y^2/2}\Big|_{y=0} = y\, e^{y^2/2}\big|_{y=0} = 0.$$

To obtain a nonzero result, the differentiation must be paired:

$$\left(\frac{d}{dy}\right)^2 e^{y^2/2}\Big|_{y=0} = y^2\, e^{y^2/2}\big|_{y=0} + e^{y^2/2}\big|_{y=0} = 1.$$

Noting that the result we get by the paired differentiation is 1, we conclude that the value of the integral (7.9) is equal to *the number of pairing schemes* consisting of v_j vertices of degree j for every $j = 1, 2, \cdots, 2m$. Thus we have obtained

PROPOSITION 7.3. *Let $v_1, v_2, \cdots, v_{2m}$ be non-negative integers. Then the integral*

$$\int_{-\infty}^{\infty} e^{-x^2/2} x^{v_1 + 2v_2 + \cdots + (2m)v_{2m}} \frac{dx}{\sqrt{2\pi}}$$

is equal to the number of pairing schemes with v_1 vertices of degree 1, v_2 vertices of degree 2, $\cdots$, and v_{2m} vertices of degree $2m$.

EXAMPLE 7.1. By a straightforward calculation we obtain

$$\int_{-\infty}^{\infty} e^{-x^2/2} x^{4v} \frac{dx}{\sqrt{2\pi}} = \left(\frac{d}{dy}\right)^{4v} e^{y^2/2}\Big|_{y=0} = \frac{(4v)!}{(2v)! \cdot 2^{2v}}.$$

It is also equal to

The number of ways of making $2v$ pairs out of $4v$ dots

$$\begin{aligned} &= \binom{4v}{2}\binom{4v-2}{2}\binom{4v-4}{2}\cdots\binom{4}{2}\binom{2}{2} \Big/ (2v)! \\ &= \frac{4v(4v-1)}{2} \cdot \frac{(4v-2)(4v-3)}{2} \cdots \frac{4 \cdot 3}{2} \cdot \frac{2 \cdot 1}{2} \Big/ (2v)! \\ &= \frac{(4v)!}{(2v)! \cdot 2^{2v}}. \end{aligned}$$

Let $\mathcal{P}(v_1, \cdots, v_{2m})$ denote the set of all pairing schemes with v_j vertices of degree j for each $j = 1, 2, \cdots, 2m$. The group

$$G(v_1, \cdots, v_{2m}) = \prod_{j=1}^{2m} \mathfrak{S}_{v_j} \rtimes (\mathfrak{S}_j)^{v_j} \tag{7.10}$$

acts on $\mathcal{P}(v_1, \cdots, v_{2m})$. We defined a $G(v_1, \cdots, v_{2m})$-orbit

$$G(v_1, \cdots, v_{2m}) \cdot P$$

starting at $P \in \mathcal{P}(v_1, \cdots, v_{2m})$ as the graph Γ associated with the pairing scheme P in Section 1 of Chapter 1. The isotropy subgroup of $G(v_1, \cdots, v_{2m})$ that stabilizes the pairing scheme P is the automorphism group of the graph Γ. Since

$$|G(v_1, \cdots, v_{2m})/\mathrm{Aut}(\Gamma)| = |G(v_1, \cdots, v_{2m}) \cdot P|,$$

we obtain a counting formula

$$\sum_{\substack{\mathrm{Graph}\Gamma \\ v_j(\Gamma)=v_j}} \frac{1}{|\mathrm{Aut}(\Gamma)|} = \frac{|\mathcal{P}(v_1, \cdots, v_{2m})|}{|G(v_1, \cdots, v_{2m})|}$$

$$= \prod_{j=1}^{2m} \frac{1}{v_j! \cdot (j!)^{v_j}} \int_{-\infty}^{\infty} e^{-x^2/2} x^{v_1+2v_2+\cdots+(2m)v_{2m}} \frac{dx}{\sqrt{2\pi}},$$

where the summation runs all graphs Γ such that the number of vertices of degree j is v_j for every $j = 1, 2, \cdots, 2m$. Summarizing, we have established

THEOREM 7.4. *As a holomorphic function in*

$$t = (t_1, t_2, \cdots, t_{2m-1}, t_{2m}) \in \mathbb{C}^{2m-1} \times \Omega_\epsilon,$$

$Z(t, m)$ admits the asymptotic expansion

$$\mathcal{A}\left(\int_{-\infty}^{\infty} e^{-x^2/2} \exp\left(\sum_{j=1}^{2m} \frac{t_j}{j!} x^j \right) \frac{dx}{\sqrt{2\pi}} \right) = \sum_{\substack{\textit{Graph } \Gamma \textit{ with} \\ \textit{vertices of degree } \leq 2m}} \frac{1}{|\mathrm{Aut}(\Gamma)|} \cdot \prod_{j=1}^{2m} t_j^{v_j(\Gamma)}$$

at $t = 0$, where $v_j(\Gamma)$ denotes the number of vertices of degree j in Γ.

The above method of computing the asymptotic expansion is the celebrated *Feynman diagram expansion*. Note that the asymptotic series is a well-defined element of the formal power series ring

$$\mathbb{Q}[[t_1, t_2, \cdots, t_{2m}]],$$

because there are only finitely many graphs for given numbers $v_1(\Gamma)$, $v_2(\Gamma)$, $\cdots$, $v_{2m}(\Gamma)$.

Let us now consider the relation between general graphs and connected graphs (see Definition 2.6).

THEOREM 7.5. *As a formal power series in*

$$\mathbb{Q}[[t_1, t_2, \cdots, t_{2m}]],$$

we have an equality

$$\sum_{\substack{\textit{Graph } \Gamma \textit{ with} \\ \textit{vertices of degree } \leq 2m}} \frac{1}{|\mathrm{Aut}(\Gamma)|} \cdot \prod_{j=1}^{2m} t_j^{v_j(\Gamma)}$$

$$= \exp\left(\sum_{\substack{\textit{Connected graph } \Gamma \textit{ with} \\ \textit{vertices of degree } \leq 2m}} \frac{1}{|\mathrm{Aut}(\Gamma)|} \cdot \prod_{j=1}^{2m} t_j^{v_j(\Gamma)} \right). \tag{7.11}$$

PROOF. Note that we classify the empty graph as a non-connected graph. Thus the formal power series

$$\sum_{\substack{\text{Connected graph } \Gamma \text{ with} \\ \text{vertices of degree } \leq 2m}} \frac{1}{|\mathrm{Aut}(\Gamma)|} \cdot \prod_{j=1}^{2m} t_j^{v_j(\Gamma)}$$

takes value 0 if we set $t = 0$. Thus

$$\begin{aligned}
&\exp\left(\sum_{\substack{\text{Connected graph } \Gamma \text{ with} \\ \text{vertices of degree } \leq 2m}} \frac{1}{|\mathrm{Aut}(\Gamma)|} \cdot \prod_{j=1}^{2m} t_j^{v_j(\Gamma)}\right) \\
&= 1 + \left(\sum_{\substack{\text{Connected graph } \Gamma \text{ with} \\ \text{vertices of degree } \leq 2m}} \frac{1}{|\mathrm{Aut}(\Gamma)|} \cdot \prod_{j=1}^{2m} t_j^{v_j(\Gamma)}\right) \\
&\quad + \frac{1}{2!}\left(\sum_{\substack{\text{Connected graph } \Gamma \text{ with} \\ \text{vertices of degree } \leq 2m}} \frac{1}{|\mathrm{Aut}(\Gamma)|} \cdot \prod_{j=1}^{2m} t_j^{v_j(\Gamma)}\right)^2 \\
&\quad + \frac{1}{3!}\left(\sum_{\substack{\text{Connected graph } \Gamma \text{ with} \\ \text{vertices of degree } \leq 2m}} \frac{1}{|\mathrm{Aut}(\Gamma)|} \cdot \prod_{j=1}^{2m} t_j^{v_j(\Gamma)}\right)^3 + \cdots .
\end{aligned}$$

Each term of the above expansion gives

$$\begin{aligned}
&\frac{1}{n!}\left(\sum_{\substack{\text{Connected graph } \Gamma \text{ with} \\ \text{vertices of degree } \leq 2m}} \frac{1}{|\mathrm{Aut}(\Gamma)|} \cdot \prod_{j=1}^{2m} t_j^{v_j(\Gamma)}\right)^n \\
&= \frac{1}{n!} \sum_{\substack{\Gamma_1, \cdots, \Gamma_n \\ \text{connected graphs with} \\ \text{vertices of degree } \leq 2m}} \frac{1}{|\mathrm{Aut}(\Gamma_1)| \cdots |\mathrm{Aut}(\Gamma_n)|} \cdot \prod_{j=1}^{2m} t_j^{v_j(\Gamma_1)+\cdots+v_j(\Gamma_n)} \\
&= \sum_{\substack{\text{Graph } \Gamma \text{ with} \\ \text{vertices of degree } \leq 2m \\ \text{and } n \text{ connected components}}} \frac{1}{|\mathrm{Aut}(\Gamma)|} \cdot \prod_{j=1}^{2m} t_j^{v_j(\Gamma)}.
\end{aligned}$$

This is because if we define a disconnected graph

$$\Gamma = \Gamma_1 \cup \cdots \cup \Gamma_n$$

with n connected components $\Gamma_1, \cdots, \Gamma_n$, then

$$v_j(\Gamma) = v_j(\Gamma_1) + \cdots + v_j(\Gamma_n)$$

and

$$\frac{1}{|\mathrm{Aut}(\Gamma)|} = \frac{1}{n!} \cdot \prod_{\ell=1}^{n} \frac{1}{|\mathrm{Aut}(\Gamma_\ell)|},$$

which follows from

$$\mathrm{Aut}(\Gamma) = \mathfrak{S}_n \rtimes \prod_{\ell=1}^{n} \mathrm{Aut}(\Gamma_\ell). \tag{7.12}$$

Summing up all terms for $n = 0, 1, 2, \cdots$, we obtain the desired formula. This completes the proof. □

Let us introduce a valuation

$$val_t : \mathbb{C}[[t_1, t_2, \cdots, t_{2m}]] \longrightarrow \{0, 1, 2, \cdots, \infty\} \tag{7.13}$$

by defining $\deg(t_j) = j$. For an element $f \in \mathbb{C}[[t_1, t_2, \cdots, t_{2m}]]$ of valuation greater than 0, we define

$$\log(1 - f) = -\sum_{n=0}^{\infty} \frac{1}{n} f^n,$$

which is a well-defined element of $\mathbb{C}[[t_1, t_2, \cdots, t_{2m}]]$. Thus we have

$$\begin{aligned} &\log\left(\sum_{\substack{\text{Graph } \Gamma \text{ with} \\ \text{vertices of degree } \leq 2m}} \frac{1}{|\mathrm{Aut}(\Gamma)|} \cdot \prod_{j=1}^{2m} t_j^{v_j(\Gamma)} \right) \\ &= \sum_{\substack{\text{Connected graph } \Gamma \text{ with} \\ \text{vertices of degree } \leq 2m}} \frac{1}{|\mathrm{Aut}(\Gamma)|} \cdot \prod_{j=1}^{2m} t_j^{v_j(\Gamma)}. \end{aligned} \tag{7.14}$$

Corollary 7.6. *The asymptotic series containing only connected graphs is given by*

$$\begin{aligned} &\log \mathcal{A}\left(\int_{-\infty}^{\infty} e^{-x^2/2} \exp\left(\sum_{j=1}^{2m} \frac{t_j}{j!} x^j \right) \frac{dx}{\sqrt{2\pi}} \right) \\ &\qquad = \sum_{\substack{\textit{Connected graph } \Gamma \textit{ with} \\ \textit{vertices of degree } \leq 2m}} \frac{1}{|\mathrm{Aut}(\Gamma)|} \cdot \prod_{j=1}^{2m} t_j^{v_j(\Gamma)}. \end{aligned}$$

3. Hermitian Matrix Integrals and Ribbon Graph Expansion

Let $\mathcal{H}_q$ denote the space of $q \times q$ Hermitian matrices. It is a q^2-dimensional Euclidean space with a metric

$$\sqrt{\mathrm{trace}(X - Y)^2}, \qquad X, Y \in \mathcal{H}_q.$$

The standard volume form on $\mathcal{H}_q$, which is compatible with the above metric, is given by

$$d\mu(X) = dx_{11} \wedge dx_{22} \wedge \cdots \wedge dx_{qq} \wedge \left(\bigwedge_{i<j} d(Re x_{ij}) \wedge d(Im x_{ij}) \right)$$

for $X = [x_{ij}] \in \mathcal{H}_q$. The metric and the volume form of $\mathcal{H}_q$ are invariant under the conjugation $X \longmapsto UXU^{-1}$ by a unitary matrix $U \in U(n)$. The main subject of

this section is the *Hermitian matrix integral*

$$Z_q(t,m)=\int_{\mathcal{H}_q}\exp\left(-\frac{1}{2}\mathrm{trace}(X^2)\right)\exp\left(\mathrm{trace}\sum_{j=3}^{2m}\frac{t_j}{j}X^j\right)\frac{d\mu(X)}{N}, \tag{7.15}$$

where

$$N=\int_{\mathcal{H}_q}\exp\left(-\frac{1}{2}\mathrm{trace}(X^2)\right)d\mu(X)=2^{q/2}\cdot\pi^{q^2/2} \tag{7.16}$$

is a normalization constant to make $Z_q(0,m)=1$.

There are several differences between (7.15) and (7.6). First of all, the *coupling constant* t_j has a coefficient $1/j$ instead of $1/j!$. Secondly, we do not include the t_1 and t_2 terms in the integral. This is because of our interests in topology of the moduli spaces of Riemann surfaces, which will become clearer as we proceed. From the point of view of graphs, we do not allow degree 1 and 2 vertices in the graphs in this section.

We note that $Z_q(t,m)$ is a holomorphic function in $(t_3,t_4,\cdots,t_{2m-1})\in\mathbb{C}^{2m-3}$ and

$$t_{2m}\in\Omega_\epsilon=\{t\in\mathbb{C}|\pi/2+\epsilon<\arg(t)<3\pi/2-\epsilon\}$$

($\epsilon>0$), because the dominating term $\mathrm{trace}(X^{2m})$ is positive definite on $\mathcal{H}_q$. Thus we can expand $Z_q(t,m)$ as a convergent power series in t_3, t_4, $\cdots$, t_{2m-1} about 0 and as an asymptotic series in t_{2m} at $t_{2m}=0$, as before.

Corresponding to the fact that the integral (7.15) has richer structure than (7.6), the Feynman diagrams appearing in the asymptotic expansion of $Z_q(t,m)$ have more information than just a graph as in Theorem 7.4. As we are going to see below, the new information we have from the Hermitian matrix integral is that the graph is a ribbon graph.

THEOREM 7.7. *The asymptotic expansion of the Hermitian matrix integral $Z_q(t,m)$ as a holomorphic function in*

$$t=(t_3,t_4,\cdots,t_{2m-1},t_{2m})\in\mathbb{C}^{2m-3}\times\Omega_\epsilon$$

at $t=0$ is given by

$$\mathcal{A}\left(\int_{\mathcal{H}_q}\exp\left(-\frac{1}{2}\mathrm{trace}(X^2)\right)\exp\left(\mathrm{trace}\sum_{j=3}^{2m}\frac{t_j}{j}X^j\right)\frac{d\mu(X)}{N}\right)$$
$$=\sum_{\substack{\textit{Ribbon graph } \Gamma \textit{ with}\\ \textit{vertices of degree } 3,4,\cdots,2m}}\frac{1}{|\mathrm{Aut}(\Gamma)|}q^{b(\Gamma)}\cdot\prod_{j=3}^{2m}{t_j}^{v_j(\Gamma)},$$

where $b(\Gamma)$ denotes the number of boundary components and $v_j(\Gamma)$ the number of degree j vertices of the ribbon graph Γ.

REMARK. For given values of $v_3(\Gamma),\cdots,v_{2m}(\Gamma)$, the number of ribbon graphs is finite. Thus the above asymptotic series is a well-defined element of

$$\big(\mathbb{Q}[q]\big)[[t_3,t_4,\cdots,t_{2m}]].$$

PROOF. The proof breaks down into several parts.

First, the same technique we used in the previous section to prove (7.8) can be applied to show

$$\begin{aligned}(7.17)\quad & \mathcal{A}\left(\int_{\mathcal{H}_q}\exp\left(-\frac{1}{2}\mathrm{trace}(X^2)\right)\exp\left(\mathrm{trace}\sum_{j=3}^{2m}\frac{t_j}{j}X^j\right)\frac{d\mu(X)}{N}\right)\\ &=\sum_{v_3=0}^{\infty}\cdots\sum_{v_{2m}=0}^{\infty}\prod_{j=3}^{2m}\frac{{t_j}^{v_j}}{v_j!\cdot j^{v_j}}\int_{\mathcal{H}_q}\exp\left(-\frac{1}{2}\mathrm{trace}(X^2)\right)\prod_{j=3}^{2m}\left(\mathrm{trace}(X^j)\right)^{v_j}\frac{d\mu(X)}{N}.\end{aligned}$$

We need another matrix $Y=[y_{ij}]\in\mathcal{H}_q$ and a matrix of differential operators

$$\frac{\partial}{\partial Y}=\left[\frac{\partial}{\partial y_{ij}}\right]$$

to evaluate the above integral.

LEMMA 7.8. *For every $j>0$ and $v>0$, we have*

$$(7.18)\qquad \left(\mathrm{trace}\left(\frac{\partial}{\partial Y}\right)^j\right)^v e^{\mathrm{trace}(X^t\cdot Y)}\Big|_{Y=0}=\left(\mathrm{trace}(X^j)\right)^v.$$

PROOF. Suppose that Y and X are both arbitrary complex matrices of size q. Then for each $j>0$, we have

$$\begin{aligned}&\mathrm{trace}\left(\frac{\partial}{\partial Y}\right)^j e^{\mathrm{trace}(X^t\cdot Y)}\Big|_{Y=0}\\ &\quad=\sum_{i_1,i_2,i_3,\cdots,i_j=1}^{q}\frac{\partial}{\partial y_{i_1i_2}}\frac{\partial}{\partial y_{i_2i_3}}\cdots\frac{\partial}{\partial y_{i_ji_1}}\exp\left(\sum_{k,\ell=1}^{q}x_{k\ell}\cdot y_{k\ell}\right)\Big|_{Y=0}\\ &\quad=\sum_{i_1,i_2,i_3,\cdots,i_j=1}^{q}x_{i_1i_2}x_{i_2i_3}\cdots x_{i_ji_1}=\mathrm{trace}X^j.\end{aligned}$$

Repeating it v times, we obtain the desired formula (7.18) for general complex matrices. Certainly, the formula holds after changing coordinates:

$$\begin{cases}y_{ij}=u_{ij}+\sqrt{-1}w_{ij} & \text{for } i<j\\ y_{ji}=u_{ij}-\sqrt{-1}w_{ij} & \text{for } i<j\\ y_{ii}=u_{ii}, & \end{cases}$$

where u_{ij} and w_{ij} are complex variables. Since (7.18) is an algebraic formula, it holds for an arbitrary field of characteristic 0. In particular, (7.18) holds for real u_{ij} and w_{ij}, which proves the lemma. □

Therefore, we have

(7.19)

$$\begin{aligned}
&\int_{\mathcal{H}_q} \exp\left(-\frac{1}{2}\mathrm{trace}(X^2)\right) \prod_{j=3}^{2m} \left(\mathrm{trace}(X^j)\right)^{v_j} \frac{d\mu(X)}{N} \\
&= \int_{\mathcal{H}_q} \exp\left(-\frac{1}{2}\mathrm{trace}(X^2)\right) \prod_{j=3}^{2m} \left(\mathrm{trace}\left(\frac{\partial}{\partial Y}\right)^j\right)^{v_j} e^{\mathrm{trace}(X^t \cdot Y)}\Big|_{Y=0} \frac{d\mu(X)}{N} \\
&= \prod_{j=3}^{2m} \left(\mathrm{trace}\left(\frac{\partial}{\partial Y}\right)^j\right)^{v_j} \int_{\mathcal{H}_q} \exp\left(-\frac{1}{2}\mathrm{trace}(X - Y^t)^2\right) \cdot e^{1/2\mathrm{trace}(Y^t)^2}\Big|_{Y=0} \frac{d\mu(X)}{N} \\
&= \prod_{j=3}^{2m} \left(\mathrm{trace}\left(\frac{\partial}{\partial Y}\right)^j\right)^{v_j} e^{1/2\mathrm{trace}Y^2}\Big|_{Y=0} \\
&= \prod_{j=3}^{2m} \left(\sum_{\alpha_1,\cdots,\alpha_j} \frac{\partial}{\partial y_{\alpha_1\alpha_2}} \frac{\partial}{\partial y_{\alpha_2\alpha_3}} \cdots \frac{\partial}{\partial y_{\alpha_{j-1}\alpha_j}} \frac{\partial}{\partial y_{\alpha_j\alpha_1}}\right)^{v_j} \exp\left(\frac{1}{2}\sum_{\mu,\nu} y_{\mu\nu}y_{\nu\mu}\right)\Big|_{Y=0}.
\end{aligned}$$

The only nontrivial contribution of the differentiation comes from a paired derivatives:

$$\frac{\partial}{\partial y_{ij}} \frac{\partial}{\partial y_{k\ell}} \exp\left(\frac{1}{2}\sum_{i,j} y_{ij}y_{ji}\right)\Big|_{Y=0} = \frac{\partial}{\partial y_{ij}} y_{\ell k} = \delta_{i\ell} \cdot \delta_{jk}.$$

If we denote by $\bullet_{ij}$ the differential operator $\frac{\partial}{\partial y_{ij}}$, then we have a pairing scheme consisting of v_j sets of j dots for each $j = 3, 4, \cdots, 2m$, and the pairing of two dots $\bullet_{ij}$ and $\bullet_{k\ell}$ contributes $\delta_{i\ell} \cdot \delta_{jk}$ to the integral. The differential operator

$$\mathrm{trace}\left(\frac{\partial}{\partial Y}\right)^j$$

is represented by a sequence of j indexed dots

$$V_\alpha = \bullet_{\alpha_1\alpha_2} \bullet_{\alpha_2\alpha_3} \bullet_{\alpha_3\alpha_4} \cdots \bullet_{\alpha_{j-1}\alpha_j} \bullet_{\alpha_j\alpha_1}$$

with a cyclic ordering, which forms a vertex of the pairing scheme

$$P \in \mathcal{P}(v_3, v_4, \cdots, v_{2m}).$$

There are

$$v = v_3 + v_4 + \cdots + v_{2m}$$

vertices and

$$e = \frac{1}{2}(3v_3 + 4v_4 + \cdots + (2m)v_{2m})$$

edges in P. Let us label all edges

$$E_1, E_2, \cdots, E_e$$

of P so that E_μ connects $\bullet_{k_{\mu 1}k_{\mu 2}}$ and $\bullet_{k_{\mu 3}k_{\mu 4}}$. Then the last line of (7.19) is a sum with all indices running from 1 to q of a sum of $|\mathcal{P}(v_3, v_4, \cdots, v_{2m})|$-terms of the products of $2e$ Kronecker δ-symbols:

$$\prod_{j=3}^{2m}\left(\sum_{\alpha_1,\cdots,\alpha_j}\frac{\partial}{\partial y_{\alpha_1\alpha_2}}\frac{\partial}{\partial y_{\alpha_2\alpha_3}}\cdots\frac{\partial}{\partial y_{\alpha_{j-1}\alpha_j}}\frac{\partial}{\partial y_{\alpha_j\alpha_1}}\right)^{v_j}\exp\left(\frac{1}{2}\sum_{\mu,\nu}y_{\mu\nu}y_{\nu\mu}\right)\Bigg|_{Y=0}$$
$$=\sum_{P\in\mathcal{P}(v_3,\cdots,v_{2m})}\sum_{k_{11},\cdots,k_{14}=1}^{q}\cdots\sum_{k_{e1},\cdots,k_{e4}=1}^{q}\prod_{\mu=1}^{e}\delta_{k_{\mu1}k_{\mu4}}\delta_{k_{\mu2}k_{\mu3}}.$$

Since each vertex of P has a cyclic ordering, it has a boundary (Definition 2.11). A boundary component is a sequence of directed edges with a cyclic ordering. If E_p ends at $\bullet_{jk}$ of a vertex V, then E_{p+1} starts at $\bullet_{ij}$ of the same vertex V (Figure 7.3).

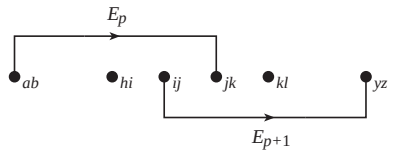

FIGURE 7.3. A Boundary Component at a Vertex

In each term of the summation, the $2e$ Kronecker δ-symbols are partitioned into $b(\Gamma)$ sets, where Γ denotes the ribbon graph associated with the pairing scheme P with cyclic ordering at each vertex, and $b(\Gamma)$ is the number of boundary components of Γ. Let $(E_{\mu_1}, E_{\mu_2}, \cdots, E_{\mu_s})$ be a boundary component of P. It contributes a factor of the form

$$\delta_{i_1i_2}\delta_{i_2i_3}\delta_{i_3i_4}\cdots\delta_{i_{n-1}i_n}\delta_{i_ni_1} \tag{7.20}$$

in the product. After summing up all the indices from 1 to q, (7.20) contributes q in the product. Therefore,

$$\sum_{k_{11},\cdots,k_{14}=1}^{q}\cdots\sum_{k_{e1},\cdots,k_{e4}=1}^{q}\prod_{\mu=1}^{e}\delta_{k_{\mu1}k_{\mu4}}\delta_{k_{\mu2}k_{\mu3}}=q^{e(\Gamma)}. \tag{7.21}$$

Recall that the group

$$G_{or}(v_3,v_4,\cdots,v_{2m})=\prod_{j=3}^{2m}\mathfrak{S}_{v_j}\rtimes(\mathbb{Z}/j\mathbb{Z})^{v_j}$$

of the orientation preserving isomorphisms of pairing schemes acts on the set $\mathcal{P}(v_3, v_4, \cdots, v_{2m})$, an orbit

$$G_{or}(v_3,v_4,\cdots,v_{2m})\cdot P$$

of this action is the ribbon graph associated with the pairing scheme, and that the automorphism group $\mathrm{Aut}(\Gamma)$ of the ribbon graph Γ is the isotropy subgroup of $G_{or}(v_3, v_4, \cdots, v_{2m})$ that stabilizes P. The computation (7.21) gives the same result for each element of the orbit. Therefore, we obtain

$$\int_{\mathcal{H}_q}\exp\left(-\frac{1}{2}\mathrm{trace}(X^2)\right)\prod_{j=3}^{2m}\left(\mathrm{trace}(X^j)\right)^{v_j}\frac{d\mu(X)}{N} \tag{7.22}$$
$$=\sum_{\Gamma\in\mathcal{P}(v_3,\cdots,v_{2m})/G_{or}(v_3,\cdots,v_{2m})}|G_{or}(v_3,\cdots,v_{2m})\cdot P|\cdot q^{b(\Gamma)}$$

$$= \sum_{\Gamma \in \mathcal{P}(v_3,\cdots,v_{2m})/G_{or}(v_3,\cdots,v_{2m})} \left| \frac{G_{or}(v_3,\cdots,v_{2m})}{\mathrm{Aut}(\Gamma)} \right| q^{b(\Gamma)}.$$

From (7.17) and (7.22), we obtain

$$\begin{aligned}
&\mathcal{A}\left(\int_{\mathcal{H}_q} \exp\left(-\frac{1}{2}\mathrm{trace}(X^2)\right) \exp\left(\mathrm{trace} \sum_{j=3}^{2m} \frac{t_j}{j} X^j\right) \frac{d\mu(X)}{N} \right) \\
&= \sum_{v_3=0}^{\infty} \cdots \sum_{v_{2m}=0}^{\infty} \prod_{j=3}^{2m} \frac{{t_j}^{v_j}}{v_j! \cdot j^{v_j}} \sum_{\Gamma \in \mathcal{P}(v_3,\cdots,v_{2m})/G_{or}(v_3,\cdots,v_{2m})} \left| \frac{G_{or}(v_3,\cdots,v_{2m})}{\mathrm{Aut}(\Gamma)} \right| q^{b(\Gamma)} \\
&= \sum_{\substack{\text{Ribbon graph } \Gamma \text{ with} \\ \text{vertices of degree } 3,4,\cdots,2m}} \frac{1}{|\mathrm{Aut}(\Gamma)|} q^{b(\Gamma)} \cdot \prod_{j=3}^{2m} {t_j}^{v_j(\Gamma)}.
\end{aligned}$$

This completes the proof. □

The relation between connected ribbon graphs and arbitrary ribbon graphs are the same as in the previous section. In particular, since (7.12) also holds for ribbon graphs, application of the logarithm gives us

$$\begin{aligned}
&\log \mathcal{A}\left(\int_{\mathcal{H}_q} \exp\left(-\frac{1}{2}\mathrm{trace}(X^2)\right) \exp\left(\mathrm{trace} \sum_{j=3}^{2m} \frac{t_j}{j} X^j\right) \frac{d\mu(X)}{N} \right) \\
&\qquad = \sum_{\substack{\text{Connected ribbon graph } \Gamma \\ \text{with maximum degree } 2m}} \frac{1}{|\mathrm{Aut}(\Gamma)|} q^{b(\Gamma)} \cdot \prod_{j=3}^{2m} {t_j}^{v_j(\Gamma)}.
\end{aligned} \tag{7.23}$$

We can rearrange the summation in terms of the genus of a compact oriented surface $C(\Gamma)$ and the number of marked points on it.

$$\begin{aligned}
&\log \mathcal{A}\left(Z_q(t,m)\right) \\
&= \sum_{\substack{g \geq 0, n > 0 \\ 2-2g-n<0}} \left(\sum_{\substack{\text{Connected ribbon graph } \Gamma \\ \text{with vertices of degree } 3,4,\cdots,2m, \\ \chi(\Gamma)=2-2g-n, b(\Gamma)=n}} \frac{q^n}{|\mathrm{Aut}(\Gamma)|} \cdot \prod_{j=3}^{2m} t_j^{v_j(\Gamma)} \right),
\end{aligned} \tag{7.24}$$

where $\chi(\Gamma) = v(\Gamma) - e(\Gamma)$ is the Euler characteristic of Γ.

4. Asymptotic Series in an Infinite Number of Variables

In the previous section we considered the asymptotic expansion of a holomorphic function $Z_q(t,m)$ in $t = (t_3, \cdots, t_{2m-1}, t_{2m})$. The asymptotic series is given by ribbon graphs with vertices of degree $3, 4, \cdots, 2m$. To apply the ribbon graph expansion to the moduli spaces of Riemann surfaces with marked points, we have to deal with ribbon graphs with vertices of arbitrary degree. This means we have to take the limit $m \to \infty$.

The power series

$$\sum_{\substack{g\geq 0, n>0\\ 2-2g-n<0}} \left(\sum_{\substack{\text{Connected ribbon graph } \Gamma\\ \text{with vertices of degree } 3,4,\cdots,2m,\\ \chi(\Gamma)=2-2g-n, b(\Gamma)=n}} \frac{q^n}{|\mathrm{Aut}(\Gamma)|} \cdot \prod_{j=3}^{2m} t_j^{v_j(\Gamma)} \right) \tag{7.25}$$

is an element of the formal power series ring

$$\big(\mathbb{Q}[q]\big)[[t_3, t_4, \cdots, t_{2m}]].$$

Let $\big(\mathbb{Q}[q]\big)[[t_3, t_4, \cdots]]$ be the formal power series ring in infinitely many variables. The *adic* topology of this ring is given by the degree

$$\deg t_k = k, \qquad k \geq 3$$

and the ideal $\mathfrak{I}_k(t)$ of $\big(\mathbb{Q}[q]\big)[[t_3, t_4, \cdots]]$ generated by polynomials in $t_3, t_4, \cdots$ of degree greater than or equal to k with coefficients in $\mathbb{Q}[q]$. There is a natural projection

$$\pi_k : \big(\mathbb{Q}[q]\big)[[t_3, t_4, \cdots]] \longrightarrow \big(\mathbb{Q}[q]\big)[[t_3, t_4, \cdots]]/\mathfrak{I}_k(t) = \big(\mathbb{Q}[q]\big)[[t_3, \cdots, t_{k-1}]]/\mathfrak{I}_k(t).$$

The degree of the monomial in (7.25) is

$$\deg \left(\prod_{j=3}^{2m} t_j^{v_j(\Gamma)} \right) = 3v_3(\Gamma) + 4v_4(\Gamma) + \cdots + (2m)v_{2m}(\Gamma) = v(\Gamma). \tag{7.26}$$

If we consider only the terms in (7.25) of degree less than or equal to k for $k \leq 2m$, then they do not depend on m at all. Therefore, for each fixed $k \geq 0$, the projection image

$$\pi_k\big(\log \mathcal{A}\big(Z_q(t,m)\big)\big) \in \big(\mathbb{Q}[q]\big)[[t_3, t_4, \cdots]]/\mathfrak{I}_k(t) = \big(\mathbb{Q}[q]\big)[[t_3, \cdots, t_{k-1}]]/\mathfrak{I}_k(t)$$

is stable for all $2m \geq k$.

Since the formal power series ring is defined by the projective system

$$\big(\mathbb{Q}[q]\big)[[t_3, t_4, \cdots]] = \varprojlim_k \big(\mathbb{Q}[q]\big)[[t_3, t_4, \cdots]]/\mathfrak{I}_k(t)$$

and since

$$\big\{\pi_{2m}\big(\log \mathcal{A}\big(Z_q(t,m)\big)\big)\big\}_{m\geq 2}$$

defines an element of this projective system, it gives a well-defined formal power series in infinitely many variables. We denote it symbolically by

$$\begin{aligned} &\lim_{m\to\infty} \log \mathcal{A}\big(Z_q(t,m)\big) \\ &\qquad = \big\{\pi_{2m}\big(\log \mathcal{A}\big(Z_q(t,m)\big)\big)\big\}_{m\geq 2} \in \big(\mathbb{Q}[q]\big)[[t_3, t_4, \cdots]]. \end{aligned} \tag{7.27}$$

Going back to the Feynman diagram expansion, we have established the following:

THEOREM 7.9. *Recall that $RG_{g,n}$ is the set of all isomorphism classes of connected ribbon graphs with $\chi(\Gamma) = 2-2g-n$ and $b(\Gamma) = n$. We have*

$$\lim_{m\to\infty} \log \mathcal{A}\big(Z_q(t,m)\big) = \sum_{\substack{g\geq 0, n\geq 1\\ 2-2g-n<0}} \left(\sum_{\Gamma\in RG_{g,n}} \frac{q^n}{|\mathrm{Aut}(\Gamma)|} \cdot \prod_{j\geq 3} t_j^{v_j(\Gamma)} \right) \tag{7.28}$$

as an element of $\big(\mathbb{Q}[q]\big)[[t_3, t_4, \cdots]]$.

For each fixed g and n, the maximum possible degree of vertices of the ribbon graphs in the second summation is $4g + 2n - 2$. To see this, let Γ be a graph with the largest possible degree ℓ. Since the Euler characteristic of Γ is given by $2-2g-n = v(\Gamma)-e(\Gamma)$, the degree becomes maximum when Γ has only one vertex. Thus

$$2 - 2g - n = 1 - \frac{1}{2}\ell.$$

This shows us that the right hand side of (7.28) does not have any infinite products.

CHAPTER 8

Computation of the Euler Characteristic of the Moduli Space

In this chapter we compute the Euler characteristic of the moduli space of Riemann surfaces with marked points and positive real numbers. The evaluation of $\chi\left(\mathfrak{M}_{g,n}\times\mathbb{R}_+^n\right)$ requires some analysis. In particular, a rigorous analytic technique of asymptotic series in infinitely many variables has to be established. We supply here everything we need, and complete the computation of the Euler characteristic in terms of a special value of the Riemann zeta function.

1. The Euler Characteristic of the Moduli Space

We give a proof of the following theorem due to Harer and Zagier [**10**] in this chapter.

THEOREM 8.1. *The Euler characteristic of the orbifold $\mathfrak{M}_{g,n}\times\mathbb{R}_+^n$ is given by*

$$\chi\left(\mathfrak{M}_{g,n}\times\mathbb{R}_+^n\right)=-\frac{(2g+n-3)!(2g)(2g-1)}{(2g)!}\zeta(1-2g) \tag{8.1}$$

for every $g\geq 0$ and $n\geq 1$ subject to $2-2g-n<0$ and $(g,n)\neq(1,1)$, where ζ is the Riemann zeta function. For $(g,n)=(1,1)$, we have

$$\chi\left(\mathfrak{M}_{1,1}\times\mathbb{R}_+\right)=-2\zeta(-1)=\frac{1}{6}.$$

The idea of the proof is that the generating function of $\chi\left(\mathfrak{M}_{g,n}\times\mathbb{R}_+^n\right)$ is given by a Hermitian matrix integral, and that the asymptotic expansion of the integral is exactly computable. We follow closely the line of arguments of [**21**], but our actual computation is based on the asymptotic analysis of [**18**].

Let us start with the generating function

$$F(q,z)=\sum_{\substack{g\geq 0,n\geq 1\\ 2-2g-n<0}}\left(\sum_{\Gamma\in RG_{g,n}}\frac{(-1)^{e(\Gamma)}}{|\mathrm{Aut}(\Gamma)|}\right)q^n(-z)^{-2+2g+n}. \tag{8.2}$$

Since

$$\chi\left(\mathfrak{M}_{g,n}\times\mathbb{R}_+^n\right)=n!\sum_{\Gamma\in RG_{g,n}}\frac{(-1)^{e(\Gamma)}}{|\mathrm{Aut}(\Gamma)|}$$

by (6.10), it is sufficient to know $F(q,z)$ to find the value of $\chi\left(\mathfrak{M}_{g,n}\times\mathbb{R}_+^n\right)$. If we compare (7.28)

$$\lim_{m\to\infty}\log\mathcal{A}\big(Z_q(t,m)\big)=\sum_{\substack{g\geq 0,n\geq 1\\ 2-2g-n<0}}\left(\sum_{\Gamma\in RG_{g,n}}\frac{q^n}{|\mathrm{Aut}(\Gamma)|}\cdot\prod_{j\geq 3}t_j^{v_j(\Gamma)}\right)$$

and (8.2), then we see that the substitution

$$t_j = -\left(\sqrt{z}\right)^{j-2}, \quad j = 3, 4, \cdots, \tag{8.3}$$

changes (7.28) to (8.2), where $\sqrt{z}$ is defined for $Re(z) > 0$. Indeed, for every ribbon graph Γ, we have

$$\begin{aligned}(-1)^{e(\Gamma)}(-z)^{-\chi(\Gamma)} &= (-1)^{v(\Gamma)} z^{e(\Gamma)-v(\Gamma)} \\ &= (-1)^{\sum v_j(\Gamma)} \cdot z^{\frac{1}{2}\sum j v_j(\Gamma) - \sum v_j(\Gamma)} \\ &= \prod_{j\geq 3} \left(-(\sqrt{z})^{j-2}\right)^{v_j(\Gamma)}.\end{aligned}$$

This leads us to the *Penner model*.

2. The Penner Model

There are no known analytic methods to compute the matrix integral $Z_q(t, m)$ for general m. Penner observed that at the limit of $m \to \infty$, the specialization (8.3) of $Z_q(t, m)$ is actually computable.

The condition

$$\pi/2 + \epsilon < \arg(t_{2m}) < 3\pi/2 - \epsilon$$

of t_{2m} translates into the condition

$$|\arg(z)| < \frac{\pi}{2m-2} \tag{8.4}$$

of z. Thus we have a holomorphic function

$$\begin{aligned}&P_q(z, m) \\ &= \int_{\mathcal{H}_q} \exp\left(-\frac{1}{2}\mathrm{trace}(X^2)\right) \exp\left(-\sum_{j=3}^{2m} \frac{(\sqrt{z})^{j-2}}{j}\mathrm{trace}(X^j)\right) \frac{d\mu(X)}{N} \\ &= \int_{\mathcal{H}_q} \exp\left(-\sum_{j=2}^{2m} \frac{(\sqrt{z})^{j-2}}{j}\mathrm{trace}(X^j)\right) \frac{d\mu(X)}{N}\end{aligned} \tag{8.5}$$

defined on the region of the complex plane given by (8.4) (Figure 8.1).

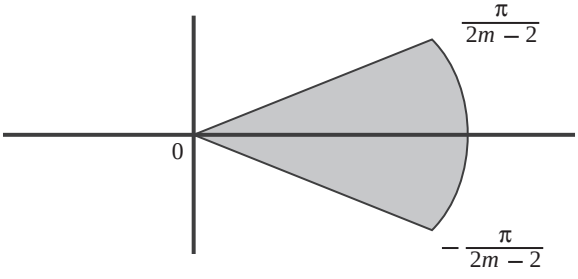

FIGURE 8.1. A Wedge-shape Domain

We note that the domain in Figure 8.1 still makes sense as the positive real axis when we take the limit $m \to \infty$. The quantity N is the same normalization constant as in (7.16).

The asymptotic expansion of (8.5) at $z = 0$ can be calculated by making the same substitution (8.3) in (7.28). Taking the logarithm, we obtain

$$\begin{aligned}&\log \mathcal{A}\left(P_q(z,m)\right)\\ &= \sum_{\substack{g\geq 0, n\geq 1\\ 2-2g-n<0}} \left(\sum_{\substack{\text{Connected ribbon graph } \Gamma\\ \text{with vertices of degree } 3,4,\cdots,2m,\\ \chi(\Gamma)=2-2g-n, b(\Gamma)=n}} \frac{(-1)^{e(\Gamma)}}{|\mathrm{Aut}(\Gamma)|} \right) q^n \cdot (-z)^{2g+n-2}.\end{aligned} \tag{8.6}$$

Note that the right hand side of (8.6) is a well-defined element of $\big(\mathbb{Q}[q]\big)[[z]]$. For every $\nu > 0$, the terms in $\log \mathcal{A}\left(P_q(z,m)\right)$ of degree less than or equal to ν with respect to z are stable for all $m \geq \nu + 1$. Again by the same argument we used in the previous section, we can define an element

$$\lim_{m\to\infty} \log \mathcal{A}\left(P_q(z,m)\right) \in \big(\mathbb{Q}[q]\big)[[z]].$$

Thus we have an equality

$$\begin{aligned}&\lim_{m\to\infty} \log \mathcal{A}\left(\int_{\mathcal{H}_q} \exp\left(-\sum_{j=2}^{2m} \frac{(\sqrt{z})^{j-2}}{j} \mathrm{trace}(X^j) \right) \frac{d\mu(X)}{N} \right)\\ &= \sum_{\substack{g\geq 0, n\geq 1\\ 2-2g-n<0}} \left(\sum_{\Gamma \in RG_{g,n}} \frac{(-1)^{e(\Gamma)}}{|\mathrm{Aut}(\Gamma)|} \right) q^n \cdot (-z)^{2g+n-2}\\ &= F(q,z)\end{aligned} \tag{8.7}$$

as a well-defined element of $\big(\mathbb{Q}[q]\big)[[z]]$. We recall that the number of ribbon graphs for fixed g and n is finite.

3. Asymptotic Analysis of Penner Model

In this section we calculate the asymptotic expansion of Penner model analytically. The standard analytic technique to compute Hermitian matrix integrals is the following.

THEOREM 8.2. *Let $f(X)$ be a function on $X \in \mathcal{H}_q$ which is invariant under the conjugation by a unitary matrix $U \in U(q)$:*

$$f(X) = f(U^{-1} \cdot X \cdot U) = f(k_0, k_1, \cdots, k_{q-1}),$$

where $k_0, k_1, \cdots, k_{q-1}$ are the eigenvalues of the Hermitian matrix X. If $f(X)$ is integrable on $\mathcal{H}_q$ with respect to the measure $d\mu(X)$, then

$$\int_{\mathcal{H}_q} f(X) d\mu(X) = c(q) \cdot \int_{\mathbb{R}^q} f(k_0, k_1, \cdots, k_{q-1}) \Delta(k)^2 dk_0 dk_1 \cdots dk_{q-1}, \tag{8.8}$$

where

$$c(q) = \frac{\pi^{q(q-1)/2}}{q! \cdot (q-1)! \cdots 2! \cdot 1!}, \tag{8.9}$$

and

$$\Delta(k) = \Delta\big(k_0, k_1 \cdots, k_{q-1}\big) = \det \begin{pmatrix} 1 & k_0 & k_0^2 & \dots & k_0^{q-1} \\ 1 & k_1 & k_1^2 & \dots & k_1^{q-1} \\ 1 & k_2 & k_2^2 & \dots & k_2^{q-1} \\ \vdots & \vdots & \vdots & \ddots & \vdots \\ 1 & k_{q-1} & k_{q-1}^2 & \dots & k_{q-1}^{q-1} \end{pmatrix} = \prod_{i>j} (k_i - k_j)$$

is the Vandermonde determinant.

PROOF. Let $\overset{\circ}{\mathcal{H}}_q$ denote the open dense subset of $\mathcal{H}_q$ consisting of non-singular Hermitian matrices of size q with q distinct eigenvalues. If $f(X)$ is a regular integrable function on $\mathcal{H}_q$, then

$$\int_{\mathcal{H}_q} f(X) d\mu(X) = \int_{\overset{\circ}{\mathcal{H}}_q} f(X) d\mu(X).$$

We denote by $\overset{\circ}{\mathbb{R}}{}^q$ the space of real diagonal matrices of all distinct, non-zero eigenvalues. Here again integration over $\mathbb{R}^q$ is equal to integration over $\overset{\circ}{\mathbb{R}}{}^q$. Since every Hermitian matrix is diagonalizable by a unitary matrix, we have a surjective map

$$U(q) \times \overset{\circ}{\mathbb{R}}{}^q \ni \left(U, \begin{bmatrix} k_0 & & \\ & \ddots & \\ & & k_{q-1} \end{bmatrix} \right) \longmapsto U \cdot \begin{bmatrix} k_0 & & \\ & \ddots & \\ & & k_{q-1} \end{bmatrix} \cdot U^{-1} \in \overset{\circ}{\mathcal{H}}_q.$$

The fiber of this map is the set of all unitary matrices that are commutative with a generic real diagonal matrix, which can be identified with the product of two subgroups

$$T^q \cdot W_q \subset U(q),$$

where $T^q \subset U(q)$ is the maximal torus of $U(q)$, and $W_q \subset U(q)$ the group of permutation matrices of size q. Note that

$$\dim U(q) = \dim \mathcal{H}_q = q^2, \quad \dim T^q = q.$$

Therefore, the induced map

$$h : U(q)/T^q \times \overset{\circ}{\mathbb{R}}{}^q \longrightarrow \overset{\circ}{\mathcal{H}}_q$$

is a covering map of degree $|W_q| = q!$. We need the Jacobian determinant of h. Put

$$X = \big[x_{ij}\big] = U \cdot \begin{bmatrix} k_0 & & \\ & \ddots & \\ & & k_{q-1} \end{bmatrix} \cdot U^{-1} \in \overset{\circ}{\mathcal{H}}_q,$$

and denote

$$dX = \big[dx_{ij}\big].$$

Then

$$dX = dU \cdot \begin{bmatrix} k_0 & & \\ & \ddots & \\ & & k_{q-1} \end{bmatrix} \cdot U^{-1} + U \cdot \begin{bmatrix} dk_0 & & \\ & \ddots & \\ & & dk_{q-1} \end{bmatrix} \cdot U^{-1}$$

$$
\begin{aligned}
&- U \cdot \begin{bmatrix} k_0 & & \\ & \ddots & \\ & & k_{q-1} \end{bmatrix} \cdot U^{-1} \cdot dU \cdot U^{-1} \\
&= U \cdot \begin{bmatrix} dk_0 & & \\ & \ddots & \\ & & dk_{q-1} \end{bmatrix} \cdot U^{-1} + \big[dU \cdot U^{-1}, X\big] \\
&= U \cdot \left(\begin{bmatrix} dk_0 & & \\ & \ddots & \\ & & dk_j \end{bmatrix} + \left[U^{-1} \cdot dU, \begin{bmatrix} k_0 & & \\ & \ddots & \\ & & k_{q-1} \end{bmatrix} \right] \right) \cdot U^{-1} \\
&= U \cdot \left(\begin{bmatrix} dk_0 & & \\ & \ddots & \\ & & dk_{q-1} \end{bmatrix} + \big[(k_j - k_i) d\omega_{ij} \big] \right) \cdot U^{-1},
\end{aligned}
$$

where

$$U^{-1} \cdot dU = \big[d\omega_{ij}\big],$$

which is a skew-Hermitian matrix. In terms of the above expression, we compute

$$d\mu(X) = dk_0 \wedge \cdots \wedge dk_{q-1} \wedge \left(\bigwedge_{i<j} (k_j - k_i)^2 Re(d\omega_{ij}) \wedge Im(d\omega_{ij}) \right).$$

Thus the integration on $\overset{\circ}{\mathcal{H}}_q$ is separated to integration on $U(q)/T^q$ and $\overset{\circ}{\mathbb{R}}^q$. Let

$$c(q) = \frac{1}{q!} \int_{U(q)/T^q} \bigwedge_{i<j} Re(d\omega_{ij}) \wedge Im(d\omega_{ij}).$$

Then we obtain

$$\int_{\overset{\circ}{\mathcal{H}}_q} f(X) d\mu(X) = c(q) \int_{\overset{\circ}{\mathbb{R}}^q} \Delta(k)^2 f(k_0, \cdots, k_{q-1}) dk_0 \cdots dk_{q-1}.$$

For the computation of $c(q)$, we refer to Bessis-Itzykson-Zuber [**2**]. □

Using formula (8.8), we can reduce our integral to

$$P_q(z,m) = \frac{c(q)}{N} \int_{\mathbb{R}^q} \Delta(k)^2 \prod_{i=0}^{q-1} \left(\exp\left(-\sum_{j=2}^{2m} \frac{(\sqrt{z})^{j-2}}{j} k_i^j \right) dk_i \right).$$

The following is our key idea to compute the Penner model.

THEOREM 8.3 ([**18**]). *Let $\mathfrak{I}_\nu(z) = z^\nu \cdot \mathbb{C}[[z]]$ denote the ideal of $\mathbb{C}[[z]]$ generated by z^ν, and*

$$\pi_\nu : \mathbb{C}[[z]] \longrightarrow \mathbb{C}[[z]]/\mathfrak{I}_\nu(z)$$

the natural projection. For an arbitrary polynomial $p(k) \in \mathbb{C}[k]$, consider the following two asymptotic series:

$$a(z,m) = \mathcal{A}\left(\int_{-\infty}^{\infty} p(k) \cdot \exp\left(-\sum_{j=2}^{2m} \frac{(\sqrt{z})^{j-2}}{j} k^j \right) dk \right) \in \mathbb{C}[[z]]$$

as $z \to +0$ *with* $|\arg(z)| < \frac{\pi}{2m-2}$, *and*

$$b(z) = \mathcal{A}\left(\sqrt{z}(ez)^{1/z}\int_0^\infty p\left(\frac{1-zx}{\sqrt{z}}\right)\cdot x^{1/z}\cdot e^{-x}\cdot dx\right) \in \mathbb{C}[[z]]$$

as $z \to +0$ *with* z *real and positive. Then for every* $m > 2$, *we have*

$$\pi_m\big(a(z,m)\big) = \pi_m\big(b(z)\big)$$

as an element of $\mathbb{C}[[z]]/\mathfrak{I}_m(z)$. *In other words,*

$$\lim_{m\to\infty}\mathcal{A}\left(\int_{-\infty}^\infty p(k)\cdot\exp\left(-\sum_{j=2}^{2m}\frac{(\sqrt{z})^{j-2}}{j}k^j\right)dk\right)$$
$$= \mathcal{A}\left(\sqrt{z}(ez)^{1/z}\int_0^\infty p\left(\frac{1-zx}{\sqrt{z}}\right)\cdot x^{1/z}\cdot e^{-x}\cdot dx\right)$$

holds with respect to the $\mathfrak{I}_m(z)$*-adic topology of* $\mathbb{C}[[z]]$.

Remark. The above integrals are not equal as holomorphic functions in z. The limit $m \to \infty$ makes sense only for real positive z, and the equality holds only asymptotically.

Proof. Putting $y = \sqrt{z}k$, we have

$$\int_{-\infty}^\infty p(k)\cdot\exp\left(-\sum_{j=2}^{2m}\frac{(\sqrt{z})^{j-2}}{j}k^j\right)dk$$
$$= \frac{1}{\sqrt{z}}\int_{-\infty}^\infty p\left(\frac{y}{\sqrt{z}}\right)\cdot\exp\left(-\frac{1}{z}\sum_{j=2}^{2m}\frac{y^j}{j}\right)dy$$
$$= \int_{-\infty}^\infty d\nu(y,m),$$

where

$$d\nu(y,m) = \frac{1}{\sqrt{z}}\cdot p\left(\frac{y}{\sqrt{z}}\right)\cdot\exp\left(-\frac{1}{z}\sum_{j=2}^{2m}\frac{y^j}{j}\right)dy.$$

Let us decompose the integral into three pieces:

$$\int_{-\infty}^\infty d\nu(y,m) = \int_{-\infty}^{-1} d\nu(y,m) + \int_{-1}^1 d\nu(y,m) + \int_1^\infty d\nu(y,m). \tag{8.10}$$

Note that the polynomial $\sum_{j=2}^{2m}\frac{y^j}{j}$ of degree $2m$ takes positive values on the intervals $(-\infty,-1]$ and $[1,\infty)$. Since $p(k)$ is a polynomial, it is obvious that the asymptotic expansion of the first and the third integrals of the right hand side of (8.10) for $z \to +0$ with $z > 0$ is the 0-series. Therefore, we have

$$\int_{-\infty}^\infty d\nu(y,m) \overset{A}{\equiv} \int_{-1}^1 d\nu(y,m).$$

On the interval $[-1,1]$, if we fix a z such that $Re(z) > 0$, then the convergence

$$\lim_{m\to\infty}\exp\left(-\frac{1}{z}\sum_{j=2}^{2m}\frac{y^j}{j}\right) = (1-y)^{1/z}\cdot e^{y/z}$$

is absolute and uniform with respect to y. Thus, for a new variable $t = 1 - y$, we have

$$\begin{aligned}
&\lim_{m\to\infty}\int_{-1}^{1} d\nu(y,m) \\
&= \frac{1}{\sqrt{z}}\int_{-1}^{1} p\left(\frac{y}{\sqrt{z}}\right)(1-y)^{1/z}e^{y/z}dy \\
&= \frac{1}{\sqrt{z}}e^{1/z}\int_{0}^{2} p\left(\frac{1-t}{\sqrt{z}}\right)t^{1/z}e^{-t/z}dt \\
&= \frac{1}{\sqrt{z}}e^{1/z}\int_{0}^{\infty} p\left(\frac{1-t}{\sqrt{z}}\right)t^{1/z}e^{-t/z}dt - \frac{1}{\sqrt{z}}e^{1/z}\int_{2}^{\infty} p\left(\frac{1-t}{\sqrt{z}}\right)t^{1/z}e^{-t/z}dt.
\end{aligned}$$

This last integral is

$$\frac{1}{\sqrt{z}}e^{1/z}\int_{2}^{\infty} p\left(\frac{1-t}{\sqrt{z}}\right)t^{1/z}e^{-t/z}dt = \frac{1}{\sqrt{z}}\int_{2}^{\infty} p\left(\frac{1-t}{\sqrt{z}}\right)e^{(1+\log t - t)/z}dt.$$

Since $1 + \log t - t < 0$ for $t \geq 2$, the asymptotic expansion of this integral as $z \to +0$ with $z > 0$ is the 0-series. Therefore, since the integrals do not depend on the integration variables, we have

$$\begin{aligned}
&\lim_{m\to\infty}\mathcal{A}\left(\int_{-\infty}^{\infty} p(k)\cdot\exp\left(-\sum_{j=2}^{2m}\frac{(\sqrt{z})^{j-2}}{j}k^j\right)dk\right) \\
&\qquad = \mathcal{A}\left(\frac{1}{\sqrt{z}}e^{1/z}\int_{0}^{\infty} p\left(\frac{1-t}{\sqrt{z}}\right)t^{1/z}e^{-t/z}dt\right) \\
&\qquad = \mathcal{A}\left(\sqrt{z}e^{1/z}z^{1/z}\int_{0}^{\infty} p\left(\frac{1-zx}{\sqrt{z}}\right)x^{1/z}e^{-x}dx\right)
\end{aligned}$$

as a formal power series in z. This completes the proof of Theorem. □

By applying Theorem 8.3 for each k_i, we obtain

$$\begin{aligned}
&\lim_{m\to\infty}\mathcal{A}\left(\int_{\mathbb{R}^q}\Delta(k)^2\cdot\prod_{i=0}^{q-1}\exp\left(-\sum_{j=2}^{2m}\frac{(\sqrt{z})^{j-2}}{j}k_i^j\right)dk_i\right) \\
&= \mathcal{A}\left(\left(\sqrt{z}e^{1/z}z^{1/z}\right)^q\int_0^\infty\cdots\int_0^\infty\Delta\left(\frac{1-zx}{\sqrt{z}}\right)^2\cdot\prod_{i=0}^{q-1}x_i^{1/z}e^{-x_i}dx_i\right) \qquad (8.11) \\
&= \mathcal{A}\left(\left(\sqrt{z}e^{1/z}z^{1/z}\right)^q z^{\frac{q(q-1)}{2}}\int_0^\infty\cdots\int_0^\infty\Delta(x)^2\cdot\prod_{i=0}^{q-1}x_i^{1/z}e^{-x_i}dx_i\right),
\end{aligned}$$

where we used the multilinear property of the Vandermonde determinant. We can use the standard technique of orthogonal polynomials to compute the above integral. Let $p_j(x)$ be a monic orthogonal polynomial in x of degree j with respect to the measure

$$d\lambda(x) = x^{1/z}e^{-x}dx$$

defined on $K = [0,\infty)$ for a positive $z > 0$, i.e.,

$$\int_K p_i(x)p_j(x)d\lambda(x) = \delta_{ij} \parallel p_j(x) \parallel^2 .$$

Because of the multilinearity of the determinant, we have once again

$$\Delta(x) = \det\left(x_i^j\right) = \det\left(p_j(x_i)\right).$$

Therefore,

$$\begin{aligned}
&\int_{K^q} \Delta(x)^2 d\lambda(x_0)\cdots d\lambda(x_{q-1}) \\
&= \int_{K^q} \det\left(p_j(x_i)\right) \det\left(p_j(x_i) d\lambda(x_i)\right) \\
&= \int_{K^q} \sum_{\sigma\in\mathfrak{S}_q} \sum_{\tau\in\mathfrak{S}_q} \operatorname{sign}(\sigma)\operatorname{sign}(\tau) \prod_{i=0}^{q-1} p_{\sigma(i)}(x_i) \prod_{i=0}^{q-1} p_{\tau(i)}(x_i) d\lambda(x_i) \\
&= \sum_{\sigma\in\mathfrak{S}_q} \sum_{\tau\in\mathfrak{S}_q} \operatorname{sign}(\sigma)\operatorname{sign}(\tau) \prod_{i=0}^{q-1} \int_K p_{\sigma(i)}(x) p_{\tau(i)}(x) d\lambda(x) \\
&= \sum_{\sigma\in\mathfrak{S}_q} \operatorname{sign}(\sigma)^2 \prod_{i=0}^{q-1} \int_K p_{\sigma(i)}(x) p_{\sigma(i)}(x) d\lambda(x) \\
&= q! \prod_{i=0}^{q-1} \parallel p_i(x) \parallel^2 .
\end{aligned} \tag{8.12}$$

For a real number $z > 0$, the *Laguerre* polynomial

$$L_m^{1/z}(x) = \sum_{j=0}^{m} \binom{m+1/z}{m-j} \frac{(-1)^j}{j!} x^j = \frac{(-1)^m}{m!} x^m + \cdots$$

of degree m satisfies the orthogonality condition

$$\int_0^\infty L_i^{1/z}(x) L_j^{1/z}(x) e^{-x} x^{1/z} dx = \delta_{ij} \frac{(j+1/z)!}{j!}. \tag{8.13}$$

Thus we can use

$$p_i(x) = (-1)^i \cdot i! \cdot L_i^{1/z}(x) \tag{8.14}$$

for the computation. From (8.11), (8.12), (8.13) and (8.14), we have

$$\begin{aligned}
&\lim_{m\to\infty} \mathcal{A}\left(\int_{\mathbb{R}^q} \Delta(k)^2 \cdot \prod_{i=0}^{q-1} \exp\left(-\sum_{j=2}^{2m} \frac{(\sqrt{z})^{j-2}}{j} k_i^j \right) dk_i \right) \\
&= \mathcal{A}\left(\left(\sqrt{z} e^{1/z} z^{1/z}\right)^q z^{\frac{q(q-1)}{2}} q! \prod_{i=0}^{q-1} i! \cdot \left(i + \frac{1}{z}\right)! \right) \\
&= \mathcal{A}\left((ez)^{\frac{n}{z}} \cdot z^{\frac{q^2}{2}} \cdot q! \prod_{i=0}^{q-1} i! \cdot \left(-1 + \frac{1}{z}\right)! \cdot \left(i + \frac{1}{z}\right)^{q-i} \right).
\end{aligned} \tag{8.15}$$

Thus we conclude

$$\begin{aligned}
&\lim_{m\to\infty}\log\mathcal{A}\left(\frac{1}{N}\int_{\mathcal{H}_q}\exp\left(-\sum_{j=2}^{2m}\frac{(\sqrt{z})^{j-2}}{j}\mathrm{trace}(X^j)\right)d\mu(X)\right)\\
&=\log\mathcal{A}\left(\frac{1}{N}\cdot\pi^{\frac{q(q-1)}{2}}\cdot(ez)^{\frac{q}{z}}\cdot z^{\frac{q^2}{2}}\cdot\prod_{i=0}^{q-1}\left(-1+\frac{1}{z}\right)!\cdot\left(i+\frac{1}{z}\right)^{q-i}\right)\\
&=\log\mathcal{A}\left(\frac{1}{N}\cdot\pi^{\frac{q(q-1)}{2}}\cdot(ez)^{\frac{q}{z}}\cdot z^{\frac{q^2}{2}}\cdot\left(\Gamma\left(\frac{1}{z}\right)\right)^q\cdot\prod_{i=0}^{q-1}\left(i+\frac{1}{z}\right)^{q-i}\right)\\
&=\mathrm{const}+\frac{n}{z}+\frac{q}{z}\log z+\frac{q^2}{2}\log z+q\log\mathcal{A}\left(\Gamma\left(\frac{1}{z}\right)\right)\\
&\quad+\sum_{i=0}^{q-1}(q-i)\log\frac{1+iz}{z}\\
&=\mathrm{const}+\frac{q}{z}+\frac{q}{z}\log z-\frac{q}{2}\log z+q\log\mathcal{A}\left(\Gamma\left(\frac{1}{z}\right)\right)\\
&\quad+\sum_{r=1}^{\infty}\frac{(-1)^{r-1}}{r}\left(\sum_{i=0}^{q-1}(q-i)i^r\right)z^r.
\end{aligned}\tag{8.16}$$

Let us recall Stirling's formula:

$$\log\mathcal{A}\left(\Gamma\left(\frac{1}{z}\right)\right)=-\frac{1}{z}\log z-\frac{1}{z}+\frac{1}{2}\log z+\sum_{r=1}^{\infty}\frac{b_{2r}}{2r(2r-1)}z^{2r-1}+\mathrm{const},\tag{8.17}$$

where b_r is the Bernoulli number defined by

$$\frac{x}{e^x-1}=\sum_{r=0}^{\infty}\frac{b_r}{r!}x^r.$$

We are not interested in the constant term (the term independent of z) of (8.17) because the asymptotic series $F(q,z)$ has no constant term. We can see that substitution of (8.17) in (8.16) eliminates all the logarithmic terms as desired:

$$\begin{aligned}
&\lim_{m\to\infty}\log\mathcal{A}\left(\frac{1}{N}\int_{\mathcal{H}_q}\exp\left(-\sum_{j=2}^{2m}\frac{(\sqrt{z})^{j-2}}{j}\mathrm{trace}(X^j)\right)d\mu(X)\right)\\
&\qquad=\sum_{r=1}^{\infty}\frac{b_{2r}}{2r(2r-1)}\cdot q\cdot z^{2r-1}+\sum_{r=1}^{\infty}\frac{(-1)^{r-1}}{r}\left(\sum_{i=0}^{q-1}(q-i)i^r\right)z^r.
\end{aligned}$$

Let

$$\phi_r(x)=\sum_{\mu=0}^{r-1}\binom{r}{\mu}b_\mu x^{r-\mu}$$

denote the Bernoulli polynomial. Then we have

$$\sum_{i=1}^{q-1}i^r=\frac{\phi_{r+1}(q)}{r+1}.$$

Thus for $r>0$,

$$\begin{aligned}\sum_{i=0}^{q-1}(q-i)i^r &= \frac{q\phi_{r+1}(q)}{r+1} - \frac{\phi_{r+2}(q)}{r+2}\\ &= \sum_{\mu=0}^{r}\frac{1}{r+1}\binom{r+1}{\mu}b_\mu\cdot q^{r+2-\mu} - \sum_{\mu=0}^{r+1}\frac{1}{r+2}\binom{r+2}{\mu}b_\mu\cdot q^{r+2-\mu}\\ &= \sum_{\mu=0}^{r}\frac{r!(1-\mu)}{\mu!(r+2-\mu)!}b_\mu\cdot q^{r+2-\mu} - b_{r+1}\cdot q.\end{aligned}$$

Therefore, we have

$$\begin{aligned}&\sum_{r=1}^{\infty}\frac{b_{2r}}{2r(2r-1)}\cdot q\cdot z^{2r-1} + \sum_{r=1}^{\infty}\frac{(-1)^{r-1}}{r}\left(\sum_{i=0}^{q-1}(q-i)i^r\right)z^r\\ &= -\sum_{r=1}^{\infty}\frac{1}{2r}b_{2r}\cdot q\cdot z^{2r-1} + \sum_{r=1}^{\infty}\sum_{\mu=0}^{r}(-1)^r\frac{(r-1)!(\mu-1)}{\mu!(r+2-\mu)!}b_\mu\cdot q^{r+2-\mu}\cdot z^r\\ &= -\sum_{r=1}^{\infty}\frac{1}{2r}b_{2r}\cdot q\cdot z^{2r-1} + \sum_{r=1}^{\infty}(-1)^{r-1}\frac{1}{r(r+1)(r+2)}q^{r+2}\cdot z^r\\ &\quad + \sum_{r=2}^{\infty}\sum_{\mu=1}^{[r/2]}(-1)^r\frac{(r-1)!(2\mu-1)}{(2\mu)!(r+2-2\mu)!}b_{2\mu}\cdot q^{r+2-2\mu}\cdot z^r.\end{aligned}\tag{8.18}$$

It is time to switch the summation indices r and μ to g and n as in (8.7). The first sum of the third line of (8.18) is the case when we specify a single point on a Riemann surface of arbitrary genus $g = r$. The second sum is for genus 0 case with more than two points specified. So we use $n = r + 2$ for the number of points. In the third sum, $\mu = g \geq 0$ is the genus and $r + 2 - 2\mu = n \geq 2$ is the number of points. Thus (8.18) is equal to

$$\begin{aligned}&\sum_{g=1}^{\infty}\zeta(1-2g)\cdot q\cdot z^{2g-1} + \sum_{n=3}^{\infty}(-1)^{n-1}\frac{1}{n(n-1)(n-2)}q^n\cdot z^{n-2}\\ &+ \sum_{g=1}^{\infty}\sum_{n=2}^{\infty}(-1)^{n-1}\frac{(2g+n-3)!}{(2g-2)!n!}\zeta(1-2g)\cdot q^n\cdot z^{-2+2g+n},\end{aligned}\tag{8.19}$$

where we used Euler's formula

$$\zeta(1-2g) = -\frac{b_{2g}}{2g},$$

and the fact that $b_0 = 1$ and $b_{2q+1} = 0$ for $q \geq 1$. Note that the first two summations of (8.19) are actually the special cases of the third summation corresponding to $n = 1$ and $g = 0$. Thus we have established:

THEOREM 8.4.

$$\begin{aligned}&\lim_{m\to\infty}\log\mathcal{A}\left(\frac{1}{N}\int_{\mathcal{H}_q}\exp\left(-\sum_{j=2}^{2m}\frac{(\sqrt{z})^{j-2}}{j}\mathrm{trace}(X^j)\right)d\mu(X)\right)\\ &= -\sum_{\substack{g\geq 0, n\geq 1\\ 2-2g-n<0}}\frac{(2g+n-3)!(2g)(2g-1)}{(2g)!n!}\zeta(1-2g)\cdot q^n\cdot(-z)^{-2+2g+n}.\end{aligned}$$

Since the asymptotic expansion is unique, from (8.7) *we obtain*

$$\sum_{\Gamma\in RG_{g,n}} \frac{(-1)^{e(\Gamma)}}{|\mathrm{Aut}(\Gamma)|} = -\frac{(2g+n-3)!(2g)(2g-1)}{(2g)!n!}\zeta(1-2g) \tag{8.20}$$

for every $g \geq 0$ *and* $n > 0$ *subject to* $2-2g-n < 0$.

Remark. If we have taken into account the values of $c(q)$ and N in the above computation, then we will see that all the constant terms appearing in the computation automatically cancel out.

The Euler characteristic $\chi(\mathfrak{M}_{g,n} \times \mathbb{R}_+^n)$ can be computed from (8.20) except for $(g,n) = (1,1)$, which has been already done in Section 2 of Chapter 5. This completes the proof of Theorem 8.1.

The Euler characteristic of

$$\mathfrak{M}_{g,1} = \coprod_{\Gamma\in RG_{g,1}} \frac{\Delta(123\cdots e(\Gamma))}{\mathrm{Aut}(\Gamma)}.$$

of (6.18) is also computed from (8.20). The result is a very simple formula:

$$\chi(\mathfrak{M}_{g,1}) = \zeta(1-2g). \tag{8.21}$$

4. Examples of the Computation

Let us examine a couple of examples of (8.20).

Example 8.1. The simplest case is $g = 0$ and $n = 3$. The ribbon graph Γ has the topological type of S^2 minus three points, which satisfies

$$\chi(\Gamma) = v(\Gamma) - e(\Gamma) = 2 - 2g - n = -1$$

and

$$3v(\Gamma) \leq 2e(\Gamma).$$

They correspond to the Euler characteristic of a tri-punctured sphere and the restriction that every vertex of Γ has degree at least 3. It follows from these conditions that

$$e(\Gamma) \leq 3.$$

There are three graphs in this case, as shown in Figure 8.2.

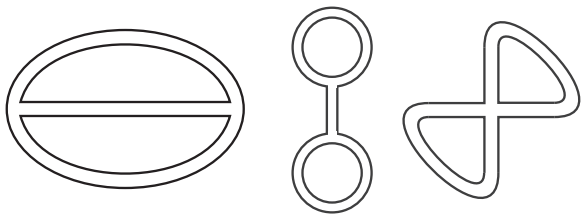

Figure 8.2. Ribbon Graphs for $g = 0, n = 3$

The automorphism groups of these ribbon graphs are $\mathfrak{S}_2 \rtimes \mathbb{Z}/3\mathbb{Z} = \mathfrak{S}_3$, $\mathbb{Z}/2\mathbb{Z}$, and again $\mathbb{Z}/2\mathbb{Z}$, respectively. Thus the left hand side of (8.20) is

$$\frac{(-1)^3}{3!} + \frac{(-1)^3}{2} + \frac{(-1)^2}{2} = -\frac{1}{6}.$$

The right hand side is coming from the term $q^3(-z)^1$ of the second summation in (8.19). The value is

$$-\frac{1}{3(3-1)(3-2)} = -\frac{1}{6}.$$

The computation using the Riemann zeta function gives us

$$-\frac{(2g+n-3)!(2g)(2g-1)}{(2g)!n!}\zeta(1-2g) = \frac{(2g)(2g-1)b_{2g}}{(2g)!3!(2g)} = -\frac{1}{6}.$$

EXAMPLE 8.2. The next simple case is $g = n = 1$. Since the Euler characteristic condition of the ribbon graphs is the same as in Example 8.1, the only possibilities are again graphs with 1 vertex and 2 edges or 2 vertices and 3 edges. There are two ribbon graphs satisfying the conditions (Figure 8.3). Their automorphism groups are $\mathfrak{S}_2 \times \mathbb{Z}/3\mathbb{Z}$ and $\mathbb{Z}/4\mathbb{Z}$. Formula (8.20) gives us

$$\frac{(-1)^3}{6} + \frac{(-1)^2}{4} = \frac{1}{12} = -\zeta(-1).$$

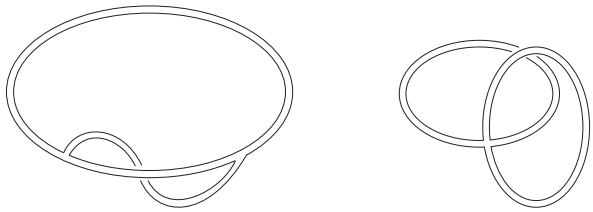

FIGURE 8.3. Ribbon Graphs for $g = 1, n = 1$

Part 3

The Theory of Kadomtsev-Petviashvili Equations

CHAPTER 9

The Kadomtsev-Petviashvili Equations

The Kadomtev-Petviashvili (KP) equation was introduced in 1970 [**?**] to study transversal stability of 1-dimensional solitons that satisfy the Korteweg-de Vries (KdV) equation. The rich mathematical structures of the KP equation were immediately recognized right after its discovery. The equation is the 0-curvature condition of a connection [**?**]. It determines isospectral deformations of linear ordinary differential operators [**?**]. Riemann theta functions of a Riemann surface give solutions to the KP equation [**?**]. The KP equation is linearlized on the Jacobian variety of a Riemann surface [**?**].

And then came a breakthrough: Sato [**24**] realized that the system of KP equation and its higher-order analogue is equivalent to the system of Plücker relations that determine the Grassmannians in the projective spaces. This new point of view of the KP equation provided many further developments, including the relation to loop groups and affine Kac-Moody Lie algebras ([**?**], [**?**]), the application to the Riemann-Schottky problem ([**1**], [**14**], [**27**]), the contribution to conformal field theory ([**?**], [**?**], [**?**], [**?**]), and the application to matrix models and the moduli theory of Riemann surfaces ([**?**], [**13**]), just naming a few.

In this chapter we introduce the KP equation as an equation for isospectral deformations of a linear ordinary differential operator. This is the most natural point of view of the KP equation to motivate the introduction of Sato's infinite-dimensional Grassmannian and to explain the deep relation with algebraic geometry of Jacobians, algebraic curves, and vector bundles defined on them.

In the next chapter, we derive the KP equation purely geometrically from the infinite-dimensional Grassmannian and the properties of the characters of tensor irreducible representations of the general linear groups.

1. The KP Equation and its Soliton Solutions

The KP euqation is a nonlinear partial differential equation

$$\frac{3}{4}u_{yy} = \left(u_t - \frac{1}{4}u_{xxx} - 3uu_x\right)_x \tag{9.1}$$

for an unknown function $u = u(x, y, t)$ in three variables, where the subscripts indicate the partial derivatives:

$$u_x = \frac{\partial u}{\partial x}, \quad u_y = \frac{\partial u}{\partial y}, \quad u_t = \frac{\partial u}{\partial t}, \quad \text{etc.}$$

The coefficients of these terms are not important as long as they are non-zero, because they can be arbitrarily chosen by a coordinate transformation

$$\begin{cases} u \longmapsto \alpha \cdot u \\ x \longmapsto \beta \cdot x \\ y \longmapsto \gamma \cdot y \\ t \longmapsto \delta \cdot t \end{cases}$$

with $\alpha\beta\gamma\delta \neq 0$. The reason of our choice of the form (9.1) will become clear later.

One of the most appealing features of the KP equation is that it describes interacting solitons. Before taking a look at KP solitons, let us consider the KdV equation that describes one-dimensional wave propagation.

The KdV equation is a nonlinear partial differential equation

$$u_t = \frac{1}{4}u_{xxx} + 3uu_x \tag{9.2}$$

for $u = u(x,t)$. the KdV equation is a special case of the KP equation when the unknown function does not depend on y. This equation was derived from the Navier-Stokes equation by taking the shallow water limit, which means that the ratio of the depth and the wave length is brought to 0. The kdV equation has a *solitary wave* solution

$$u(x,t) = c\big(\operatorname{sech}^2(\sqrt{c}(x+ct))\big) \tag{9.3}$$

that travels from the right to the left at the constant speed c without changing the shape of the wave. We note from the formula (9.3) that the velocity $-c$, the wave length $\sqrt{c}$, and the height c of the wave are all related: the wave length is proportional to the square root of the height, and the speed is proportional to the height. For example, the height of the solitary wave of Figure 9.1 is 4 and its wave length is about 2. In the real world situation, the unit length of the horizontal direction is infinitely large compared to the unit length of height.

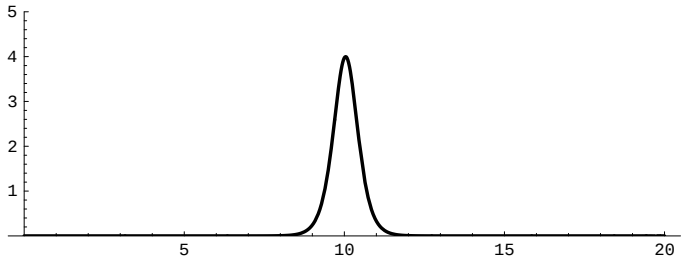

FIGURE 9.1. A Solitary Wave

More interesting solutions to the KdV equation are interacting *soliton* solutions. Let us look at Figure 9.2. The first wave looks like another solitary wave, but it decays into four solitons immediately. To be precise, it is not a decay process, because one of the waves coming out is much taller than the initial wave. After forming four bumps, the identity of each soliton is preserved for all time.

The entire nonlinear interaction is described in Figure 9.3. From this figure we can see that the taller the soliton is, the faster it travels. It is consistent with the property of the solitary wave solution of (9.3). Since the taller solitons are behind

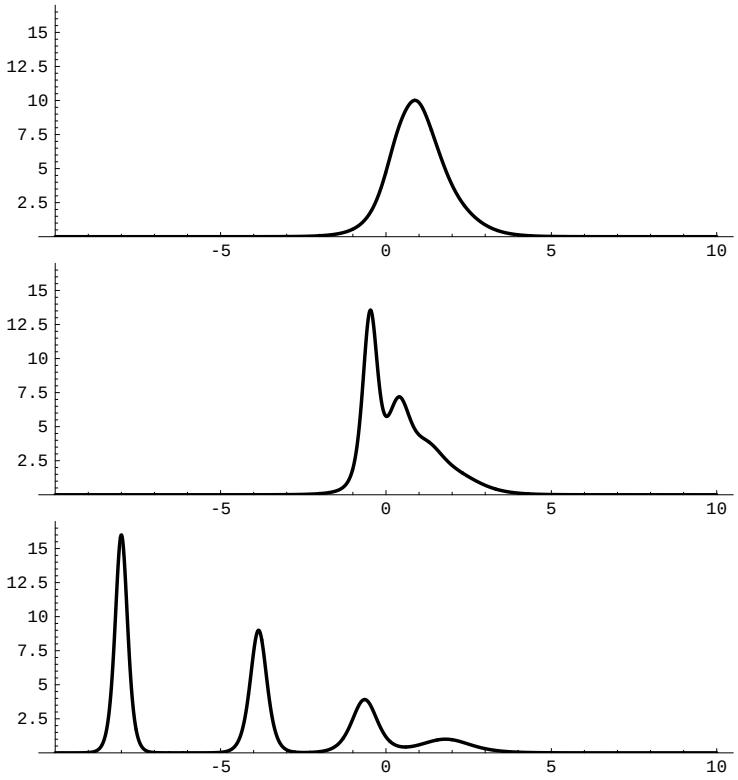

FIGURE 9.2. Nonlinear Collision of Four Solitons

the shorter solitons, the taller ones catch up the shorter ones and eventually they all collide. The first picture of Figure 9.2 shows the very moment of the simultaneous collision. Since the height of this collision wave is shorter than the tallest in-coming wave, the interaction is nonlinear.

If we ignore the very moment of collision, then the interaction looks like just four solitary waves passing each other without any interaction. Since the KdV equation is nonlinear, such linear superposition of solitary waves is impossible. Actually, if we look at Figure 9.3 more carefully, then we recognize that the collision kicks off the tallest and fastest wave while bounces back the shortest and slowest one. The position of the four solitons after collision is not exactly the same as what we expect from the behavior of the in-coming waves. This also shows the essential nonlinear nature of the interaction.

Another important feature of the KdV solitons is the conservation of soliton number. In the above example, the number of bumps is four before and after the collision.

Now let us go back to the KP equation. It describes shallow water wave propagation of two-dimensional medium, such as a big tsunami wave on the ocean surface. Figure 9.4 shows the moment of collision of two tsunami waves. The height of these waves are the same, but the one in left moves faster than the one on the right. Both waves travel from left to right.

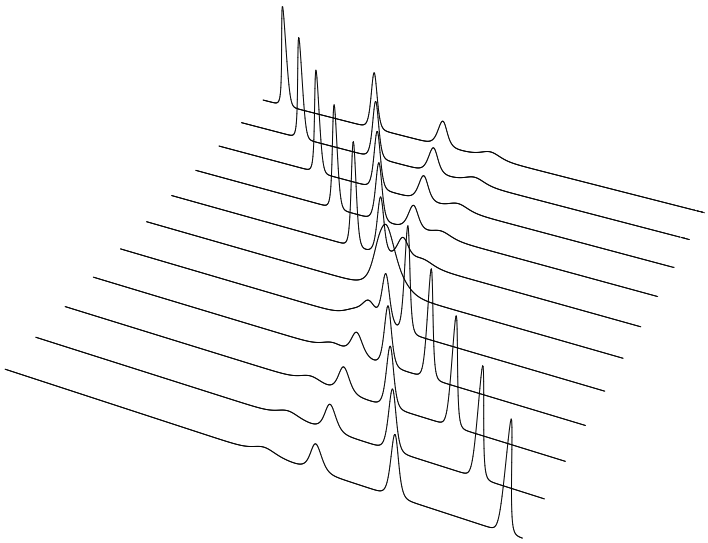

FIGURE 9.3. Interaction of Four Solitons

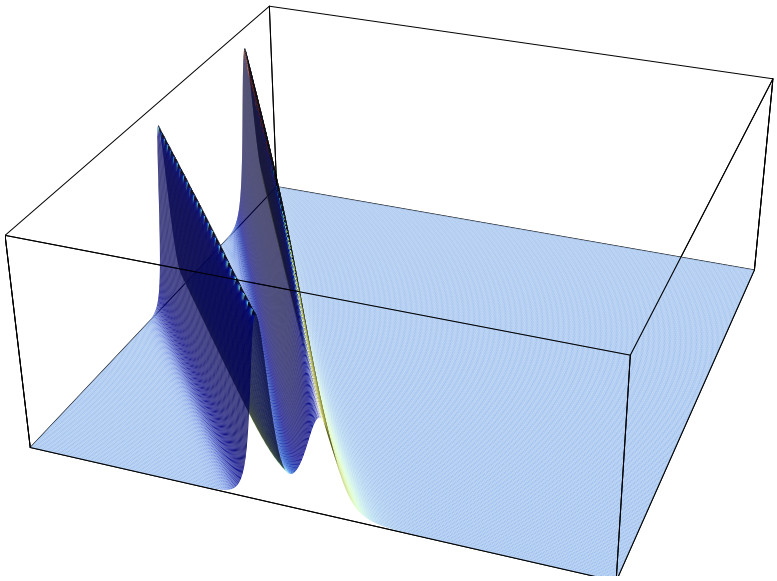

FIGURE 9.4. Collision of Two Tsunami Waves

After the collision, the tall tsunami waves collapse into three small waves of the equal height and different speeds. There are two input waves, but three waves come out of collision.

The wave at the front moves out with the largest speed after the collision, while the waves behind travel much slowly.

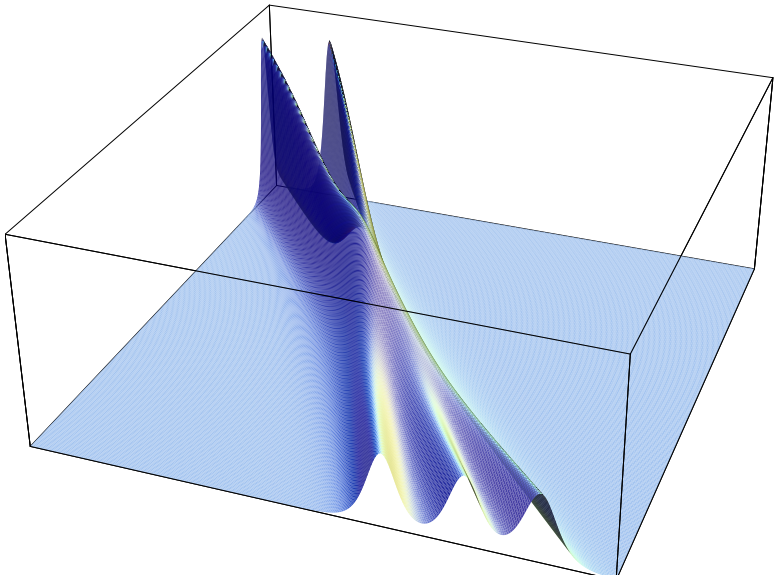

FIGURE 9.5. $1 + 1 = 3$?

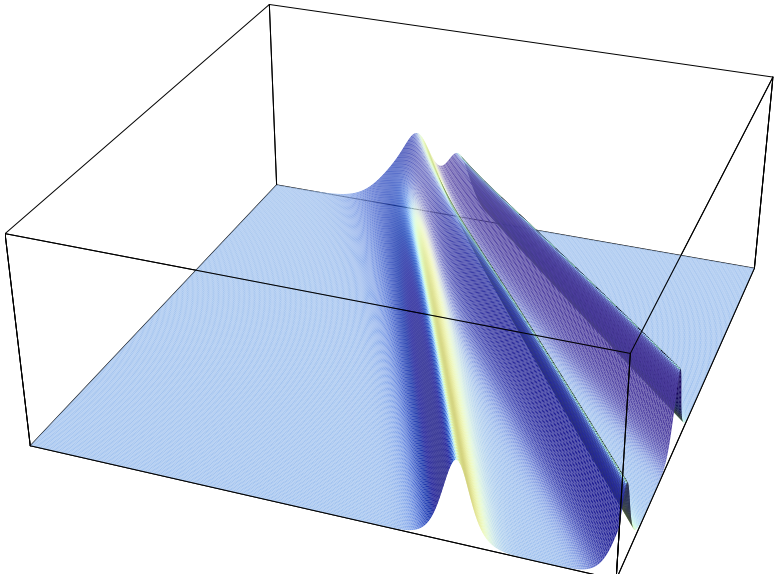

FIGURE 9.6. Collapsing into Three Tsunami Waves

This type of two-dimensional waves can be seen quite often on a sea shore. The interaction we see on a beach appears to be more stable. Actually, what we see globally is the shape of Figure 9.5 moving straight away from us, rather than two waves coming in from the left and collapsing into three while traveling to the right.

If we walk along the wave of Figure 9.5, then we see that the whole wave moves at the constant speed withough changing its shape.

2. The Micro-Differential Operators in 1-variable and the Lax Equation

Our interests of the KP equation does not lie in the fact that it describes the shallow water wave propagation. The KP equation has a two-fold relation to the moduli spaces of Riemann surfaces, and this point is what we are going to investigate in this and the next chapters.

Although we have given the KP equation already as a nonlinear parital differential equation in (9.1), the form of the equation does not tell us anything about its relation to the geometry. We have to give a more fundamental definition of the KP equation. In this section, we define the KP equation as the master equation of all possible *isospectral deformations* of a linear ordinary differential opertor.

Let us consider an $n \times n$ matrix L and a family $U(t)$ of invertible $n \times n$ matrices depending on the parameter t differentiably. Then the matrices of the family

$$L(t) = U(t) \cdot L \cdot U(t)^{-1} \tag{9.4}$$

have the same eigenvalues for all t, because the characteristic polynomial of $L(t)$ is independent of t. From (9.4) it follows

$$\frac{\partial L(t)}{\partial t} = [B(t), L(t)], \tag{9.5}$$

where

$$B(t) = \frac{\partial U(t)}{\partial t} U(t)^{-1}. \tag{9.6}$$

Equation of the form (9.5) is called the *Lax equation*.

We consider the Lax equation in the case when the quantities $L(t)$ and $B(t)$ are differential operators in the other variable x. As an example, let us take

$$\begin{cases} L(t) = \left(\frac{d}{dx}\right)^2 + 2u(x,t) \\ B(t) = \left(\frac{d}{dx}\right)^3 + 3u(x,t)\frac{d}{dx} + \frac{3}{2}u(x,t)_x \end{cases}. \tag{9.7}$$

Recall that for a differentiable function $f(x)$, we have the *commutation relation*

$$\left[\frac{d}{dx}, f(x)\right] = \frac{d}{dx} \circ f(x) - f(x) \circ \frac{d}{dx} = f(x)_x. \tag{9.8}$$

This is essentially the Leibniz rule. Thus we compute

$$[B(t), L(t)] = \frac{1}{2}u_{xxx} + 6uu_x.$$

Since

$$\frac{\partial L(t)}{\partial t} = 2u_t,$$

the Lax equation of the operators of (9.7) implies the KdV equation (9.2).

This is just a computation. The mystery behind the scene lies in the fact that the commutator $[B(t), L(t)]$ is a function, or a 0-th order differential operator. Since $B(t)$ is of order 3 and $L(t)$ has order 2, we expect that the commutator has a positive order. Actually, $B(t)$ is determined by $L(t)$ so that the commutator becomes a function. We will see how the form of $B(t)$ is determined shortly.

Let us turn our attention to the *isospectral* property of the Lax equation.

DEFINITION 9.1. Let L be a linear ordinary differential operator. A one-parameter family $L(t)$ of differential operators, where the coefficients of $L(t)$ depend on the deformation parameter t, is said to be a *family of isospectral deformations* if $L = L(0)$ and there is another linear ordinary differential operator $B(t)$ such that the system of linear equations

$$\begin{cases} L(t)\psi(x,t) = \lambda\psi(x,t) \\ \frac{\partial\psi(x,t)}{\partial t} = B(t)\psi(x,t) \end{cases} \tag{9.9}$$

has a solution $\psi(x,t)$ for every eigenvalue λ of L.

The first equation of (9.9) is the eigenvalue problem of the operator $L(t)$ for each t with an eighenvalue λ, which is constant with respect to x and t, though the operator $L(t)$ changes with t. The second equation determines the t dependence of the eigenfunction $\psi(x,t)$. If L has only discrete eigenvalues, then the meaning of isospectral family is clear, and the first equation of (9.9) suffices to define it. But if L has a continuous spectrum, then it is not clear what we mean by saying that $L(t)$ has the same spectum of L. We are appealing to (9.4) and (9.6) again to define an isospectral family. Indeed, (9.4) corresponds to the first equation of (9.9), and (9.6) corresponds to the second equation. The mechanism of the Lax equation is the same as the case of matrices:

PROPOSITION 9.2. *Suppose that t-depending operators $L(t)$ and $B(t)$ satisfy the condition that the system*

$$\begin{cases} L(t)\psi(x,t) = \lambda(t)\psi(x,t) \\ \frac{\partial\psi(x,t)}{\partial t} = B(t)\psi(x,t) \end{cases} \tag{9.10}$$

has a solution for every eigenvalue $\lambda(t)$ of $L(t)$. Then $L(t)$ is an isospectral family of $L = L(0)$ if and only $L(t)$ and $B(t)$ satisfy the Lax equation

$$\frac{\partial L(t)}{\partial t} = [B(t), L(t)].$$

PROOF. Let us differentiate the first equation of (9.10) with respect to t:

$$\begin{aligned} L(t)_t\psi + L(t)\psi_t - \lambda(t)_t\psi - \lambda(t)\psi_t & \\ = (L(t)_t + L(t)B(t) - \lambda(t)B(t) - \lambda(t)_t)\psi & \\ = (L(t)_t - [B(t), L(t)] - \lambda(t)_t)\psi = 0. & \end{aligned}$$

Therefore, $L(t)_t - [B(t), L(t)] = 0$ if and only if $\lambda(t)_t = 0$. □

REMARK. In the above argument, some completeness condition of the eigenfunctions of $L(t)$ is assumed. Since we are interested in geometry of the Lax equation rather than its analysis, we do not go into any functional analytic detail of the equation here.

The KdV equation describes a one-parameter isospectral deformation of a second order differential operator

$$L = \left(\frac{d}{dx}\right)^2 + 2u(x).$$

It is natural to ask a question: what is the largest possible family of nontrivial isospectral deformations of L? More generally, we can ask: how can we determine

the largest possible family of nontrivial isospectral deformations of an arbitrary linear ordinary differential operator?

This question leads us to defining the *system of KP equations*, or the *KP system*, which is a master equation for the universal family of isospectral deformations of an arbitrary linear ordinary differential operator.

So far we have not specified the space of functions on which our differential operators act. To develop a systematic investigation, let us choose a commutative $\mathbb{C}$-algebra R with a *derivation* operator

$$\partial : R \longrightarrow R, \tag{9.11}$$

which is a $\mathbb{C}$-linear map satisfying the Leibniz rule

$$\partial(fg) = \partial(f) \cdot g + f \cdot \partial(g), \qquad f, g \in R. \tag{9.12}$$

We assume that the derivation operator is surjective, and that the kernel of ∂ contains $\mathbb{C}$:

$$\mathbb{C} \subset \mathrm{Ker}(\partial) \subset R.$$

In other words, a first order linear differential equation

$$\partial(f) = g \tag{9.13}$$

has a solution $f \in R$ for every $g \in R$, and $\partial(c) = 0$ if $c \in \mathbb{C}$. In our investigation of this book, we exclusively consider the case

$$(R, \partial) = \left(\mathbb{C}[[x]], \frac{d}{dx} \right),$$

but the theory can be generalized by using many different differential algebras [**19**].

Definition 9.3. The ring D of linear ordinary differential operators with coefficients in R is the associative algebra generated by R and ∂ with the commutation relation

$$[\partial, f] = \partial \circ f - f \circ \partial = \partial(f) \in R, \tag{9.14}$$

which is understood as a multiplication operator acting on R.

Let us define a $\mathbb{C}$-linear subspace $D^{(\nu)}$ of D by

$$D^{(\nu)} = \left\{ \sum_{j=0}^{\nu} a_j \circ \partial^j \;\middle|\; a_j \in R \right\}, \tag{9.15}$$

and define

$$R[\partial] = \bigcup_{\nu=0}^{\infty} D^{(\nu)}.$$

The commutation relation (9.14) gives

$$\partial \circ f = f \circ \partial + \partial(f) \in D^{(1)}.$$

Thus there is a $\mathbb{C}$-linear isomorphism

$$D \xrightarrow{\sim} R[\partial],$$

with which we identify D and $R[\partial]$ from now on. The relation (9.14) also gives an explicit way of computing the product of two differential operators. By induction, we can show a useful formula

$$\partial^\nu \circ f = \sum_{i=0}^{\nu} \binom{\nu}{i} \partial^i(f) \circ \partial^{\nu-i} \in D^{(\nu)}, \qquad \nu \geq 0. \tag{9.16}$$

We use the notation

$$\partial^n(f) = f^{(n)}, \tag{9.17}$$

and call it the n-th derivative of f.

A differential operator $P \in D$ is of *order* ν if

$$P = \sum_{j=0}^{\nu} a_j \circ \partial^j \in D^{(\nu)},$$

and *monic* if the leading coefficient a_ν is equal to 1, and *normalized* if $a_\nu = 1$ and $a_{\nu-1} = 0$.

Although the KP system is for a differential operator, it is best described in terms of micro-differential operators.

Definition 9.4. A *micro-differential operator* is an element of the set

$$E = \bigcup_{\nu \in \mathbb{Z}} E^{(\nu)}, \tag{9.18}$$

where

$$E^{(\nu)} = \left\{ \sum_{j=0}^{\infty} a_j \circ \partial^{\nu-j} \;\middle|\; a_j \in R \right\} \tag{9.19}$$

is a $\mathbb{C}$-linear space of formal sums. An element of $E^{(\nu)} \setminus E^{(\nu-1)}$ is called a micro-differential operator of *order* ν.

The vector space E has a filtration

$$\cdots E^{(\nu-1)} \subset E^{(\nu)} \subset E^{(\nu+1)} \cdots \tag{9.20}$$

that satisfies

$$\bigcap_{\nu \in \mathbb{Z}} E^{(\nu)} = \{0\}. \tag{9.21}$$

We introduce the natural topology in E such that $\{E^{(\nu)}\}_{\nu \in \mathbb{Z}}$ forms the basis of open neighborhood of $0 \in E$. The formal sum of the elements of E is convergent with respect to this topology because of (9.21). The set $\{0\}$ is a closed subset of E because its complement is the union of infinitely many open sets:

$$\bigcup_{\nu \in \mathbb{Z}} \bigcup_{a \in R \setminus \{0\}} (a \circ \partial^\nu + E^{(\nu-1)}).$$

Thus $\{P\}$ is a closed set for every $P \in E$.

Let us define a commutation relation

$$[\partial^{-1}, f] = \partial^{-1} \circ f - f \circ \partial^{-1} = \sum_{i=1}^{\infty} (-1)^i f^{(i)} \circ \partial^{-1-i}. \tag{9.22}$$

Note that the sum of the right hand side is again a convergent sum in $E^{(-1)}$. The relation of (9.22) makes sense because

$$\begin{aligned}\partial \circ (\partial^{-1} \circ f) &= \partial \circ \sum_{i=0}^{\infty} (-1)^i f^{(i)} \circ \partial^{-1-i} \\ &= \sum_{i=0}^{\infty} (-1)^i f^{(i+1)} \circ \partial^{-1-i} + \sum_{i=0}^{\infty} (-1)^i f^{(i)} \circ \partial^{-i} \\ &= -\sum_{i=1}^{\infty} (-1)^i f^{(i)} \circ \partial^{-i} + \sum_{i=0}^{\infty} (-1)^i f^{(i)} \circ \partial^{-i} = f.\end{aligned}$$

Again by induction, we can show the general Leibniz rule

$$\partial^\nu \circ f = \sum_{i=0}^{\infty} \binom{\nu}{i} f^{(i)} \circ \partial^{\nu-i} \in E^{(\nu)}, \tag{9.23}$$

where

$$\binom{\nu}{i} = \frac{\nu(\nu-1)(\nu-2)\cdots(\nu-i+1)}{i!}$$

for $\nu \in \mathbb{Z}$ and $i \geq 0$. Note that it generalizes both (9.16) and (9.22).

Using the general Leibniz rule (9.23), we can introduce a multiplication in E. It is just a computation to show that this multiplication defines the structure of an associative algebra in E. Since (9.23) is a generalization of the usual Leibniz rule, D is a subalgebra of E. We have a natural *polarization*

$$E = D \oplus E^{(-1)}, \tag{9.24}$$

where both D and $E^{(-1)}$ are subalgebras of E but the direct sum is only as $\mathbb{C}$-linear spaces. The set D is a closed subset of E because its complement is give by

$$\bigcup_{P \in D} \bigcup_{\nu < 0} \bigcup_{a \in R \setminus \{0\}} (P + a \circ \partial^\nu + E^{(\nu-1)}).$$

We call an element of the subalgebra $E^{(-1)}$ a *formal Volterra integral operator*. Following the porlarization (9.24), we write

$$P = P_+ + P_-,$$

where $P \in E$, $P_+ \in D$, and $P_- \in E^{(-1)}$. P_+ is the differential operator part, and P_- is the Volterral operator part, of P.

The ring D acts naturally on R, but E does not. Since $\partial : R \to R$ has a non-trivial kernel, ∂^{-1} is not a map of R into itself. For the case of $R = \mathbb{C}[[x]]$, we can construct an operand of E as we will see below, but in general a micro-differential operator does not act on a function. Thus the use of the name "Volterra integral operator" for an element of $E^{(-1)}$ is an abuse of terminology. The rationale of this usage comes from the fact that every element $P \in E^{(-1)}$ is *nilpotent* in the general sense, i.e.,

$$\lim_{n \to \infty} P^n = 0. \tag{9.25}$$

This follows from $P^n \in E^{(-n)}$ and

$$\bigcap_{n=1}^{\infty} E^{(-n)} = \{0\}.$$

The above consideration shows us that if $P \in E^{(-1)}$, then

$$(1+P)^{-1} = 1 - P + P^2 - P^3 + \cdots \tag{9.26}$$

is a convergent expression and determines a well-defined element of $E^{(0)}$. Note that if $Q \in E^{(-1)}$, then

$$(1+P)\circ(1+Q) = 1 + P + Q + P \circ Q \in 1 + E^{(-1)}.$$

Continuing the abuse of terminology, we define:

Definition 9.5. The *Volterra group* is the subset of E defined by

$$G = 1 + E^{(-1)}. \tag{9.27}$$

The inverse of an element $1+P$ of G, where $P \in E^{(-1)}$ is a formal Volterra integral operator, is defined by (9.26).

Proposition 9.6 (Standard form of a normalized micro-differential operator). *Every normalized micro-differential operator P of order other than 0 is conjugate to ∂^ν by an element of the Volterra group G, where ν is the order of P.*

Proof. We have to solve the equation

$$P \circ S = S \circ \partial^\nu \tag{9.28}$$

for

$$S = \sum_{n=0}^{\infty} s_n \circ \partial^{-n} \in G,$$

where $s_0 = 1$. Let

$$P = \sum_{i=0}^{\infty} a_i \circ \partial^{\nu - i},$$

where $a_0 = 1$ and $a_1 = 0$. Then

$$\begin{aligned} 0 = P\circ S - S \circ \partial^\nu &= \sum_{i=0}^{\infty}\sum_{j=0}^{\infty}\sum_{n=0}^{\infty} \binom{\nu - i}{j} a_i s_n^{(j)} \circ \partial^{\nu - i - j - n} - \sum_{m=0}^{\infty} s_m \circ \partial^{\nu - m} \\ &= \sum_{m=0}^{\infty}\left(\sum_{n=0}^{m}\sum_{j=0}^{m-n}\binom{\nu-(m-n-j)}{j} a_{m-n-j} s_n^{(j)} - s_m\right)\circ\partial^{\nu-m} \\ &= \sum_{m=1}^{\infty}\left(\sum_{n=0}^{m-1}\sum_{j=0}^{m-n}\binom{\nu-(m-n-j)}{j} a_{m-n-j} s_n^{(j)}\right)\circ\partial^{\nu-m}. \end{aligned}$$

Thus we have

$$s_{m-1}^{(1)} = -\frac{1}{\nu}\sum_{n=0}^{m-2}\sum_{j=0}^{m-n}\binom{\nu-(m-n-j)}{j} a_{m-n-j} s_n^{(j)}. \tag{9.29}$$

Since $\partial : R \to R$ is surjective, we can solve (9.29) recursively starting from $s_0 = 1$ to determine a group element $S \in G$. This completes the proof. □

Remark. (1) The above procedure does not work if the order of P is 0. It is because the only operator that is conjugate to the identity is the identity operator itself.

(2) Solving the differential equation (9.29) involves determining a constant of integration at each step. Thus the operator S is not unique. From the computation, it is easy to see that the ambiguity is precisely

$$S \longrightarrow S \circ S_{\text{const}}, \tag{9.30}$$

where S_{const} is an element of the Volterra group whose coefficients are in $\text{Ker}(\partial)$. We have

$$P = S \circ \partial^\nu \circ S^{-1} = (S \circ S_{\text{const}}) \circ \partial^\nu (S \circ S_{\text{const}})^{-1},$$

because

$$S_{\text{const}} \circ \partial^\nu \circ S_{\text{const}}^{-1} = \partial^\nu.$$

COROLLARY 9.7 (Existence of the inverse and the n-th root of a normalized operator). *Let $P \in E$ be a normalized micro-differential operator of order $n > 0$. Then there is a unique normalized operator P^{-1} of order $-n$, and also a unique normalized operator $P^{1/n}$ of order 1.*

PROOF. Let $P = S \circ \partial^n \circ S^{-1}$. Then

$$P^{-1} = S \circ \partial^{-n} \circ S^{-1}$$

and

$$P^{1/n} = S \circ \partial \circ S^{-1}.$$

The ambiguity (9.30) does not affect these definitions. □

The KP equations are about deformations of a differential operator. Thus we need to specify the deformation parameters before defining the KP system. Since our goal is to relate the moduli theory of Part 1, matrix integrals of Par 2, and the KP theory of Part 3, we use $\mathbb{C}[[t_1, t_2, t_3, \cdots]]$ for the set of deformation parameters. We recall that this ring has a filtration

$$\mathbb{C}[[t_1, t_2, t_3, \cdots]] = \mathfrak{I}_0 \supset \mathfrak{I}_1 \supset \mathfrak{I}_2 \supset \mathfrak{I}_3 \supset \cdots,$$

where $\mathfrak{I}_n$ is the ideal of $\mathbb{C}[[t_1, t_2, t_3, \cdots]]$ generated by homogeneous polynomials of degree n, and we have defined that

$$\deg(t_j) = j.$$

We denote by $R[[t]]$ the ring of all formal power series in $t = (t_1, t_2, t_3, \cdots)$ with coefficients in R. We assume that the derivation ∂ and elements of $\mathbb{C}[[t_1, t_2, t_3, \cdots]]$ are commutative. The ring $D[[t]]$ of differential operators and the ring $E[[t]]$ of micro-differential operators with coefficients in $R[[t]]$ are defined in exactly the same way as before.

DEFINITION 9.8 (Definition of the KP system). The KP system is the system of nonlinear partial differential equations

$$\frac{\partial L}{\partial t_n} = [(L^n)_+, L], \qquad n = 1, 2, 3, \cdots, \tag{9.31}$$

for a normalized micro-differential operator $L \in E[[t]]$ of order 1.

EXAMPLE 9.1. Let

$$L = (\partial^2 + 2u)^{1/2} = \partial + u\partial^{-1} - \frac{u^{(1)}}{2}\partial^{-2} + \left(\frac{u^{(2)}}{4} - \frac{1}{2}u^2\right)\partial^{-3} + \cdots.$$

Then from (9.31), we derive

$$\frac{\partial L^2}{\partial t_3} = [(L^3)_+, L^2] = \left[\partial^3 + 3u\partial + \frac{3}{2}u^{(1)}, \partial^2 + 2u\right].$$

Since $L^3 = (L^3)_+ + (L^3)_-$,

$$[(L^3)_+, L^2] = [L^3, L^2] - [(L^3)_-, L^2] = [(L^3)_-, L^2].$$

Note that $[(L^3)_+, L^2] \in D[[t]]$, while the order of $[(L^3)_-, L^2] \in E[[t]]$ is at most $-1 + 2 - 1 = 0$. Thus $[(L^3)_+, L^2]$ is just an element of $R[[t]]$. This is the reson of the mysterious Lax form of the KdV equation (9.7).

Since L of Definition 9.8 is a normalized operator, $\partial L/\partial t_n \in E^{(-1)}[[t]]$. As in Example 9.1, we have

$$[(L^n)_+, L] = -[(L^n)_-, L] \in E^{(-1)}[[t]].$$

Thus the KP system (9.31) is an equation in $E^{(-1)}[[t]]$.

Let $P \in D$ be a normalized differential operator. Its isospectral deformation is given by a Lax equation

$$\frac{\partial P}{\partial t} = [Q, P] \tag{9.32}$$

for some differential operator $Q \in D$. If the order of P is m, then (9.32) is equivalent to

$$\frac{\partial L}{\partial t} = [Q, L] \tag{9.33}$$

for the m-th root $L = P^{1/m}$. Since L is normalized and of order 1, the deformation operator Q has to satisfy the condition that $[Q, L] \in E^{(-1)}$.

PROPOSITION 9.9 (Determining all possible isospectral deformations). *Let $L \in E$ be a normalized micro-differential operator of order 1, and define*

$$F_L = \{Q \in D \mid [Q, L] \in E^{(-1)}\}. \tag{9.34}$$

Then F_L is the set of all finite sums of the form

$$Q = \sum_{j=0}^{\nu} a_j \circ (L^j)_+ \tag{9.35}$$

for $\nu \geq 0$ and $a_j \in \mathrm{Ker}(\partial)$.

PROOF. From the same argument as above, we have

$$[Q, L] = \left[\sum_{j=0}^{\nu} a_j \circ (L^j)_+, L\right] = -\left[\sum_{j=0}^{\nu} a_j \circ (L^j)_-, L\right] \in E^{(-1)}.$$

Conversely, let $Q \in F_L$, and assume that the order of Q is $\nu \geq 0$. Thus Q is written as

$$Q = a_\nu \circ (L^\nu)_+ + Q_1$$

with $Q_1 \in D^{(\nu-1)}$. Since

$$L = \partial + (L)_-,$$

the highest order term of

$$[Q, L] = [a_\nu \circ (L^\nu)_+ + Q_1, \partial + (L)_-]$$

is $a_\nu^{(1)} \circ \partial^\nu$. The condition $[Q, L] \in E^{(-1)}$ implies that $a_\nu^{(1)} = 0$. Thus $a_\nu \in \mathrm{Ker}(\partial)$. Then $a_\nu \circ (L^\nu)_+ \in F_L$, hence $Q_1 \in F_L$. Since the order of Q_1 is smaller that ν, we can use the induction on ν. □

If $R = \mathbb{C}[[x]]$, then $\mathrm{Ker}(\partial) = \mathbb{C}$. Therefore, the KP system (9.31) for $L = P^{1/m}$ exhausts all possible isospectral deformations of a normalized differential operator P of order m up to linear combination. Thus we claim that the KP system is the master equation for all possible isospectral deformations of an arbitrary normalized differential operator.

3. The KP Equations and the Grassmannian

From now on, we choose

$$(R, \partial) = \left(\mathbb{C}[[x]], \frac{d}{dx}\right)$$

for our differential algebra. There is a filtration

$$\mathbb{C}[[x]] \supset \mathbb{C}[[x]]x \supset \mathbb{C}[[x]]x^2 \supset \mathbb{C}[[x]]x^3 \supset \cdots \tag{9.36}$$

in $\mathbb{C}[[x]]$ that satisfies

$$\bigcap_{n=0}^{\infty} \mathbb{C}[[x]]x^n = \{0\}.$$

The Krull topology of $\mathbb{C}[[x]]$ is defined by taking $\mathbb{C}[[x]]x^n$'s as a basis for open neighborhood of 0. A formal power series $f(x)$ has *valuation* n if

$$f(x) \in \mathbb{C}[[x]]x^n \setminus \mathbb{C}[[x]]x^{n+1}.$$

The algebra E of micro-differential operators does not act on $\mathbb{C}[[x]]$. Let us first construct the space V_x of functions on which E naturally acts. The derivation defines a projective system

$$\cdots \xrightarrow{\partial} R \xrightarrow{\partial} R \xrightarrow{\partial} R \xrightarrow{\partial} \cdots. \tag{9.37}$$

Definition 9.10. The vector space V_x is a subspace of the projective limit

$$\varprojlim (R \xrightarrow{\partial} R)$$

of (9.37) consisting of the sequences $\mathbf{f} = \left(f^{(\nu)}(x)\right)_{\nu \in \mathbb{Z}}$ subject to the following conditions:

(1) $f^{(\nu)}(x) \in \mathbb{C}[[x]]$.
(2) $\partial(f^{(\nu)}(x)) = f^{(\nu+1)}(x)$.
(3) For every $\mathbf{f} \in V_x$, there are positive integers N and n such that for all $\nu > N$, $f^{(-\nu)}(x) \in \mathbb{C}[[x]]x^{\nu-n}$.

Given an integer $\nu \in \mathbb{Z}$, there is a linear projection

$$\pi_\nu : V_x \ni \left(f^{(\nu)}(x)\right)_{\nu \in \mathbb{Z}} \longmapsto f^{(\nu)}(x) \in \mathbb{C}[[x]]. \tag{9.38}$$

A micro-differential operator $P = \sum_{\nu \geq 0} a_\nu(x) \circ \partial^{m-\nu}$ of order m now acts on an element $\mathbf{f} = \left(f^{(\nu)}(x)\right)_{\nu \in \mathbb{Z}}$ of V_x by

$$\begin{aligned} \pi_0(P(\mathbf{f})) &= \sum_{\nu \geq 0} a_\nu(x) f^{(m-\nu)}(x) \\ \pi_\mu(P(\mathbf{f})) &= \pi_0((\partial^\mu \circ P)(\mathbf{f})) \end{aligned} \tag{9.39}$$

Since there is an integer n for every $\mathbf{f}$ such that

$$\mathrm{val}_x(a_\nu(x)f^{(m-\nu)}(x)) \geq \mathrm{val}_x(f^{(m-\nu)}(x)) \geq \nu - m - n$$

for all sufficiently large $\nu >> m$, the formal infinite sum $\pi_0(P(\mathbf{f}))$ makes sense in the Krull topology and determines a well-defined element of $\mathbb{C}[[x]]$.

4. Algebraic Solutions of the KP Equations

CHAPTER 10

Geometry of the Infinite-Grassmannian

1. The Infinite-Dimensional Grassmannian

Let $V \cong \mathbb{C}^n$ be an n-dimensional complex vector space. For $0 \leq m \leq n$, the mth wedge product space

$$\bigwedge^m V = \{v_{i_1} \wedge v_{i_2} \wedge \cdots \wedge v_{i_m} \mid v_{i_j} \in V\}$$

is a vector space of dimension $\binom{n}{m}$. Let $W \subset V$ be an m-dimensional vector subspace of V, and

$$\{w_1, w_2, \cdots, w_m\}$$

a basis for W. We can assign an element

$$w_1 \wedge w_2 \wedge \cdots \wedge w_m \in \bigwedge^m V \tag{10.1}$$

to each basis of W. The *Grassmannian* $Gr(m, n)$ is the set of all m-dimensional vector subspaces of V, which has the structure of a smooth compact complex algebraic variety of dimension $m(n-m)$ [**9**]. The assignment (10.1) defines the *Plücker embedding*

$$Gr(m, n) \longrightarrow \mathbb{P}\left(\bigwedge^m V\right) \tag{10.2}$$

of the Grassmannian into the projective space of $\bigwedge^m V$. If we choose another basis $\{u_1, u_2 \cdots, u_m\}$, of W, then there is an $m \times m$ nonsingular matrix $A \in GL_m(\mathbb{C})$ such that

$$(u_1, u_2 \cdots, u_m) = A \cdot (w_1, w_2, \cdots, w_m).$$

Then

$$u_1 \wedge u_2 \wedge \cdots \wedge u_m = \det(A) \cdot w_1 \wedge w_2 \wedge \cdots \wedge w_m. \tag{10.3}$$

Thus $u_1 \wedge u_2 \wedge \cdots \wedge u_m$ and $w_1 \wedge w_2 \wedge \cdots \wedge w_m$ belong to the same line in the vector space $\bigwedge^m V$, and hence defines the same element of the projective space $\mathbb{P}\left(\bigwedge^m V\right)$.

Let us consider an infinite-dimensional generalization. As a vector space we use the set of formal Laurent series $V = \mathbb{C}((z))$ in z. We choose a *polarization*

$$\mathbb{C}((z)) = \mathbb{C}[z^{-1}] \oplus \mathbb{C}[[z]] \cdot z \tag{10.4}$$

of $\mathbb{C}((Z))$. The topology of $\mathbb{C}((z))$ is defined by the basis of open neighborhoods

$$V^{(\mu)} = \mathbb{C}[[z]] \cdot z^{-\mu}, \qquad \mu \in \mathbb{Z} \tag{10.5}$$

of $0 \in \mathbb{C}((z))$. A formal Laurent series $f(z)$ has *order* μ if

$$f(z) \in V^{(\mu)} \setminus V^{(\mu-1)}.$$

For example, $z^{-\mu}$ has order μ. Thus we have a valuation

$$\mathrm{ord} : \mathbb{C}((z)) \setminus \{0\} \longrightarrow \mathbb{Z}.$$

The open sets define a filtration

$$\cdots \subset V^{(\mu-1)} \subset V^{(\mu)} \subset V^{(\mu+1)} \subset \cdots \tag{10.6}$$

of V, and satisfy

$$\bigcap_{\mu\in\mathbb{Z}} V^{(\mu)} = \{0\}, \qquad \bigcup_{\mu\in\mathbb{Z}} V^{(\mu)} = V. \tag{10.7}$$

We note here that

$$V^{(\mu)}/V^{(\mu-1)} \cong \mathbb{C} \tag{10.8}$$

for every $\mu \in \mathbb{Z}$. For a subset $X \subset V$, let us define the set

$$N_X = \{\mu \in \mathbb{Z} \mid \mathrm{ord}(x) = \mu \text{ for some } x \in X\} \subset \mathbb{Z} \tag{10.9}$$

of the order of elements of X. The filtration (10.6) of V induces a filtration

$$X = \bigcup_{\mu\in\mathbb{Z}} X^{(\mu)}, \qquad X^{(\mu)} = X \cap V^{(\mu)} \tag{10.10}$$

of X.

For an arbitrary vector subspace $W \subset \mathbb{C}((z))$, let

$$\gamma_W : W \longrightarrow \mathbb{C}((z))/\mathbb{C}[[z]] \cdot z \cong \mathbb{C}[z^{-1}] \tag{10.11}$$

denote the natural map. Consider an exact sequence

$$0 \longrightarrow \mathrm{Ker}(\gamma_W) \longrightarrow W \xrightarrow{\gamma_W} \mathbb{C}((z))/\mathbb{C}[[z]] \cdot z \longrightarrow \mathrm{Coker}(\gamma_W) \longrightarrow 0. \tag{10.12}$$

The map γ_W is *Fredholm* if $\mathrm{Ker}(\gamma_W)$ and $\mathrm{Coker}(\gamma_W)$ are finite-dimensional. For a Fredholm map γ_W, its *index* is defined by

$$\mathrm{index}(\gamma_W) = \dim \mathrm{Ker}(\gamma_W) - \dim \mathrm{Coker}(\gamma_W). \tag{10.13}$$

Definition 10.1. The *universal Grassmannian* Gr of Sato [**24**] is the set

$$Gr = \{W \subset V \mid \gamma_W : W \longrightarrow \mathbb{C}[z^{-1}] \text{ is Fredholm}\}. \tag{10.14}$$

It is the disjoint union

$$Gr = \bigcup_{\mu\in\mathbb{Z}} Gr(\mu)$$

of connected components

$$Gr(\mu) = \{W \subset V \mid \gamma_W : W \longrightarrow \mathbb{C}[z^{-1}] \text{ is Fredholm of index } \mu\}. \tag{10.15}$$

The *big-cell* of the Grassmannian is the subset $Gr_\emptyset$ of $Gr(0)$ consisting of vector subspaces $W \subset V$ such that γ_W of (10.11) is an isomorphism.

In (10.4), the factor $\mathbb{C}[z^{-1}]$ is a closed subset of $\mathbb{C}((z))$, because its complement is the union

$$\bigcup_{p(z^{-1})\in\mathbb{C}[z^{-1}]} \bigcup_{\mu\geq 1} \bigcup_{\substack{f(z)\in\mathbb{C}[[z]]\cdot z \\ \mathrm{ord} f(z) = -\mu}} \left(p(z^{-1}) + f(z) + \mathbb{C}[[z]] \cdot z^{\mu+1}\right)$$

of open sets. More generally, if γ_W is Fredholm, then W is a closed subspace of $\mathbb{C}((z))$. Thus the universal Grassmannian parametrozes closed vector subspaces of V.

Let $W \in Gr$. Since γ_W is Fredholm, the set N_W of orders of elements of W contains only finitely many negative integers and all but finite positive integers. The number of missing non-negative integers of N_W is the dimension of $\mathrm{Coker}(\gamma_W)$, and the number of negative integers in N_W is the dimension of $\ker(\gamma_W)$. An *admissible* basis for W is a collection

$$\{w_\mu\}_{\mu \in N_W} \tag{10.16}$$

of monic elements of W such that $\mathrm{ord}(w_\mu) = \mu$. A formal power series of order μ is monic if its leading term is $z^{-\mu}$. Every $W \in Gr$ has an admissible basis.

2. Bosonization of Fermions

Now let us restrict to the case of index zero Grassmannian $Gr(0)$. It is more convenient to use $\{0, 1, 2, \cdots\}$ as the index set of a basis for $W \in Gr(0)$ than N_W. So let

$$\{w_0, w_1, w_2, \cdots\}$$

be an admissible basis for W such that $\mathrm{ord}(w_j) < \mathrm{ord}(w_{j+1})$. The index condition implies that

$$\mathrm{ord}(w_j) = j \qquad \text{for all } j >> 0. \tag{10.17}$$

For such an admissible basis for $W \in Gr(0)$, we can define a formal expression

$$w_0 \wedge w_1 \wedge w_2 \wedge \cdots \tag{10.18}$$

called a *half-infinite wedge product*. Let us denote by $\bigwedge^{\infty/2}(V)$ the space of linear combinations of half-infinite wedge products for all $W \in Gr(0)$. Since

$$\dim W^{(\mu)}/W^{(\mu-1)} = \begin{cases} 1 & \text{if } \mu \in N_W \\ 0 & \text{otherwise,} \end{cases} \tag{10.19}$$

two admissible bases for W are related by the multiplication of an upper-diagonal matrix

$$(w_0', w_1', w_2', w_3', \cdots) = (w_0, w_1, w_2, w_3, \cdots) \begin{pmatrix} 1 & a_{01} & a_{02} & a_{03} & \dots \\ & 1 & a_{12} & a_{13} & \dots \\ & & 1 & a_{23} & \dots \\ & & & 1 & \dots \\ & & & & \ddots \end{pmatrix}. \tag{10.20}$$

The infinite-dimensional version of (10.3) is simply

$$w_0 \wedge w_1 \wedge w_2 \wedge \cdots = w_0' \wedge w_1' \wedge w_2' \wedge \cdots,$$

because the determinant of the upper-triangular matrix of (10.20) is 1. Following Dirac [**5**], we use the *ket vector* natation

$$|W\rangle = w_0 \wedge w_1 \wedge w_2 \wedge \cdots \in \bigwedge^{\frac{\infty}{2}}(V).$$

The infinite-dimensional Plücker embedding is the map

$$i : Gr(0) \ni W \longmapsto [w_0 \wedge w_1 \wedge w_2 \wedge \cdots] \in \mathbb{P}\left(\bigwedge^{\frac{\infty}{2}}(V)\right). \tag{10.21}$$

Let $e_\mu = z^{-\mu} \in V$. Then $\{e_\mu\}_{\mu\in\mathbb{Z}}$ forms a formal basis for V. Let e_μ^* be the dual basis for the formal dual V^*. We have

$$\langle e_\mu^* | e_\nu \rangle = \delta_{\mu\nu}.$$

This pairing can be extended to the space of the half-infinite forms in the following restricted manner. Let $W \in Gr(0)$ and $\{w_0, w_1, w_2, \cdots\}$ be an addmissible basis for W. We define

$$\langle \cdots \wedge e_2^* \wedge e_1^* \wedge e_0^* | w_0 \wedge w_1 \wedge w_2 \wedge \cdots \rangle = \langle e_0^* | w_0 \rangle \cdot \langle e_1^* | w_1 \rangle \cdot \langle e_2^* | w_2 \rangle \cdot \cdots . \tag{10.22}$$

Since $\mathrm{ord}(w_j) = j$ for all large j,

$$\langle e_j^* | w_j \rangle = 1$$

for all $j >> 0$. Thus the infinite product (10.22) is actually a well-defined finite product. Again following Dirac, we write

$$\langle 0| = \cdots \wedge e_2^* \wedge e_1^* \wedge e_0^*$$

as a *bra vector*, so that the *braket* give us

$$\langle 0|W\rangle = \langle \cdots \wedge e_2^* \wedge e_1^* \wedge e_0^* | w_0 \wedge w_1 \wedge w_2 \wedge \cdots \rangle.$$

As a function on $Gr(0)$, $\langle 0|W\rangle$ takes values either 0 or 1:

$$\langle 0|W\rangle = \begin{cases} 1 & \text{if } W \in Gr_\emptyset \\ 0 & \text{otherwise.} \end{cases} \tag{10.23}$$

The function $\langle 0|*\rangle$ can be extended linearly to the whole $\bigwedge^{\frac{\infty}{2}}(V)$.

When V is a finite-dimensional vector space, the Grassmann algebra over V is also finite-dimensional, hence it cannot be isomorphic to a polynomial ring. In the case of infinite dimensions, the situation is different. Consider a weighted homogeneous polynomial $p_r(t)$ in $\mathbb{Q}[t_1, \cdots, t_{2m}]$ of degree r defined by

$$p_r(t) = \sum_{n_1+2n_2+3n_3+\cdots+(2m)n_{2m}=r} \frac{t_1^{n_1} \cdot t_2^{n_2} \cdot t_3^{n_3} \cdots t_{2m}^{n_{2m}}}{n_1! \cdot n_2! \cdot n_3! \cdots n_{2m}!}. \tag{10.24}$$

We have a relation

$$\exp\left(\sum_{\alpha=1}^{2m} t_\alpha k^\alpha\right) = \sum_{r=0}^{\infty} p_r(t) k^r \tag{10.25}$$

as an entire function in $t_1, \cdots, t_{2m}$ and k. As before, we can take the limit of $m \to \infty$, and we have an equation

$$\exp\left(\sum_{\alpha=1}^{\infty} t_\alpha k^\alpha\right) = \sum_{r=0}^{\infty} p_r(t) k^r \tag{10.26}$$

as an element in $\mathbb{C}[[t_1, t_2, t_3, \cdots]]$ for every $k \in \mathbb{C}$. For a given r, there are finitely many non-negative numbers n_j such that

$$\sum_{j=1}^{\infty} j n_j = r.$$

Therefore,

$$p_r(t) = \sum_{n_1+2n_2+3n_3+\cdots=r} \frac{t_1^{n_1} \cdot t_2^{n_2} \cdot t_3^{n_3} \cdots}{n_1! \cdot n_2! \cdot n_3! \cdots} \tag{10.27}$$

is still a weighted homogeneous polynomial of degree r. The *time evolution operator* is an expression

$$H(t) = \exp\left(\sum_{\alpha=1}^{\infty} t_\alpha z^{-\alpha}\right) = \sum_{r=0}^{\infty} p_r(t) z^{-r} \in (\mathbb{C}((z)))\,[[t_1, t_2, t_3, \cdots]]. \tag{10.28}$$

We note that $H(t)$ does not make sense as an element of

$$(\mathbb{C}[[t_1, t_2, t_3, \cdots]])\,((z)).$$

The time evolution operator defines a map

$$H(t) : V \ni w \longmapsto w(t) = H(t) \cdot w \in (\mathbb{C}((z)))\,[[t_1, t_2, t_3, \cdots]].$$

For a point W of the Grassmannian, we define

$$W(t) = \{H(t) \cdot w \mid w \in W\} \subset (\mathbb{C}((z)))\,[[t_1, t_2, t_3, \cdots]]. \tag{10.29}$$

We wish to define an element

$$\langle 0|W(t)\rangle \in \mathbb{C}[[t_1, t_2, t_3, \cdots]].$$

For this purpose, let us introduce an infinte matrix representation of the points of the Grassmannian. An element

$$w(z) = \sum_{\mu=-\infty}^{\infty} c_\mu z^\mu \in V$$

is identified with a column vector of infinite length

$$w = \begin{bmatrix} \vdots \\ c_{-2} \\ c_{-1} \\ c_0 \\ c_1 \\ c_2 \\ \vdots \end{bmatrix}. \tag{10.30}$$

The multiplication of z^{-1} to $w(z)$ corresponds to shifting the entries of (10.30)

$$z^{-1} \cdot w = \begin{bmatrix} \ddots & & & & & & & \\ & 0 & 1 & & & & & \\ & & 0 & 1 & & & & \\ & & & 0 & 1 & & & \\ & & & & 0 & 1 & & \\ & & & & & 0 & & \\ & & & & & & \ddots & \end{bmatrix} \begin{bmatrix} \vdots \\ c_{-2} \\ c_{-1} \\ c_0 \\ c_1 \\ c_2 \\ \vdots \end{bmatrix} = \begin{bmatrix} \vdots \\ c_{-1} \\ c_0 \\ c_1 \\ c_2 \\ c_3 \\ \vdots \end{bmatrix}. \tag{10.31}$$

Thus the time evolution operator $H(t)$ has the matrix representation as shown in Figure 10.1, where $p_r = p_r(t)$.

Let $W \in Gr(0)$ be a point of the index 0 Grassmannian, and $\{w_j\}_{j\geq 0}$ an admissible basis for W. Since $\deg(w_j) = j$ for $j >> 0$, there is an integer N such that $\deg(w_j) = j$ for all $j \geq N$. We can arrange the basis vectors such that

$$w_j = z^{-m_j} + \sum_{i=1}^{\infty} c_{-m_j+i,-j} z^{-m_j+i} \qquad 0 \leq j < N \tag{10.32}$$

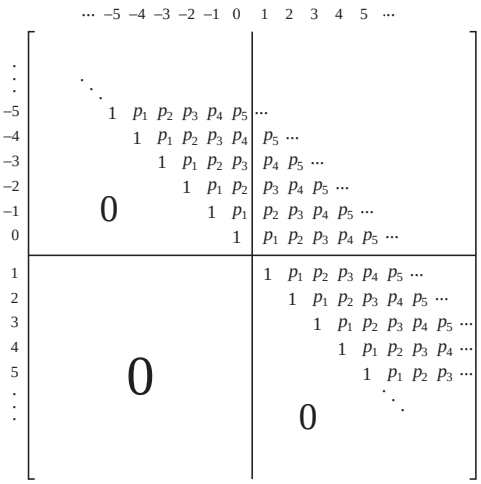

FIGURE 10.1. The Matrix Representation of the Time Evolution Operator

$$w_j = z^{-j} + \sum_{i=1}^{\infty} c_{-N+i,-j} z^{-j+i} \qquad j \geq N, \tag{10.33}$$

where $\{m_0, m_1, m_2, \cdots\} = N_W$ is the set of the order of elements of W. The matrix representation of the admissible basis is given in Figure 10.2.

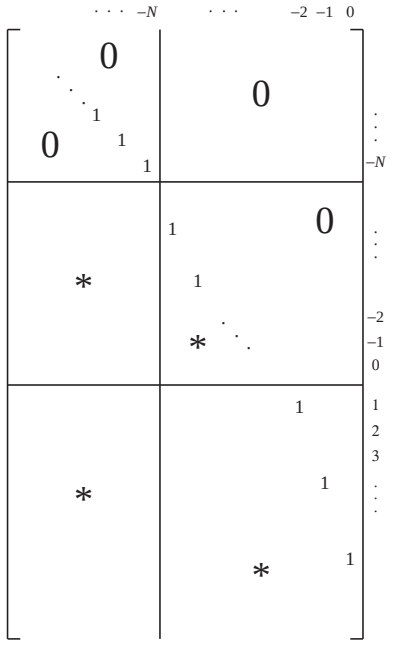

FIGURE 10.2. The Matrix Representation of a Point of the Grassmannian

The product of any row of the matrix of Figure 10.1 and any column of the matrix of Figure 10.1 is a well-defined element of $\mathbb{C}[[t_1, t_2, t_3, \cdots]]$. We use $\mathfrak{I}_r$ to denote the ideal of $\mathbb{C}[[t_1, t_2, t_3, \cdots]]$ generated by weighted homogeneous polynomials of degree r.

3. Schur Polynomials

4. Plücker Relations

5. Tau-Functions and the KP Equations

CHAPTER 11

Hermitian Matrix Integrals and the KP Equations

1. The Hermitian Matrix Integral as a τ-Function

There are no analytic methods to evaluate the Hermitian matrix integral

$$Z_q(t,m) = \int_{\mathcal{H}_q} \exp\left(-\frac{1}{2}\mathrm{trace}(X^2)\right) \exp\left(\mathrm{trace}\sum_{j=3}^{2m}\frac{t_j}{j}X^j\right)\frac{d\mu(X)}{N}.$$

However, the integral as a function in t can be characterized by the fact that *it satisfies the system of the KP equations*. In this section we prove this statement.

To investigate the most general case, let us define

$$Z_q(t,m,\phi) = \int_{\mathcal{H}_q} \exp\left(\mathrm{trace}\sum_{j=1}^{2m}\frac{t_j}{j}X^j\right)\phi(X)\frac{d\mu(X)}{N}, \tag{11.1}$$

where

(11.2)

$$\phi(X) = \phi(k_0,k_1,\cdots k_{q-1}) = \frac{\det\begin{pmatrix}\phi_0(k_0) & \phi_1(k_0) & \dots & \phi_{q-1}(k_0)\\ \phi_0(k_1) & \phi_1(k_1) & \dots & \phi_{q-1}(k_1)\\ \vdots & \vdots & \ddots & \vdots\\ \phi_0(k_{q-1}) & \phi_1(k_{q-1}) & \dots & \phi_{q-1}(k_{q-1})\end{pmatrix}}{\Delta\big(k_0,k_1\cdots,k_{q-1}\big)}$$

is a $U(q)$-invariant function on $\mathcal{H}_q$ determined by q functions $\phi_0(k),\cdots,\phi_{q-1}(k)$ in one variable, and $k_0,\cdots,k_{q-1}$ are eigenvalues of X. Unlike (7.15), we allow terms containing t_1X and t_2X^2 in the integral (11.1). Using (8.8), we have

$$\begin{aligned} Z_q(t,m,\phi) &= \int_{\mathcal{H}_q}\exp\left(\mathrm{trace}\sum_{\alpha=1}^{2m}\frac{t_\alpha}{\alpha}X^\alpha\right)\phi(X)\cdot\frac{d\mu(X)}{N}\\ &= \frac{c(q)}{N}\int_{\mathbb{R}^q}\exp\left(\sum_{i=0}^{q-1}\sum_{\alpha=1}^{2m}\frac{t_\alpha}{\alpha}k_i^\alpha\right)\Delta(k_0,\cdots,k_{q-1})\det\left(\phi_j(k_i)\right)dk_0\cdots dk_{q-1}. \end{aligned}$$

Here we need a simple formula to proceed further. Let $\phi_0(k),\cdots,\phi_{q-1}(k)$ and $\psi_0(k),\cdots,\psi_{q-1}(k)$ be $2q$ arbitrary functions in k. Then

$$\det\left[\phi_i(k_\ell)\right]\cdot\det\left[\psi_j(k_\ell)\right] = \sum_{\sigma\in\mathfrak{S}_q}\det\left[\phi_i(k_{\sigma(j)})\cdot\psi_j(k_{\sigma(j)})\right], \tag{11.3}$$

where σ runs over all permutations of $\mathfrak{S}_q$. To prove (11.3), we calculate the left hand side by the usual product formula of the determinant. It is a summation of q^q terms. Because of the multilinearity of the determinants, only $q!$ of these terms

are nonzero. Rearranging the $q!$ terms, we obtain the above formula. Using this formula for $\psi_j(k) = k^j$, we obtain

$$\begin{aligned}
&Z_q(t, m, \phi) \\
&= \frac{c(q)}{N} \int_{\mathbb{R}^q} \exp\left(\sum_{i=0}^{q-1}\sum_{\alpha=1}^{2m} \frac{t_\alpha}{\alpha} k_i^\alpha\right) \sum_{\sigma\in\mathfrak{S}_q} \det\left(\phi_j(k_{\sigma(i)})k_{\sigma(i)}^i\right) dk_0\cdots dk_{q-1} \\
&= \frac{c(q)}{N} \int_{\mathbb{R}^q} \sum_{\sigma\in\mathfrak{S}_q} \exp\left(\sum_{i=0}^{q-1}\sum_{\alpha=1}^{2m} \frac{t_\alpha}{\alpha} k_{\sigma(i)}^\alpha\right) \det\left(\phi_j(k_{\sigma(i)})k_{\sigma(i)}^i\right) dk_0\cdots dk_{q-1} \\
&= \frac{c(q)}{N} \sum_{\sigma\in\mathfrak{S}_q} \det\left(\int_{\mathbb{R}^q} \exp\left(\sum_{\alpha=1}^{2m} \frac{t_\alpha}{\alpha} k_{\sigma(i)}^\alpha\right)\phi_j(k_{\sigma(i)})k_{\sigma(i)}^i\right) dk_0\cdots dk_{q-1} \\
&= q!\cdot\frac{c(q)}{N} \det\left(\int_{-\infty}^{\infty} \exp\left(\sum_{\alpha=1}^{2m} \frac{t_\alpha}{\alpha} k_i^\alpha\right)\phi_j(k_i)k_i^i dk_i\right) \\
&= q!\cdot\frac{c(q)}{N} \det\left(\int_{-\infty}^{\infty} \exp\left(\sum_{\alpha=1}^{2m} \frac{t_\alpha}{\alpha} k^\alpha\right)\phi_j(k)k^i dk\right).
\end{aligned}$$

The above computation makes sense as a complex analytic function in

$$(t_1, \cdots, t_{2m-1}, t_{2m}) \in \mathbb{C}^{2m-1} \times \Omega_\epsilon,$$

on which the integral converges provided that $|\phi_j(k)|$ grows slower than $\exp(k^{2m})$. To compare our t_j's with the standard time variables in the KP theory, let us set

$$T_\alpha = \frac{t_\alpha}{\alpha}.$$

From (10.25), we have

$$\begin{aligned}
Z_q(t, m, \phi) = q!\cdot\frac{c(q)}{N} \det\left(\int_{-\infty}^{\infty} \sum_{r=0}^{\infty} p_r(T)k^r\phi_j(k)k^i dk\right) \\
= q!\cdot\frac{c(q)}{N} \det\left(\int_{-\infty}^{\infty} \sum_{r=0}^{\infty} p_{r-i}(T)k^r\phi_j(k)dk\right),
\end{aligned}$$

where we define $p_r(T) = 0$ for $r < 0$.

LEMMA 11.1. *Let $\phi_j(k)$, $j = 0, \cdots, q-1$, be a function defined on $\mathbb{R}$ such that*

$$\int_{-\infty}^{\infty} k^r\phi_j(k)dk$$

exists for all $r \geq 0$. Then as a holomorphic function defined for $Re(t_{2m}) < 0$, we have

$$\mathcal{A}\left(\int_{-\infty}^{\infty} \exp\left(\sum_{\alpha=1}^{2m} \frac{t_\alpha}{\alpha} k^\alpha\right)\phi_j(k)k^i dk\right) = \sum_{r=0}^{\infty} p_{r-i}(T)\int_{-\infty}^{\infty} k^r\phi_j(k)dk$$

as $t_{2m} \to 0$.

PROOF. The argument is the same as the one we used in Section **??**. We choose a fixed t_{2m} so that $Re(t_{2m}) < 0$. Because of the uniform convergence of the power

series expansion of the integrand, we can interchange the integral and the infinite sums for $\alpha = 1, \cdots, 2m-1$. Using (**??**), (**??**) and (**??**), we have

$$\begin{aligned}
&\mathcal{A}\left(\int_{-\infty}^{\infty} \exp\left(\sum_{\alpha=1}^{2m} T_\alpha k^\alpha\right)\phi_j(k)k^i dk\right) \\
&= \sum_{n_1=0}^{\infty} \frac{{T_1}^{n_1}}{n_1!} \cdots \sum_{n_{2m}=0}^{\infty} \frac{{T_{2m}}^{n_{2m}}}{n_{2m}!} \int_{-\infty}^{\infty} k^{i+n_1+2n_2+\cdots+(2m)n_{2m}}\phi_j(k)dk \\
&= \sum_{r=0}^{\infty} p_r(T) \int_{-\infty}^{\infty} k^{i+r}\phi_j(k)dk.
\end{aligned}$$

□

Thus we have established

$$\begin{aligned}
\mathcal{A}\left(Z_q(t,m,\phi)\right) &= q! \cdot \frac{c(q)}{N} \det\left(\sum_{r=0}^{\infty} p_{r-i}(T) \int_{-\infty}^{\infty} k^r \phi_j(k)dk\right) \\
&= \det\left(\sum_{r=0}^{\infty} p_{r-i}(T)\xi_{rj}\right),
\end{aligned} \tag{11.4}$$

where

$$\xi_{rj} = q! \cdot \frac{c(q)}{N} \int_{-\infty}^{\infty} k^r \phi_j(k)dk.$$

We recall that the determinant in (11.4) is an $n \times n$ determinant. Sato [**24**] proved that any size determinant of the form

$$\det\left(\sum_{r=0}^{\infty} p_{r-i}(T)\xi_{rj}\right) \tag{11.5}$$

satisfies the Hirota bilinear form of the KP equations. He also proved that every power series solution of the KP system should be written as (11.5), allowing certain infinite determinants. A necessary background of the KP theory can be found in [**16**].

We have thus proved the following theorem.

THEOREM 11.2. *If $\phi_j(k)$, $j = 0, \cdots, q-1$, satisfies that*

$$\left|\int_{-\infty}^{\infty} k^r \phi_j(k)dk\right| < +\infty$$

for all $r \geq 0$, then the asymptotic expansion of the matrix integral $Z_q(t,m,\phi)$ satisfies the KP equations with respect to $T_1, T_2, \cdots, T_{2m}$. Moreover, if we choose a value of T_{2m} such that $Re(T_{2m}) < 0$ and fix it, then $Z_q(t,m,\phi)$ itself is an entire holomorphic solution to the KP equations with respect to $(T_1, T_2, \cdots, T_{2m-1}) \in \mathbb{C}^{2m-1}$. In particular,

$$u(T_1, T_2, T_3, \cdots) = \frac{\partial^2}{\partial T_1^2} \log(Z_q(t,m,\phi))$$

is a meromorphic solution to the KP equation

$$\frac{3}{4}u_{22} = \left(u_3 - \frac{1}{4}u_{111} - 3uu_1\right)_1,$$

where u_j denotes the partial derivative of u with respect to T_j.

The formula we have just established is a continuum version of the famous Hirota soliton solution of the KP equations [**24**]. The most general soliton solution of the KP equations due to Mikio and Yasuko Sato depends on $nM+M$ parameters c_{ij} and λ_i, where $0 \leq i \leq M-1$ and $0 \leq j \leq q-1$. Let

$$\eta(T,k) = \sum_{\alpha=1}^{2m} T_\alpha k^\alpha.$$

Then Sato-Sato's soliton solution is given by

$$\sum_{0 \leq i_0 < \cdots < i_{q-1} \leq M-1} \exp\left(\sum_{j=0}^{q-1} \eta(T, \lambda_{i_j})\right) \Delta(\lambda_{i_0}, \cdots, \lambda_{i_{q-1}}) \det \begin{pmatrix} c_{i_0 0} & \cdots & c_{i_0 q-1} \\ \vdots & & \vdots \\ c_{i_{q-1} 0} & \cdots & c_{i_{q-1} q-1} \end{pmatrix}.$$

This coincides with our $Z_q(t,m,\phi)$ if we take

$$\phi_j(k) = \sum_{i=0}^{M-1} c_{ij} \delta(k - \lambda_i).$$

Therefore, our matrix integral $Z_q(t,m,\phi)$ of (**??**) with (**??**) is indeed a *continuum soliton solution* of the KP equations.

So far we have dealt with the matrix integrals with a fixed integer m in this section. As before, we can take the limit $m \to \infty$ of these integrals, which gives formal power series solutions of the whole hierarchy of the KP equations. Note that the determinant expression of (11.4) does not have any explicit mention on the integer m. Therefore, we have obtained the third asymptotic formula for the matrix integral:

$$\lim_{m \to \infty} \mathcal{A}\left(Z_q(t,m,\phi)\right) = q! \cdot \frac{c(q)}{N} \det\left(\sum_{r=0}^{\infty} p_{r-i}(T) \int_{-\infty}^{\infty} k^r \phi_j(k) dk\right). \tag{11.6}$$

2. Transcendental Solutions of the KP Equations and the sl_2 Stability

There are several different ways to construct solutions to the KP equations. The Krichever construction and its generalizations are based on the correspondence between certain points of the Grassmannian of Sato [**24**] and the algebro-geometric data consisting of an irreducible algebraic curve (possibly singular) and a torsion-free sheaf on it [**15**]. These solutions deserve to be called *algebraic*, because they carry geometric information of algebraic curves. Let us call a solution to the KP equations *transcendental* if no algebraic curve corresponds to this solution. The natural question we can ask is: how can we construct a transcendental solution?

In this section we show that the Hermitian matrix integrals we have been dealing with in the earlier sections are indeed transcendental solutions.

The technique we show that these matrix integrals are transcendental solutions is based on the observation that the points of the Grassmannian corresponding to these solutions satisfy a peculiar $sl(2)$ stability condition. Since these solutions are deeply related to the moduli theory of Riemann surfaces, the appearance of $sl(2)$ is mysteriously suggestive. At present we do not have any geometric explanation

of the relation between the KP equations, the $sl(2)$ stability on the Grassmannian, and the moduli theory of pointed Riemann surfaces.

Let W be a point of the big-cell of the Grassmannian. We can choose a basis

$$\langle w_0, w_1, w_2, \cdots \rangle$$

for W such that

$$w_j = z^{-j} + \sum_{i=1}^{\infty} c_{ij} z^i, \qquad j = 0, 1, 2, \cdots . \tag{11.7}$$

The *Bosonization* is a map

$$Gr \longrightarrow \mathbb{P}(\mathbb{C}[[T_1, T_2, T_3, \cdots]]) \tag{11.8}$$

that assigns a τ-function τ_W to each point W of the Grassmannian. For a point W of the big-cell with a basis (11.7), the Bosonization has an infinite determinant expression

$$\tau_W = \det \left(p_{i-j}(T) + \sum_{\mu=1}^{\infty} p_{\mu+i}(T) c_{\mu j} \right). \tag{11.9}$$

The infinite determinant gives a well-defined element of $\mathbb{C}[[T_1, T_2, T_3, \cdots]]$ in the same manner as we have explained in the earlier sections. Sato's formula (11.5) gives another expression of the Bosonization map. For more detail, we refer to [**16**] and [**17**].

The *commutative stabilizer* of $W \in Gr$ is defined by

$$A_W = \{a \in \mathbb{C}((z)) \mid a \cdot W \subset W\}. \tag{11.10}$$

The key idea that connects the KP equations and algebraic curves is that the commutative stabilizer is the coordinate ring of an algebraic curve. If the greatest common divisor of the pole order of elements in A_W is 1, then the Bosonization τ_W of W is essentially the Riemann theta function associated with the algebraic curve C whose coordinate ring is A_W [**14**], [**16**].

DEFINITION 11.3. A solution of the KP equations τ_W is said to be *transcendental* if

$$A_W = \mathbb{C}. \tag{11.11}$$

REMARK. It is known that if $A_W \neq \mathbb{C}$, then the Bosonization τ_W of W is a solution to the KP equation corresponding to a vector bundle $\mathcal{F}$ on an algebraic curve C such that

$$H^0(C, \mathcal{F}) = H^1(C, \mathcal{F}) = 0 \tag{11.12}$$

[**15**]. Conversely, there is a solution corresponding to an arbitrary torsion-free sheaf $\mathcal{F}$ defined on an arbitrary (possibly singular) algebraic curve C satisfying (11.12). None of these solutions are transcendental.

The Hermitian matrix integral we have discussed in Section **??** gives a transcendental solution to the KP equations.

THEOREM 11.4. *Choose arbitrary positive integers k and q, and let*

$$a = (a_1, a_2, \cdots, a_{2k}) \in \mathbb{C}^{2k}$$

be a complex vector such that $Re(a_{2k}) < 0$. Define a formal Laurent series

$$w_j = \sum_{r=0}^{\infty} \left(\int_{-\infty}^{\infty} \lambda^{r+j} \exp\left(\sum_{\mu=1}^{2k} a_\mu \lambda^\mu \right) d\lambda \right) z^{r+1-n} \in \mathbb{C}((z)) \tag{11.13}$$

for $j = 0, 1, 2, \cdots, q-1$, and let

$$W(a) = \langle w_0, w_1, \cdots, w_{q-1}, z^{-n}, z^{-q-1}, \cdots \rangle \in Gr \tag{11.14}$$

be a point of the Grassmannian spanned by $w_0, w_1, \cdots, w_{q-1}$, and $z^{-n}, z^{-q-1}, \cdots$. Then the τ-function corresponding to $W(a)$ is given by the asymptotic expansion of a Hermitian matrix integral:

(11.15)

$$\tau_{W(a)} = \lim_{m\to\infty} \mathcal{A} \left(\int_{\mathcal{H}_q} \exp\left(\sum_{j=1}^{2m} T_j \mathrm{trace}(X^j) \right) \exp\left(\sum_{\mu=1}^{2k} a_\mu \mathrm{trace}(X^\mu) \right) dX \right),$$

where we take $Re(T_{2m}) < 0$ first and then let $m \to \infty$ to determine a well-defined formal power series in $\mathbb{C}[[T_1, T_2, T_3, \cdots]]$. Define a linear differential operator

$$L_i(a) = z^{1-i} \frac{d}{dz} + \frac{(3q-1) + i(q-1)}{2} z^{-i} + \sum_{\mu=1}^{2k} \mu a_\mu z^{-i-\mu} \tag{11.16}$$

for $i = -1, 0, 1$. These differential operators satisfy the $sl(2, \mathbb{C})$ relation

$$[L_i(a), L_j(a)] = (i-j) L_{i+j}(a).$$

The point $W(a)$ of the Grassmannian satisfies the non-commutative stability condition

$$L_i(a) \cdot W(a) \subset W(a), \qquad i = -1, 0, 1. \tag{11.17}$$

Moreover, $\tau_{W(a)}$ is a transcendental solution of the KP equations.

Proof. The function

$$\exp\left(\sum_{\mu=1}^{2k} a_\mu \mathrm{trace}(X^\mu) \right)$$

is a special case of the function $\phi(X)$ defined in (**??**). Thus the results of the previous section proves that $\tau_{W(a)}$ is a τ-function of the KP equations corresponding to the point of the Grassmannian $W(a)$.

Let us first prove that the $sl(2)$ stability condition (11.17) implies that the commutative stabilizer is trivial:

$$A_{W(a)} = \mathbb{C}.$$

Suppose $f(z) \in A_{W(a)} \subset \mathbb{C}((z))$, and let $\mathrm{ord}(f) = \nu > 0$, where we define the *pole order* by

$$\mathrm{ord}(z^{-\nu}) = \nu.$$

Since $L_{-1}(a)$ and f stabilize $W(a)$,

$$[L_{-1}(a), f] = z^2 \frac{df}{dz} \in A_{W(a)}$$

also stabilizes $W(a)$. Note that

$$\mathrm{ord}([L_{-1}(a), f]) = \nu - 1.$$

Thus we can immediately conclude that

$$A_{W(a)} = \mathbb{C}[z^{-1}].$$

But then

$$L_{-1}(a) - \sum_{\mu=1}^{2k} \mu a_\mu z^{1-\mu} = z^2 \frac{d}{dz} + \frac{(3q-1)-(q-1)}{2} z \tag{11.18}$$

stabilizes $W(a)$. Since the new stabilizer (11.18) decreases the order of elements of $W(a)$ exactly by 1, $W(a)$ must have an element of arbitrary negative order. But this contradicts to the Fredholm condition of $W(a)$. This means $A_{W(a)} = \mathbb{C}$, hence $\tau_{W(a)}$ is a transcendental solution.

Now all we need is to show (11.17), which can be verified by a straightforward computation. First, we note a simple formula

$$\begin{aligned} 0 &= \int_{-\infty}^{\infty} \frac{d}{d\lambda} \left(\lambda^\alpha \exp\left(\sum_{\mu=1}^{2k} a_\mu \lambda^\mu \right) d\lambda \right) \\ &= \int_{-\infty}^{\infty} \alpha \lambda^{\alpha-1} \exp\left(\sum_{\mu=1}^{2k} a_\mu \lambda^\mu \right) d\lambda \\ &\quad + \int_{-\infty}^{\infty} \sum_{\mu=1}^{2k} \mu a_\mu \lambda^{\alpha+\mu-1} \exp\left(\sum_{\mu=1}^{2k} a_\mu \lambda^\mu \right) d\lambda. \end{aligned} \tag{11.19}$$

Let us compute the effect of the differential operators (11.16) on the basis elements of $W(a)$. First, we have

$$\begin{aligned} L_{-1}(a) w_j &= \left(z^2 \frac{d}{dz} + nz + \sum_{\mu=1}^{2k} \mu a_\mu z^{1-\mu} \right) \sum_{r=0}^{\infty} z^{r+1-n} \int_{-\infty}^{\infty} \lambda^{r+j} e^{\sum_{\mu=1}^{2k} a_\mu \lambda^\mu} d\lambda \\ &= \sum_{r=0}^{\infty} (r+1) z^{r+2-n} \int_{-\infty}^{\infty} \lambda^{r+j} e^{\sum_{\mu=1}^{2k} a_\mu \lambda^\mu} d\lambda \\ &\quad + \sum_{r=0}^{\infty} \sum_{\mu=1}^{2k} z^{r+2-n-\mu} \int_{-\infty}^{\infty} \lambda^{r+j} \mu a_\mu e^{\sum_{\mu=1}^{2k} a_\mu \lambda^\mu} d\lambda \\ &= \sum_{r=0}^{\infty} r z^{r+1-n} \int_{-\infty}^{\infty} \lambda^{r+j-1} e^{\sum_{\mu=1}^{2k} a_\mu \lambda^\mu} d\lambda \\ &\quad + \sum_{\mu=1}^{2k} \sum_{r=0}^{\mu-2} z^{r+2-n-\mu} \int_{-\infty}^{\infty} \lambda^{r+j} \mu a_\mu e^{\sum_{\mu=1}^{2k} a_\mu \lambda^\mu} d\lambda \\ &\quad + \sum_{\mu=1}^{2k} \sum_{r=\mu-1}^{\infty} z^{r+2-n-\mu} \int_{-\infty}^{\infty} \lambda^{r+j} \mu a_\mu e^{\sum_{\mu=1}^{2k} a_\mu \lambda^\mu} d\lambda \\ &= \sum_{r=0}^{\infty} r z^{r+1-n} \int_{-\infty}^{\infty} \lambda^{r+j-1} e^{\sum_{\mu=1}^{2k} a_\mu \lambda^\mu} d\lambda \\ &\quad + \sum_{\mu=1}^{2k} \sum_{r=0}^{\mu-2} z^{r+2-n-\mu} \int_{-\infty}^{\infty} \lambda^{r+j} \mu a_\mu e^{\sum_{\mu=1}^{2k} a_\mu \lambda^\mu} d\lambda \end{aligned}$$

$$
\begin{aligned}
&+\sum_{\mu=1}^{2k}\sum_{r=0}^{\infty} z^{r+1-n}\int_{-\infty}^{\infty}\lambda^{r+j+\mu-1}\mu a_\mu e^{\sum_{\mu=1}^{2k}a_\mu\lambda^\mu}d\lambda\\
&=\sum_{r=0}^{\infty} r z^{r+1-n}\int_{-\infty}^{\infty}\lambda^{r+j-1}e^{\sum_{\mu=1}^{2k}a_\mu\lambda^\mu}d\lambda\\
&+\sum_{\mu=1}^{2k}\sum_{r=0}^{\mu-2} z^{r+2-n-\mu}\int_{-\infty}^{\infty}\lambda^{r+j}\mu a_\mu e^{\sum_{\mu=1}^{2k}a_\mu\lambda^\mu}d\lambda\\
&-\sum_{r=0}^{\infty} z^{r+1-n}\int_{-\infty}^{\infty}(r+j)\lambda^{r+j-1}e^{\sum_{\mu=1}^{2k}a_\mu\lambda^\mu}d\lambda\\
=&-jw_{j-1}+\sum_{\mu=1}^{2k}\sum_{r=0}^{\mu-2} z^{r+2-n-\mu}\int_{-\infty}^{\infty}\lambda^{r+j}\mu a_\mu e^{\sum_{\mu=1}^{2k}a_\mu\lambda^\mu}d\lambda\\
&\in W(a)
\end{aligned}
$$

for all $j=0,1,2,\cdots,q-1$. Note that w_{-1} does not appear in the above computation because of the combination jw_{j-1}. For the basis elements $z^{-n}, z^{-q-1},\cdots$, we have

$$
\begin{aligned}
L_{-1}(a)z^{-n-i}&=\left(z^2\frac{d}{dz}+nz+\sum_{\mu=1}^{2k}\mu a_\mu z^{1-\mu}\right)z^{-n-i}\\
&=(-i)z^{-n-i+1}+\sum_{\mu=1}^{2k}\mu a_\mu z^{1-\mu-n-i}\in W(a)
\end{aligned}
$$

for all $i\geq 0$. We note that the term z^{-n+1} does not appear in this computation. Thus we conclude

$$L_{-1}(a)\cdot W(a)\subset W(a).$$

For $j=0$, we have

$$
\begin{aligned}
L_0(a)w_j&=\left(z\frac{d}{dz}+\frac{3q-1}{2}+\sum_{\mu=1}^{2k}\mu a_\mu z^{-\mu}\right)\sum_{r=0}^{\infty} z^{r+1-n}\int_{-\infty}^{\infty}\lambda^{r+j}e^{\sum_{\mu=1}^{2k}a_\mu\lambda^\mu}d\lambda\\
&=\sum_{r=0}^{\infty}(r+\frac{n+1}{2})z^{r+1-n}\int_{-\infty}^{\infty}\lambda^{r+j}e^{\sum_{\mu=1}^{2k}a_\mu\lambda^\mu}d\lambda\\
&+\sum_{r=0}^{\infty}\sum_{\mu=1}^{2k} z^{r+1-n-\mu}\int_{-\infty}^{\infty}\lambda^{r+j}\mu a_\mu e^{\sum_{\mu=1}^{2k}a_\mu\lambda^\mu}d\lambda\\
&=\frac{n+1}{2}w_j+\sum_{r=0}^{\infty} r z^{r+1-n}\int_{-\infty}^{\infty}\lambda^{r+j}e^{\sum_{\mu=1}^{2k}a_\mu\lambda^\mu}d\lambda\\
&+\sum_{\mu=1}^{2k}\sum_{r=0}^{\mu-1} z^{r+1-n-\mu}\int_{-\infty}^{\infty}\lambda^{r+j}\mu a_\mu e^{\sum_{\mu=1}^{2k}a_\mu\lambda^\mu}d\lambda\\
&+\sum_{\mu=1}^{2k}\sum_{r=\mu}^{\infty} z^{r+1-n-\mu}\int_{-\infty}^{\infty}\lambda^{r+j}\mu a_\mu e^{\sum_{\mu=1}^{2k}a_\mu\lambda^\mu}d\lambda
\end{aligned}
$$

$$
\begin{aligned}
&= \frac{n+1}{2} w_j + \sum_{r=0}^{\infty} r z^{r+1-n} \int_{-\infty}^{\infty} \lambda^{r+j} e^{\sum_{\mu=1}^{2k} a_\mu \lambda^\mu} d\lambda \\
&\quad + \sum_{\mu=1}^{2k} \sum_{r=0}^{\mu-1} z^{r+1-n-\mu} \int_{-\infty}^{\infty} \lambda^{r+j} \mu a_\mu e^{\sum_{\mu=1}^{2k} a_\mu \lambda^\mu} d\lambda \\
&\quad + \sum_{\mu=1}^{2k} \sum_{r=0}^{\infty} z^{r+1-n} \int_{-\infty}^{\infty} \lambda^{r+j+\mu} \mu a_\mu e^{\sum_{\mu=1}^{2k} a_\mu \lambda^\mu} d\lambda \\
&= \frac{n+1}{2} w_j + \sum_{r=0}^{\infty} r z^{r+1-n} \int_{-\infty}^{\infty} \lambda^{r+j} e^{\sum_{\mu=1}^{2k} a_\mu \lambda^\mu} d\lambda \\
&\quad + \sum_{\mu=1}^{2k} \sum_{r=0}^{\mu-1} z^{r+1-n-\mu} \int_{-\infty}^{\infty} \lambda^{r+j} \mu a_\mu e^{\sum_{\mu=1}^{2k} a_\mu \lambda^\mu} d\lambda \\
&\quad - \sum_{r=0}^{\infty} z^{r+1-n} \int_{-\infty}^{\infty} (r+j+1) \lambda^{r+j} e^{\sum_{\mu=1}^{2k} a_\mu \lambda^\mu} d\lambda \\
&= \left(\frac{n+1}{2} - j - 1 \right) w_j + \sum_{\mu=1}^{2k} \sum_{r=0}^{\mu-1} z^{r+1-n-\mu} \int_{-\infty}^{\infty} \lambda^{r+j} \mu a_\mu e^{\sum_{\mu=1}^{2k} a_\mu \lambda^\mu} d\lambda \\
&\qquad \in W(a)
\end{aligned}
$$

for all $j = 0, 1, 2, \cdots, q-1$. It is obvious that

$$L_0(a) \cdot z^{-n-i} \in W(a)$$

for $i \geq 0$. Finally, for $j = 1$, we have

$$
\begin{aligned}
&L_1(a) w_j \\
&= \left(\frac{d}{dz} + (2q-1) z^{-1} + \sum_{\mu=1}^{2k} \mu a_\mu z^{-\mu-1} \right) \sum_{r=0}^{\infty} z^{r+1-n} \int_{-\infty}^{\infty} \lambda^{r+j} e^{\sum_{\mu=1}^{2k} a_\mu \lambda^\mu} d\lambda \\
&\qquad = \sum_{r=0}^{\infty} (r+n) z^{r-n} \int_{-\infty}^{\infty} \lambda^{r+j} e^{\sum_{\mu=1}^{2k} a_\mu \lambda^\mu} d\lambda \\
&\qquad\quad + \sum_{r=0}^{\infty} \sum_{\mu=1}^{2k} z^{r-n-\mu} \int_{-\infty}^{\infty} \lambda^{r+j} \mu a_\mu e^{\sum_{\mu=1}^{2k} a_\mu \lambda^\mu} d\lambda \\
&\qquad = \sum_{r=-1}^{\infty} (r+n+1) z^{r+1-n} \int_{-\infty}^{\infty} \lambda^{r+j+1} e^{\sum_{\mu=1}^{2k} a_\mu \lambda^\mu} d\lambda \\
&\qquad\quad + \sum_{\mu=1}^{2k} \sum_{r=0}^{\mu} z^{r-n-\mu} \int_{-\infty}^{\infty} \lambda^{r+j} \mu a_\mu e^{\sum_{\mu=1}^{2k} a_\mu \lambda^\mu} d\lambda \\
&\qquad\quad + \sum_{\mu=1}^{2k} \sum_{r=\mu+1}^{\infty} z^{r-n-\mu} \int_{-\infty}^{\infty} \lambda^{r+j} \mu a_\mu e^{\sum_{\mu=1}^{2k} a_\mu \lambda^\mu} d\lambda \\
&= z^{-n} \int_{-\infty}^{\infty} \lambda^j e^{\sum_{\mu=1}^{2k} a_\mu \lambda^\mu} d\lambda + \sum_{r=0}^{\infty} (r+n+1) z^{r+1-n} \int_{-\infty}^{\infty} \lambda^{r+j+1} e^{\sum_{\mu=1}^{2k} a_\mu \lambda^\mu} d\lambda
\end{aligned}
$$

$$
\begin{aligned}
&+\sum_{\mu=1}^{2k}\sum_{r=0}^{\mu} z^{r-n-\mu}\int_{-\infty}^{\infty}\lambda^{r+j}\mu a_\mu e^{\sum_{\mu=1}^{2k}a_\mu\lambda^\mu}d\lambda\\
&+\sum_{\mu=1}^{2k}\sum_{r=0}^{\infty} z^{r+1-n}\int_{-\infty}^{\infty}\lambda^{r+j+\mu+1}\mu a_\mu e^{\sum_{\mu=1}^{2k}a_\mu\lambda^\mu}d\lambda\\
=\ & z^{-n}\int_{-\infty}^{\infty}\lambda^j e^{\sum_{\mu=1}^{2k}a_\mu\lambda^\mu}d\lambda+\sum_{r=0}^{\infty}(r+n+1)z^{r+1-n}\int_{-\infty}^{\infty}\lambda^{r+j+1}e^{\sum_{\mu=1}^{2k}a_\mu\lambda^\mu}d\lambda\\
&+\sum_{\mu=1}^{2k}\sum_{r=0}^{\mu} z^{r-n-\mu}\int_{-\infty}^{\infty}\lambda^{r+j}\mu a_\mu e^{\sum_{\mu=1}^{2k}a_\mu\lambda^\mu}d\lambda\\
&-\sum_{r=0}^{\infty} z^{r+1-n}\int_{-\infty}^{\infty}(r+j+2)\lambda^{r+j+1}e^{\sum_{\mu=1}^{2k}a_\mu\lambda^\mu}d\lambda\\
=\ & z^{-n}\int_{-\infty}^{\infty}\lambda^j e^{\sum_{\mu=1}^{2k}a_\mu\lambda^\mu}d\lambda+(n-j-1)w_{j+1}\\
&+\sum_{\mu=1}^{2k}\sum_{r=0}^{\mu} z^{r-n-\mu}\int_{-\infty}^{\infty}\lambda^{r+j}\mu a_\mu e^{\sum_{\mu=1}^{2k}a_\mu\lambda^\mu}d\lambda\\
&\in W(a)
\end{aligned}
$$

for all $j = 0, 1, 2, \cdots, q-1$. Note that the term w_q does not appear in the computation. It is again obvious that

$$L_1(a)\cdot z^{-n-i}\in W(a)$$

for $i \geq 0$. This completes the proof of the $sl(2)$ stability of $W(a)$, and hence we have established the theorem. □

The action of these $sl(2)$ generators on $W(a)$ is very subtle, and it does not seem to allow any generalization. For example, the above proof does not apply for the Virasoro generators $L_i(a)$ other than $i = -1, 0, 1$, although the operators $L_i(a)$ are defined for all $i \in \mathbb{Z}$ and they satisfy the Witt algebra relation

$$[L_i(a), L_j(a)] = (i-j)L_{i+j}(a)$$

for $i, j \in \mathbb{Z}$.

Bibliography

[1] Enrico Arbarello and C. De Concini. On a set of equations characterizing the Riemann matrices. *Annals of Mathematics*, 120:119–140, 1984.

[2] D. Bessis, C. Itzykson, and J. B. Zuber. Quantum field theory techniques in graphical enumeration. *Advances in Applied Mathematics*, 1:109–157, 1980.

[3] P. Deligne and D. Mumford. The irreducibility of the space of curves of given genus. *Publications of I. H. E. S.*, 86:75–, 1969.

[4] P. Deligne and M. Rapoport. Les schémas de modules de courbes elliptiques. In P. Deligne and W. Kuyk, editors, *Modular Functions of One Variable, II*, volume 349, pages 143–316. Springer-Verlag, 1973.

[5] Paul Adrien Maurice Dirac. *The Principles of Quantum Mechanics, Fourth Edition*. Oxford University Press, 1958.

[6] Fredderick P. Gardiner. *Teichmüller Theory and Quadratic Differentials*. John Wiley & Sons, 1987.

[7] Martin Gardner. *Time Travel and Other Mathematical Bewilderments*. W. H. Freeman and Co., 1988.

[8] James Gleick. *Genius—The Life and Science of Richard Feynman*. Pnatheon Books New York, 1992.

[9] Phillip Griffiths and Joseph Harris. *Principles of Algebraic Geometry*. John Wiley and Sons, 1978.

[10] J. Harer and D. Zagier. The Euler characteristic of the moduli space of curves. *Inventiones Mathematicae*, 85:457–485, 1986.

[11] Yasutaka Ihara. Braids, galois groups, and some arithmetic functions. In Ichiro Satake, editor, *Proceedings of the International Congress of Mathematicians 1990*, pages 99–120. Springer-Verlag, 1991.

[12] Y. Imayoshi and M. Taniguchi. *An Introduction to Teichmüller Spaces*. Springer-Verlag, 1992.

[13] Maxim Kontsevich. Intersection theory on the moduli space of curves and the matrix Airy function. *Communications in Mathematical Physics*, 147:1–23, 1992.

[14] Motohico Mulase. Cohomological structure in soliton equations and jacobian varieties. *Journal of Differential Geometry*, 19:403–430, 1984.

[15] Motohico Mulase. Category of vector bundles on algebraic curves and infinite dimensional Grassmannians. *International Journal of Mathematics*, 1:293–342, 1990.

[16] Motohico Mulase. Algebraic theory of the KP equations. In Robert C. Penner and Shing-Tung Yau, editors, *Perspectives in Mathematical Physics*, pages 151–217. International Press Inc., 1994.

[17] Motohico Mulase. Matrix integrals and integrable systems. In K. Fukaya, M. Furuta, T. Kohno, and D. Kotschick, editors, *Topology, Geometry and Field Theory*, pages 111–127. World Scientific Publishing Co., 1994.

[18] Motohico Mulase. Asymptotic analysis of a hermitian matrix integral. *International Journal of Mathematics*, 6:881–892, 1995.

[19] Motohico Mulase and Pol Vanhaecke. *The KP Theory and Algebraic Geometry*. somewhere, 1998.

[20] David Mumford, John Fogarty, and Frances Kirwan. *Geometric Invariant Theory, Third Edition*. Springer-Verlag, 1994.

[21] Robert C. Penner. Perturbation series and the moduli space of Riemann surfaces. *Journal of Differential Geometry*, 27:35–53, 1988.

[22] Giovanni Sansone and Johan Gerretsen. *Lectures on the Theory of Functions of a Complex Variable, volume I and II*. Wolters-Noordhoff Publishing, 1960, 1969.

[23] Ichiro Satake. The Gauss-Bonnet theorem for V-manifold. *Journal of the Mathematical Society of Japan*, 9:464–492, 1957.

[24] Mikio Sato. Soliton equations as dynamical systems on an infinite-dimensional Grassmann manifold. *Kokyuroku of the Research Institute for Mathematical Sciences, Kyoto University*, 439:30–46, 1981.

[25] L. Schneps. *The Grothendieck theory of dessins d'enfants*, volume 200. London Mathematical Society, 1994.

[26] Julian Schwinger. *Selected Papers on Quantum Electrodynamics*. Dover Publications, 1958.

[27] Takahiro Shiota. Characterization of jacobian varieties in terms of soliton equations. *Inventiones Mathematicae*, 83:333–382, 1986.

[28] Daniel D. Sleator, Robert E. Tarjan, and William P. Thurston. Rotation distance, triangulations, and hyperbolic geometry. *Journal of the American Mathematical Society*, 1:647–681, 1988.

[29] Kurt Strebel. *Quadratic Differentials*. Springer-Verlag, 1984.

[30] G. 'tHooft. A planer diagram theory for strong interactions. *Nuclear Physics B*, 72:461–473, 1974.

[31] William Thurston. *Three-Dimensional Geometry and Topology, volume 1 and 2*. Princeton University Press, 1997, (volume 2 to be published).

[32] Hermann Weyl. *Der Idee der Riemannschen Fläche*. Teubner, Leipzig, 1913.

[33] Edward Witten. Two dimensional gravity and intersection theory on moduli space. *Surveys in Differential Geometry*, 1:243–310, 1991.